DEVELOPMENT OF ADVANCED MATHEMATICAL PROGRAMMING METHODS FOR SUSTAINABLE ENGINEERING AND SYSTEM BIOLOGY

Pavel Vaskan

Dipòsit Legal: T 952-2014

DOCTORAL THESIS

Pavel Vaskan

DEVELOPMENT OF ADVANCED MATHEMATICAL PROGRAMMING METHODS FOR SUSTAINABLE ENGINEERING AND SYSTEM BIOLOGY

Universitat Rovira i Virgili
Department of Chemical Engineering

UNIVERSITAT ROVIRA I VIRGILI

Tarragona
2014

Pavel Vaskan

DEVELOPMENT OF ADVANCED MATHEMATICAL PROGRAMMING METHODS FOR SUSTAINABLE ENGINEERING AND SYSTEM BIOLOGY

DOCTORAL THESIS

Supervised by: Prof. **Gonzalo Guillén Gosálbez**
Prof. **Laureano Jiménez Esteller**

Universitat Rovira i Virgili
Department of Chemical Engineering
SUSCAPE research group

Tarragona
2014

UNIVERSITAT ROVIRA I VIRGILI

Departament d'Enginyeria Química
Av. Països Catalans, 26,
Campus Sescelades
43007 Tarragona (Spain)
Tel.: +34 977 55 9603
Fax: +34 977 55 9621

Gonzalo Guillén Gosálbez and Laureano Jiménez Esteller , associate professors in the Department of Chemical Engineering,

I STATE that the present study, entitled "Development of advanced mathematical programming methods for sustainable engineering and system biology", presented by Pavel Vaskan for the award of the degree of Doctor, has been carried out under our supervision at the Department of Chemical Engineering of the University Rovira i Virgili.

Tarragona, 15th January, 2014

Dr. Gonzalo Guillén Gosálbez

Dr. Laureano Jiménez Esteller

Acknowledgment

Foremost, I would like to express my sincere gratitude to my advisors Prof. Gonzalo Guillén Gosálbez and Prof. Laureano Jiménez. Thanks to Prof. Gonzalo Guillén Gosálbez for the continuous support of my Ph.D study and research, for the motivation, enthusiasm, and his immense knowledge, which he was always ready to share. Many thanks to Prof. Laureano Jiménez for this great opportunity to do doctoral program in SUSCAPE group, for his patience, advises and paternal care. Without both of you this thesis would have been impossible.

I also want to thank all members of the SUSCAPE research group who helped me in different forms. It was a pleasure to work with all of you. I would like to acknowledge the Catalan Government for granting me a three-year scholarship (FI) that has cover part of the expenses during my PhD. I also acknowledge the postgraduate coordinators Núria Juanpere, and Anna Benages for their administrative help over the whole period of my PhD trainee.

Specially I would like to thank my family. Words cannot express how grateful I am to my mother, brother, grandfather and grandmother for all of the sacrifices that you have made for me. Your support was something that sustained and inspired me being so far away from you. I love you very much.

Finally, thanks to the people who made my PhD life happy and interesting. Thanks for all of my friends, Russian-Ukraine URV community, Erasmus students and *Castellers de Sant Pere i Sant Pau*.

Summary

The main goal of this thesis was to develop mathematical programming tools to address the design and planning of sustainable engineering systems and the modeling and optimization of biological systems. This PhD dissertation is presented using five articles that have been published or are ready to be submitted to international peer reviewed journals.

The first part, which includes two publications, explores the combined use of multi-objective optimization and geographic informational systems (GIS) to assist in the problem of utilization of sewage sludge in Catalonia (north-east region of Spain). In the first paper (see 7.1), we propose an approach that integrates GIS and multi-objective mixed-integer linear programming (MILP) within a unified framework that allows exploring, in a rigorous and systematic manner a large number of alternatives for sewage sludge amendment from which the best ones (according to the decision-makers' preferences) are identified. The capabilities of our methodology are illustrated through its application to a real case study based on Catalonia. The tool presented provides as output a set of optimal alternatives for sewage sludge distribution, each one achieving a unique combination of economic and environmental performance. Our ultimate goal is to guide decision-makers towards the adoption of more sustainable patterns for sewage sludge amendment.

The combined use of GIS and optimization tools gives rise to complex MILP models due to the spatially explicit nature of the problems addressed. In these MILPs, the decision variables are defined for every pixel of the GIS map, thereby leading to mathematical models with a very large number of variables and constraints. As an illustrative example, a GIS map with 13,984 pixels leads to an MILP containing 69,920 continuous variables, 125,860 binary variables, and 153,832 equations (see 7.2, section 4). In our first paper, we overcame this limitation by considering a GIS map with low resolution (i.e., that contain a low number of pixels). Although this strategy simplifies the calculations, it offers no guarantee of convergence to the global optimum of the original problem (i.e., the one with high resolution).

In the next work (see 7.2), we proposed a rigorous decomposition algorithm for the efficient solution of GIS-based MILPs that exploits their particular mathematical structure. This strategy allows handling models based on GIS maps with high resolution. Our approach is based on de-

composing the problem into two hierarchical levels between which our algorithm iterates until a termination criterion is satisfied. We illustrate the capabilities of our strategy via its application to the optimal location of agricultural areas for sewage sludge amendment in Catalonia. Numerical results show that our approach achieves reductions of orders of magnitude in CPU time (compared to the full space GIS-based MILP) while still yielding near optimal solutions.

The next section of the PhD addresses the optimal design of heat exchanger networks (HENs) and energy production systems considering economic and environmental concerns. The design task of a HEN is posed in mathematical terms as a multi-objective mixed integer non-linear programming (MINLP) problem in which life cycle assessment (LCA) principles are used to quantify the environmental impact (see 7.3). One of the advantages of our approach is that it accounts for the simultaneous minimization of several environmental metrics, as opposed to other models that focus on minimizing a single aggregated indicator. A rigorous dimensionality reduction method based on a mixed-integer linear programming (MILP) formulation is applied to aid the post-optimal analysis of the trade-off solutions [1]. The capabilities of our approach are tested through two examples. We clearly illustrate how the use of a single overall aggregated environmental metric is inadequate in the design of HENs, since it may leave solutions that are potentially appealing for decision-makers out of the analysis. Our method is aimed at facilitating decision-making at the early stages of the design of HENs.

Next we applied our approach to the design of utility plants considering economic and environmental concerns simultaneously. The approach presented relies on the combined use of multi-objective optimization, LCA analysis and dimensionality reduction methods (see 7.4, [1]). We first pose the planning task as a multi-objective mixed integer linear problem (MILP) that simultaneously accounts for the minimization of the cost and environmental impact of the energy system. The environmental performance of the plant is quantified using several LCA-based indicators that measure the damage caused in different categories. We then apply a dimensionality reduction technique to facilitate the post-optimal analysis of the solutions found. Numerical examples show that the number of environmental objectives can be greatly reduced while still preserving the problem structure to a large extent. We clearly demonstrate that the use of any single aggregated environmental metric is inadequate, as it might change the dominance

structure of the problem in a manner such that some solutions that are optimal in the original space of objectives might be lost.

In the last part of the thesis we present a new optimization method based on Flux Balance Analysis (FBA), that allows identifying meaningful biological objective functions driving the cell's metabolic machinery under different conditions (see 7.5). Our approach, which is based on multi-level optimization coupled with mixed-integer nonlinear programming (MINLP), identifies in a rigorous and systematic manner, the most probable objective functions for a given set of experimental conditions. We benchmark the method by analyzing which combination of objective functions better explains a set of metabolic fluxes that were experimentally determined in vivo. We confirm that biomass maximization is a fundamental objective function under any experimental condition. In addition, we found that its combination with additional criteria (e.g., Nicotinamide adenine dinucleotide (NADH) consumed), improves the predictive capabilities of the FBA model.

The general approach and tools presented in this PhD Thesis can be applied to a wide variety of sectors such as energy, chemical, petrochemical, agricultural, metabolic, pharmaceutical etc. evidencing the multidisciplinary character of the approach and the potential impact of this Thesis.

Table of contents

1 Introduction

Multi-objective optimization is concerned with mathematical optimization problems involving more than one objective function to be optimized simultaneously. Multi-objective optimization has been applied in many fields of science, including, among others, engineering, economics, logistics and systems biology, where optimal decisions need to be taken in the presence of trade-offs between two or more conflicting objectives. During my PhD studies, I have focused on the development of multi-objective optimization techniques as applied to sustainable engineering and systems biology.

Traditionally, the optimization models devised by the process engineering to assist in the operation and design of industrial processes have concentrated on maximizing the economic benefit of the process. In recent years, however, there has been a growing awareness of the importance of incorporating environmental concerns along with traditional economic criteria within the optimization procedure. To answer some of these engineering trends, intensive research effort is currently being devoted for developing and adopt more sustainable design alternatives.

One of the most interesting problems in process systems engineering concerns the development of decision support tools that incorporate various stakeholders' interests during the sustainable design and planning of industrial processes. In most cases, stakeholders have different views of the problem and show conflicting interests, making it difficult to find a consensus among them.

In this thesis we have addressed this problem from different perspectives. First, we proposed a systematic tool based on mathematical programming and spatial analysis techniques (i.e., GIS) to support decision making in the management of sewage sludge in the region of Catalonia (see 7.1). Geographic informational systems (GIS) were initially developed as a tool for storing and displaying all forms of geographically referenced information. In the recent past, however, there has been a growing interest on the application of GIS in the solution of various social and economic problems. Particularly, GIS has been used in the context of spatial decision analysis for the assessment of potential locations for different types of systems considering various inputs simultaneously, with a recent growing interest placed on its application to environmental problems. As an example, Nadal et al. [2], Poggio et al. [3] investigated the use of GIS for human

health assessment, whereas Schriever et al. [4], and Johnson et al. [5] applied GIS in the assessment of the ecological exposure and environmental risk of several systems.

GIS can be combined with multicriteria decision analysis (GIS-MCDA) to address problems in which different (typically conflictive) criteria like risks, costs, benefits and stakeholders' views must be accounted for in the analysis. In this kind of problems, decisions to be made include the selection of the best potential geographical locations among a set of alternatives. This approach takes advantage of the complementary strengths of GIS (i.e., data acquisition, storage, retrieval, manipulation and analysis) and MCDA (quantification of the decision maker's preferences [6]).

Passuello et al. [7] applied GIS and MCDA to the management of sewage sludge, whereas Malczewski [8] investigated the use of GIS-based tools in land-use suitability analysis. The capabilities of GIS and spatial analysis can be further enhanced through its integration with optimization tools. Grabaum and Meyer [9] investigated the use of GIS to support decision making in planning problems. Wang et al. [10] developed a GIS model to identify the best location for future land uses in the Lake Erhai basin in China. Mapa et al. [11] combined GIS and mathematical modeling for the solution of location-allocation problems arising in the management of education facilities. Jung et al. [12] integrated GIS and optimization tools for the effective control of parcel delivery services. Marcoulaki et al. [13] developed an integrated framework based on stochastic optimization and GIS for the design of pipeline systems. Van den Broek et al. [14] integrated ArcGIS, a geographical information system with spatial and routing functions, with MARKAL, an energy bottom-up model based on linear optimization for designing a cost-effective CO_2 storage infrastructure in The Netherlands.

One problem in which the combined use of GIS and mathematical programming holds good promise is the treatment of sewage sludge in agricultural areas. The production of sewage sludge (SS) has grown rapidly during the last years, mainly due to the increase of the world population. Despite recent advances, the question on how to treat the SS still remains open. There are different alternatives for this, and one effective method is to reuse it as a fertilizer in the agricultural sector, an alternative encouraged by the European Community, which promotes the recycling of organic matter and nutrients to soils [15].

Identifying the best agricultural areas for SS amendment is a difficult task because this strat-

egy shows benefits to both soil and crops, but also disadvantages due to the potential contamination of the fields. Furthermore, several environmental aspects, such as groundwater contamination by nitrates, open waters and soil protection, as well as human exposure to the contaminants present in the sludge matrix must be considered along with economic aspects, making this task quite challenging. This is because the management of this residue concerns different stakeholders, with different views of the problem and conflicting interests. In addition, they may find that their interests are not reached, fact that leads to a low acceptance of the practice. Figure 1 briefly describes the objectives of each stakeholder.

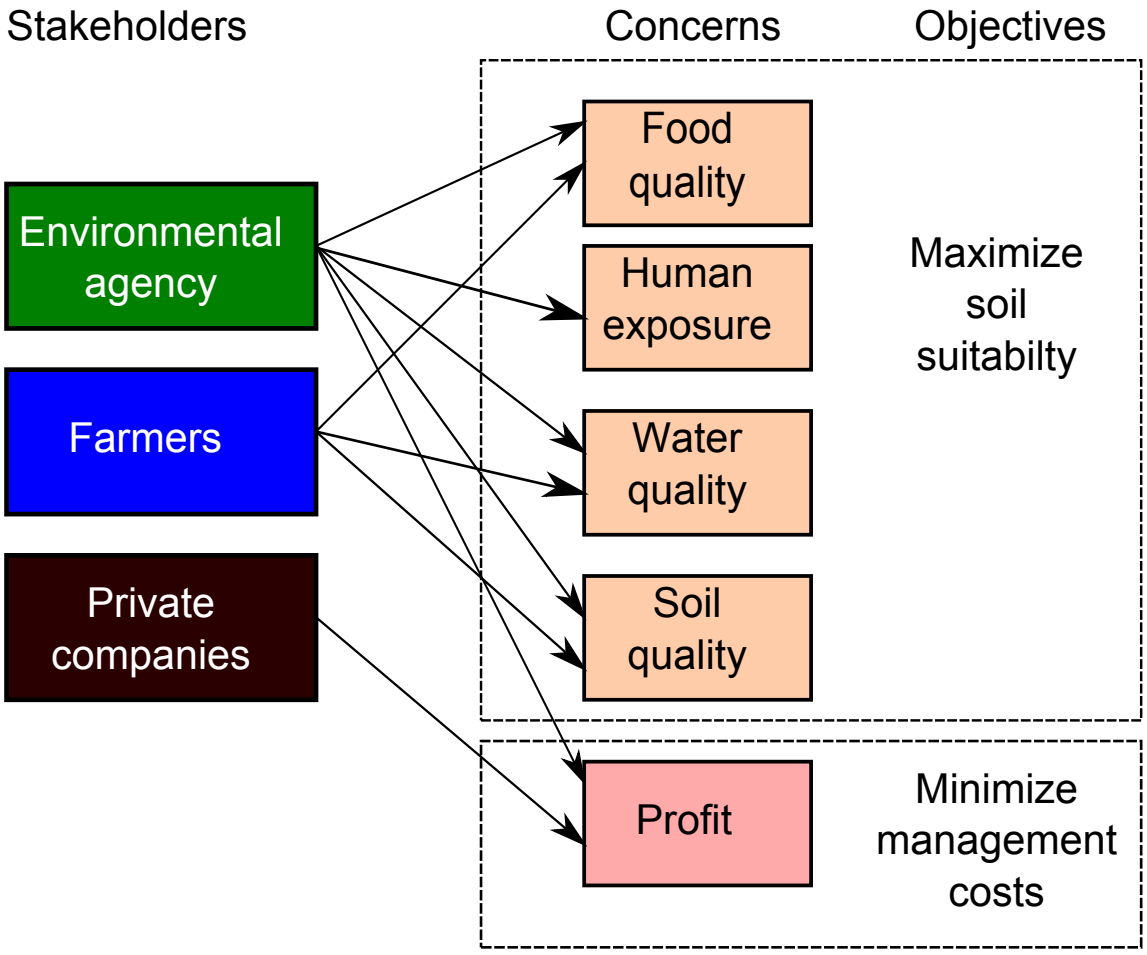

Figure 1: Relationship between the stakeholders and objectives.

Systematic tools based on multi-objective mathematical programming are well suited to tackle problems of this type, as they allow screening in a rigorous and systematic manner a large number of alternatives from which the best ones are identified.

This thesis presented a systematic spatial decision-making tool for the optimal distribution

of SS on agricultural areas based on the combined use of GIS and mathematical programming (7.1). The task of identifying the best agricultural soils for SS amendment was formulated as a mixed-integer linear programming (MILP) problem that seeks to optimize simultaneously the economic and environmental performance of the system. The multi-objective optimization model coupled with GIS data provides a comprehensive procedure to evaluate SS disposal options on agricultural areas for organic amendment.

The capabilities of our approach were tested through its application to a case study based on Catalonia. Numerical results show that it is possible to improve the environmental performance of the final solution by compromising the associated cost (Section 4 at 7.1). Our methodology is intended to assist decision-makers in such a challenging task.

One of the main advantages of our approach is that it produces solutions that reflect precisely the default preferences of the decision-makers involved in the problem. Furthermore, it relies on a rigorous and systematic mathematical approach that avoids falling in sub-optimal solutions, an undesired situation that might occur when applying heuristics or rules of thumb.

The combined use of GIS and optimization tools led to complex MILP models due to the spatially explicit nature of the problem. In these MILPs, the decision variables are defined for every pixel of the GIS map, thereby giving rise to mathematical models with a very large number of variables and constraints. Hence, in the second work presented in this Thesis (see 7.2), we proposed a rigorous decomposition algorithm for the efficient solution of GIS-based MILPs that exploits their particular structure. This strategy allows handling models defined on the basis of GIS maps with high resolution. Our approach decomposes the original MILP problem into two hierarchical levels between which the algorithm iterates until a termination criterion is satisfied. Numerical results show that our approach achieves reductions of orders of magnitude in CPU time (as compared to the full space GIS-based MILP), while still yielding near optimal solutions (Section 6 at 7.2).

Mathematical programming techniques offer a general modeling framework for including environmental concerns in the synthesis and planning of industrial processes. Despite recent progress in sustainable design, the selection of a suitable metric for the environmental assessment of processes is still an open issue in the literature. According to Cano et al. [16], there are

four main types of environmental objectives. These are the minimization of

(1) the emissions of pollutants of concern [17];

(2) the mass of waste generated [18];

(3) the contribution to specific environmental problems [19];

(4) specific aggregated indicators reflecting the overall environmental impact [20].

Regardless of the approach followed, what has become clear during the last years is that the environmental performance of a process should be assessed over its entire life cycle. Traditional process engineering approaches that included environmental concerns within the decision-making process focused at the plant level. This approach could lead to solutions that decrease the environmental impact locally at the expense of increasing the environmental burdens in other stages of the life cycle of the process, which could result in a worst overall environmental performance [19].

The life cycle assessment (LCA) methodology arose in response to this situation. LCA is an objective methodology for evaluating the environmental loads associated with a product, process, or activity over their entire life cycle [21]. This method is based on identifying and quantifying the energy and materials used in a process in order to translate them into a set of meaningful environmental indicators that inform about the impact caused in different categories (i.e., human health, eco-system quality, and resources). The performance in these damage categories is employed to assess process alternatives leading to potential environmental improvements.

The combined use of multi-objective optimization (MOO) and LCA was first proposed by Livingston and Pistikopoulous [22, 23], and then formally defined by Azapagic and Clift [24]. In the recent past, this approach has been applied to a wide variety of industrial problems, such as the design of chemical plants [25], thermodynamic cycles [26], the strategic planning of supply chains [27, 28, 29, 30], the design of heat exchanger networks [31], the design of solar energy plants [32], and the design of hydrogen infrastructures [33, 34], among others.

A critical issue in the combined use of MOO and environmental assessment methods such as LCA is the definition of suitable eco-metrics to be minimized. No agreement has been reached so far as to which universal LCA indicator should be employed in the calculations. Unfortunately, the computational burden of MOO grows rapidly with the number of objectives, which

prevents the inclusion of several LCA indicators in the optimization model. Selecting key LCA metrics for optimization purposes that keep the problem in a manageable size while still quantifying the environmental performance in an accurate manner is therefore very challenging. In this thesis we accomplished this task by using a rigorous MILP-based dimensionality reduction technique developed by Guillén-Gosálbez [1]. We applied this method to the sustainable design of heat exchanger networks (for further details see 7.3) and utility plants (see 7.4). This approach distinguish between meaningful LCA objectives and redundant ones. The former are kept in the analysis, while the later are eliminated. The method sheds light on the relationships between LCA indicators, providing valuable insight into the trade-offs that inherently exist between economic and environmental criteria.

The design of heat exchanger networks (heat exchanger network synthesis, HENS) is an important field in process systems engineering and has been the subject of intensive research over the past 50 years. Its significance can be attributed to its role in controlling the costs of energy and providing environmental benefits for a process [35]. The most common methods to solve the synthesis of HENs are the sequential and simultaneous approaches.

Sequential synthesis methods use the strategy of dividing the HEN design problem into a series of subproblems in order to reduce the computational requirements for obtaining a network design. Sequential synthesis methods are further divided into two subcategories: (1) evolutionary design methods, such as the pinch design method (PDM) by Linnhoff et al. [36, 37, 38], the dual temperature method by Trivedi [39] , and pseudo-pinch methods by Trivedi et al. [40]; and (2) mathematical programming techniques based on the sequential solution of continuous and integer linear programs, like the approaches by Cerda et al. [41] and Papoulias and Grossmann [42], as well as nonlinear optimization problems, like the approach by Floudas et al. [43]. The sequential synthesis method offers no guarantee of convergence to a HEN with minimum annual cost.

Simultaneous HENS approaches attempt to find the optimal network without decomposing the problem. Simultaneous synthesis methods rely primarily on MINLP formulations with simplifying assumptions. One of the earliest simultaneous HENS formulations was proposed by Yuan et al. [44]. The MINLP formulation proposed by Yee and Grossmann [45], is one of

the most widely used. In this case, the problem is divided into stages; in each stage any match of process streams is allowed. In addition, any cold/hot utility and hot/cold process stream can be used to heat and cool the process streams in every stage. The superstructure taken as a basis in the development of the model is presented in Figure 4.

Most HENS methods focus only on optimizing the economic performance (mainly the total cost), and disregard the environmental dimension of the problem. In this thesis we addressed the optimal design of heat exchanger networks (HENs) with economic and environmental concerns (7.3). The design task is posed in mathematical terms as a multi-objective mixed-integer non-linear programming (MINLP) problem, in which life cycle assessment (LCA) principles are used to quantify the environmental impact. One of the advantages of our approach is that it accounts for the simultaneous minimization of several environmental metrics, as opposed to other models that focus on minimizing a single aggregated indicator. A rigorous dimensionality reduction method based on a mixed-integer linear programming (MILP) formulation [1] is applied to aid the post-optimal analysis of the trade-off solutions. The capabilities of our approach are tested through two examples. We clearly illustrate how the use of a single overall aggregated environmental metric is inadequate in the design of HENs, since it may leave some solutions that are appealing for decision-makers out of the analysis (Section 5 at 7.3).

We applied next a similar approach to the sustainable design of utility plants considering several environmental metrics. Nowadays, a high percentage of the total human-originated environmental impact is energy related. The design and planning of efficient energy systems capable of satisfying the power and steam demand in the process industries is therefore a crucial issue in sustainability [46].

Several methods are available in the literature for the synthesis of utility plants. They can be roughly classified into two main groups. The first are based on thermodynamic targets and heuristics [47, 48]. As pointed out by Bruno et al. [49], these methods have as major drawback that even if the design with highest thermal efficiency is obtained, it may not be economically attractive because capital costs may be too high. The second group, to which the present work belongs, relies on rigorous optimization techniques based on mathematical programming (i.e., linear, non-linear, mixed-integer linear, and mixed-integer non-linear programming: LP, NLP,

MILP and MINLP, respectively). Specifically, the first optimization approaches based on LP and MILP techniques were introduced by Nishio and Johnson [50], Papoulias and Grossmann [42], and Petroulas and Reklaitis [51]. Following a similar approach, Hui and Natori [52] applied MINLP strategies to the optimization of site utility systems, while Bruno et al.[49] proposed another MINLP formulation for the design of utility systems.

Most of the strategies mentioned above optimize the system considering only the economic performance and disregarding its environmental impact [49, 53, 54]. In this thesis we developed a multi-objective optimization model of an utility plan that considers explicitly several environmental indicators (7.4). To facilitate the calculations, we coupled this model with an MILP-based dimensionality reduction approach [1] that identifies key environmental metrics whose optimization automatically results in the improvement of the system in all the remaining damage categories.

This analysis reduces the complexity of the underlying multi-objective optimization problem from the viewpoints of generation and interpretation of its solutions. The capabilities of this approach are illustrated through its application to two case studies. Results clearly illustrate that significant reductions in the number of environmental objectives can be attained while still preserving the main features of the problem (Section 6 at 7.4). Our approach is aimed at facilitating the decision-making process in the design of energy systems with environmental impact considerations.

The final part of this Thesis is dedicated to systems biology. System biology is a biology-based inter-disciplinary field that studies complex interactions between biological systems and their constituents, and which applies a holistic approach to biological and biomedical problems. One of the outreaching aims of systems biology is to model and discover emergent properties of cells, tissues and organisms using mathematical programming methods. In this thesis we focused on shedding light on an open important problem in systems biology: the identification of meaningful biological objective functions driving the operation of metabolic networks under various environmental conditions. Determining such functions is a central topic in systems biology. Research in this area might ultimately allow biologists to identify biological underlying design principles [55].

In general, the choice of an analytical method in system biology depends on the availability of biological knowledge. A steady state analysis can be done using only the network structure, and without knowing the velocity rate constants for a particular reaction. For example, flux balance analysis (FBA) was used to predict the switching of the metabolic pathway in Escherichia coli under different nutritional conditions based on knowledge of only the metabolic network structure [56]. On the contrary, stability analysis and sensitivity analysis provide insight into how the system's behavior changes in the face of some stimuli. Similarly, bifurcation analysis provides dynamic information of a system [57, 58].

Several in silico frameworks for determining a most-likely objective function have been proposed [59]. For example, ObjFind, was built under the assumption that natural systems optimize a linear combination of biological objectives defined on the basis of some biological reactions [60] . ObjFind seeks to determine the values of the weights (coefficients of importance, CoI) to be attached to a set of reaction fluxes such that when the resulting weighted sum of fluxes is optimized, the difference between the optimal in silico flux distribution predicted by the model and the experimentally observed distribution is minimized. In the ObjFind framework, a high CoI indicates that a reaction is important for the cellular objective function, while a small weight implies the opposite.

BOSS illustrates another type of optimization framework [61]. This method considers, as potential objectives, de novo reactions added to the stoichiometry matrix of the target network. In this approach, the objective reaction is not confined to be one of a subset of existing reactions, but rather is allowed to take on any form (e.g. an existing reaction, a combination of existing reactions, or a previously uncharacteristic reaction). This assumption provides more flexibility to the framework and makes the optimization process closer to what might have occurred during biological evolution, where changes in regulation (optimizing the CoIs of existing reactions) can be combined with gene duplication or deletion (adding new reactions to the network). A third type of framework was proposed by Knorr et al. [62]. This framework employs a Bayesian-based technique to determine meaningful biological objective functions for a system.

The aforementioned types of frameworks rely on single-objective approaches that assume the existence of a unique universal biological objective function. However, a recent study by

Sauer and co-workers has shown that there might be more than one meaningful fitness function driving the metabolic machinery [63, 64]. Particularly, these authors suggested the existence of three main biological criteria that microorganisms might attempt to optimize simultaneously: maximum ATP yield, maximum biomass yield, and minimum sum of absolute fluxes.

If we expect to understand the evolution and functional properties of complex metabolic networks, it is important to develop a rigorous framework that can identify the criteria underlying design selection in biological systems. In this thesis we report the development of a novel MINLP base optimization framework (7.5) where the KarushKuhnTucker (KKT) conditions are used to convert a bi-level optimization problem into a single-level optimization one. Hence, inspired by the ObjFind method by Burgard and Maranas [60], we propose an approach that identifies a set of meaningful biological criteria that all together explain the operation of metabolic networks.

We test the capabilities of our method through its application to the study of in vivo flux distribution in Escherichia coli's central metabolism using data derived from 13C isotopomer analysis [65]. We adapt a FBA model of that metabolism [66], considering as surrogates for cellular fitness functions biomass growth rate and a set of reaction fluxes that produce/consume ATP (Adenosine triphosphate) and redox potential. Numerical results show that biomass maximization is a fundamental objective function under the observed experimental conditions. In addition, we find that its combination with additional criteria improves the predictive capabilities of the FBA model (i.e., the multi-objective FBA model provides results that better explain the experimental observations). Our findings may have significant implications in explaining the emergence of alternative and seemingly equally fit solutions in replicate experiments of long term evolution [67].

1.1 General objectives

The objectives of this thesis can be divided into two domains: sustainable engineering and systems biology. In sustainable engineering, the main objectives of the thesis are the following:

- Propose and apply, in different engineering problems, novel optimization frameworks based on the combined use of multi-objective optimization (MOO), economic analysis, and environmental assessment tools.

- Develop a spatial decision-support tool for optimizing sewage sludge amendment by combining Geographical Information Systems (GIS) and multi-objective Mixed-Integer Linear Programming (moMILP).
- Adapt and apply a bi-level decomposition algorithm to the solution of GIS-based mathematical models in order to expedite their solution.
- Develop a Multi-Objective Optimization (MOO) framework for the environmentally conscious design and planning of Heat Exchanger Networks (HEN).
- Develop a multi-objective optimization (MOO) framework for the environmentally conscious design and planning of utility plants.
- Develop and implement effective dimensionality reduction methods for facilitating the solution of MOO problems with a large number of objectives.

The objectives regarding systems biology are:

- Develop an optimization method based on Flux Balance Analysis (FBA) for identifying meaningful biological objective functions driving the metabolic machinery.
- Investigate the existence of meaningful biological objectives, in addition to biomass growth rate maximization.

1.2 Problem statement

In this section we formally describe the problems addressed in this thesis.

1.2.1 Combined use of GIS and multi-objective optimization.

The reuse of sewage sludge (SS) as an agricultural fertilizer has traditionally received increasing interest. The SS matrix contains harm emissions, such as heavy metals and persistent organic pollutants (POPs) that can contaminate the soil, crops, groundwater, open waters, and eventually reach the human food chain (7.1, Section 3.2.2, Figure 5). The impact on the field depends on its local characteristics. Two subcriteria are considered for soil: “soil structure” and “soil characteristics” The subcriterion “soil structure” quantifies the ability of the soils to receive SS (for instance, organic soils with a fine texture are preferred due to their buffer properties), while “soil

characteristics" consider metal concentration and mobility in soil (bioavailability and lower mobility for high pH and carbonate content). Spatial decision-making tools for land classification are well suited for addressing the sewage sludge amendment problem, as they allow identifying the best regions from information available in spatial databases (7.1, Section 3.2.2, Figure 5.).

The capabilities of our methodology are illustrated through its application to a case study based on Catalonia (NE of Spain). Catalonia is a region in the Northeastern part of Spain that covers an area of 32,114 km2 (Figure 2). It extends from the Pyrenees southward along the Mediterranean. Catalonia has a diversity of soil types, mostly calcareous sediments mixed with alluvium and clay. The Catalonian agriculture was centered on the production of wine, wheat, rice, barley, olive, grapes, fruits, nuts and vegetables. The agricultural area currently available has more than 0.5 million ha (7.1, Section 2, Figure 1.)

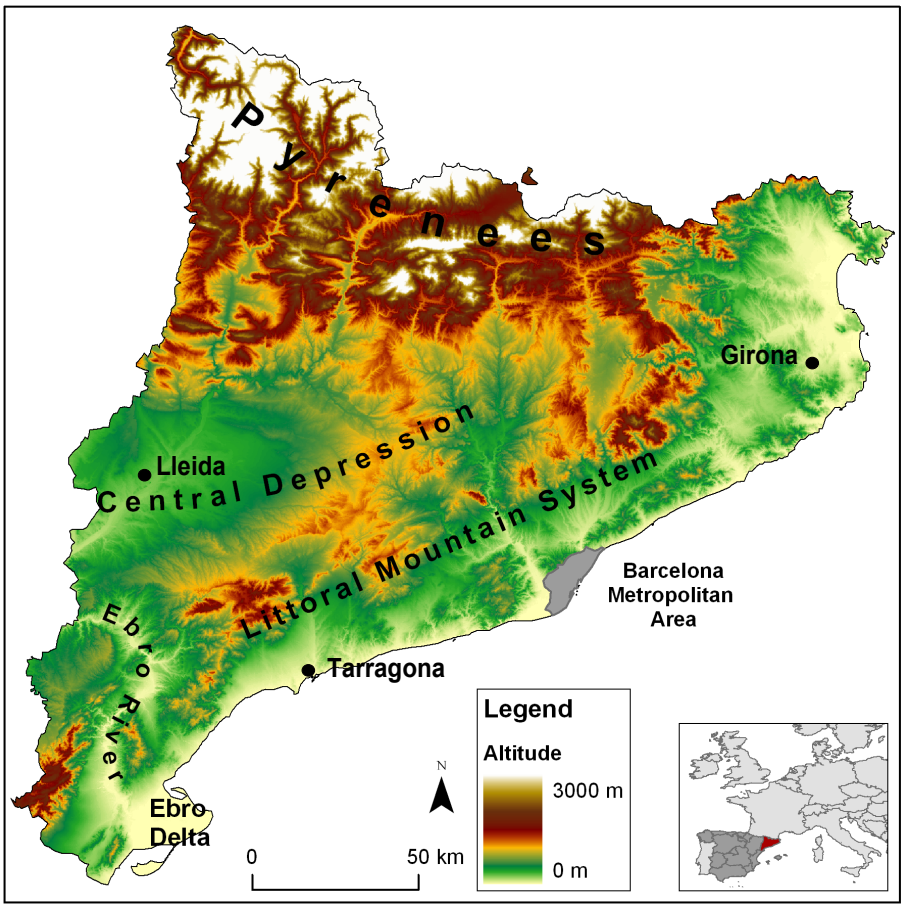

Figure 2: The map of Catalonia.

We derived a mathematical model that is based on the superstructure shown in Figure 3.

We considered a total area of 451,296 ha subdivided into 12,536 pixels, each one with a surface of 36 ha. Each of these fields is defined by a set of coordinates (in meters), an index of suitability (SUI(j)) (see 2.5, 7.1, Section 3.2.2), which quantifies the ability of the land to receive SS, an acceptable capacity (CAP(j)) in tons per year of sludge, and an application cost (in $euro\ ton^{-1}{\bullet}year^{-1}$). We are also given the set of WWTPs (waste water treatment plants) located in different cities of Catalonia (7.1, Section 2, Figure 1.) In this study we have considered the capitals of each provinces of Catalonia as the main producers of sludge (i.e., Barcelona, Tarragona, Girona, and Lleida). Each of these cities is characterized by a pair of coordinates (x,y) in meters and total production of SS in tons per year (denoted by parameter CAP(i)). The goal of the analysis is to determine the optimal distribution of SS production among the Catalonian agricultural areas that simultaneously optimizes the overall suitability and the total cost (for more details see in 7.1, Section 3.1). The mathematical formulation is posed as a Mixed-Integer Linear Programming (details can be found in 7.1, Section 3.2).

In this thesis, we also proposed a decomposition algorithm for GIS-based MILP models. The capabilities of our approach are tested using the same case study, but this time considering three different levels of aggregation in the problem (all of them for the same agricultural area of 505,176 ha): 126,294; 31,517; and 13,984 pixels, each one with a surface of 4, 16, and 36 ha, respectively. Additionally, we solved a set of problems of increasing complexity involving a different number of cities in Catalonia. We consider first the location of WWTPs in Barcelona, Girona, Tarragona, and Lleida, and then solved the same problem considering additional locations (i.e., Terrasa, Vic, Amposta, and Montblanc). The goal of the analysis is to determine the optimal distribution of SS production among a set of agricultural areas so that the total cost is minimized (further details are available in 7.2, Section 2)

1.2.2 Sustainable design of heat exchanger networks.

To formally state the problem of interest, we consider a HEN superstructure like the one depicted in Figure 4, which is an extension of the superstructure introduced by Yee and Grossmann [45]. The problem is divided into stages; in each stage any match of process streams is allowed. In addition, there exists the possibility to use any cold/hot utility available for cooling/heating the hot/cold process streams

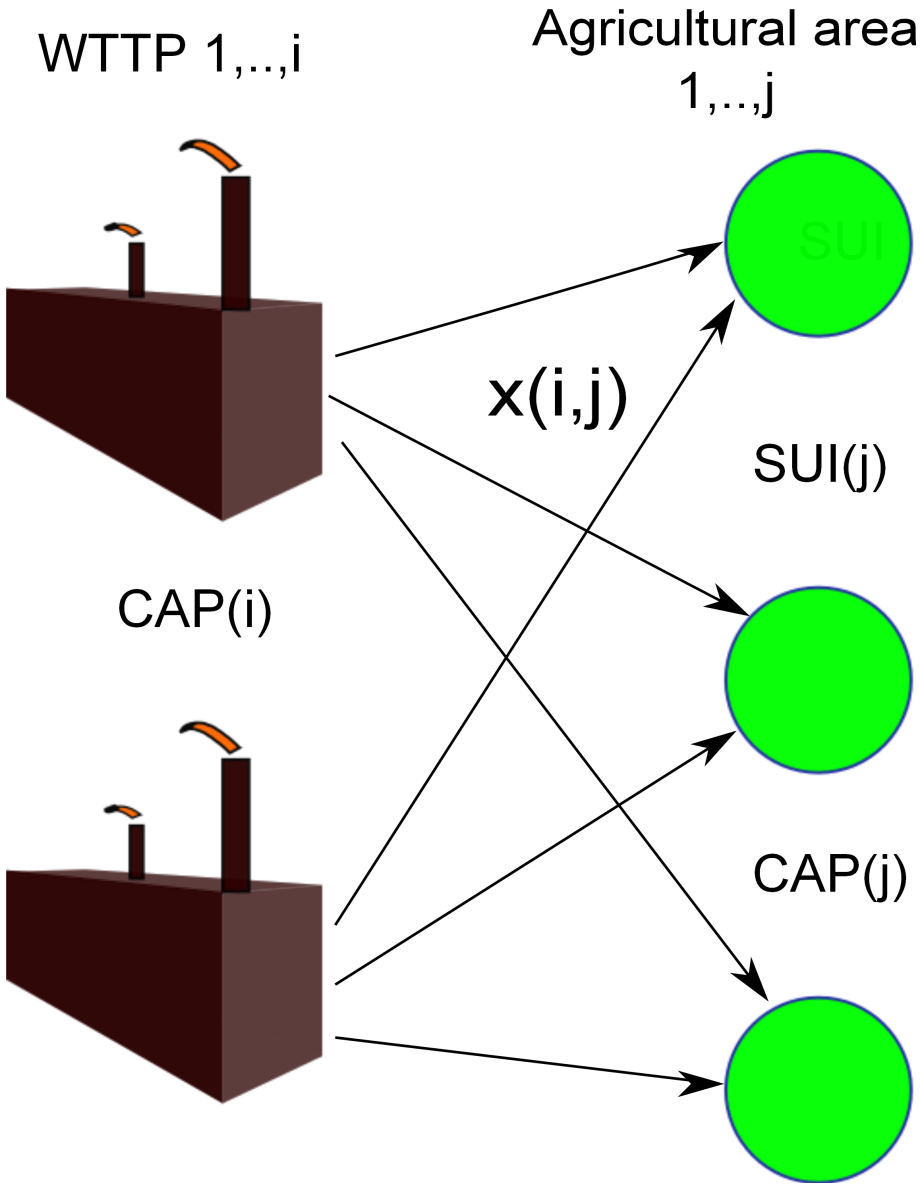

Figure 3: Superstructure of the supply chain problem.

Given are a set of hot and cold process streams to be cooled and heated, respectively, and their associated inlet and outlet temperatures. The flow rates, heat capacities and film transfer coefficients of the process streams are also provided, along with a set of available hot and cold utilities and their temperature ranges. Given also is the cost information of the heat exchangers units as well as the hot and cold utilities. Environmental data associated with every type of utility and construction material are also provided by the Ecoinvent 2.2 database, which offers international life cycle assessment (LCA) and life cycle management (LCM) data and services. The intermediate temperatures of the process streams in the limits of each stage are regarded as

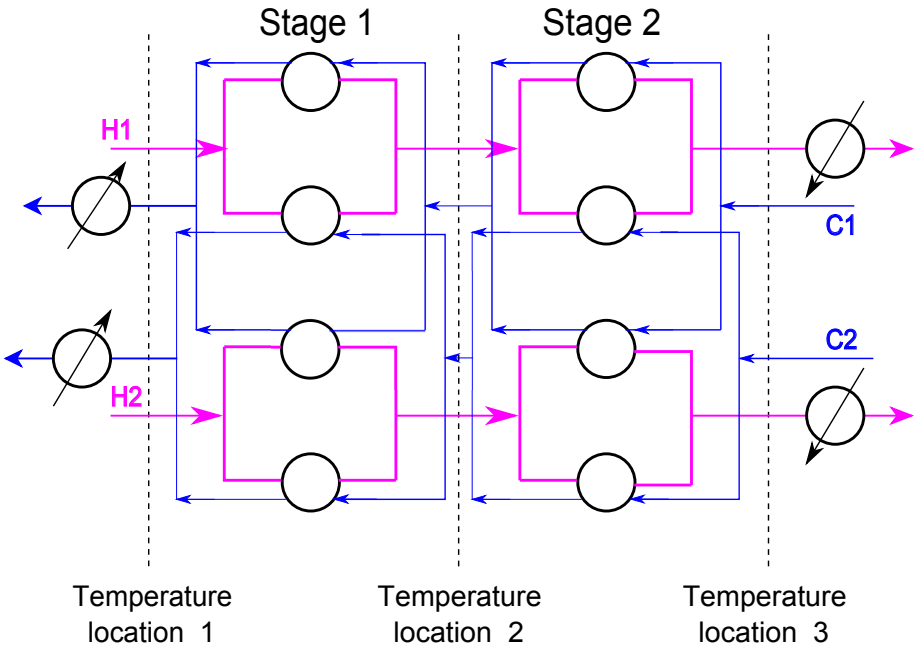

Figure 4: Superstructure for the HEN synthesis for two cold and hot streams and two stages.

decision variables. We assume isothermal mixing of streams, which simplifies the calculations.

The goal of the analysis is to determine the optimal design and operating conditions that minimize simultaneously the total cost and a set of environmental impacts, which are quantified via LCA principles. The capabilities of our approach are tested through two examples. The problem solution is defined by a set of Pareto optimal designs, each one of them achieving a unique combination of cost and environmental impact (see in 7.3, Section 2). The mathematical formulation can be found in 7.3, Section 3 and Appendix A.

1.2.3 Sustainable design of utility plants.

Energy systems utilize fuel, air and other materials to generate electricity and steam demanded by other process units in the industrial system. The system taken as reference in this work includes storage tanks to store the fuels, boilers that convert fuel into steam at high pressure and turbines that expand higher pressure steam into lower pressure steam in order to generate electricity. The details of the system are presented in Figure 5.

Given are a set of demands of electricity and steam at various pressure levels to be satisfied by the utility plant. The objective is to determine the set of planning decisions that simultaneously minimize the total cost and environmental impact. Environmental data associated with every

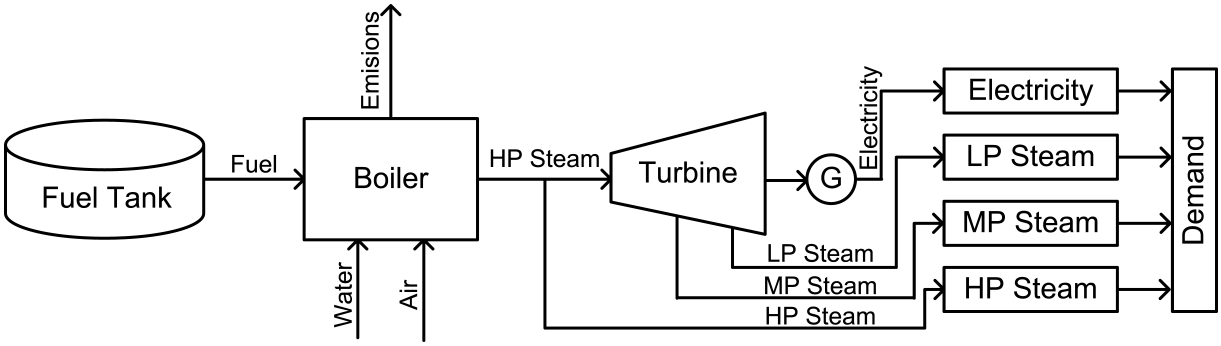

Figure 5: Energy system taken as reference

type of fuel and the purchased electricity are also provided. Decisions to be made include the amounts and types of fuels to be used in each boiler and turbine.

The capabilities of our modeling framework and solution strategy are illustrated through two case studies that address the optimal planning of an energy system that includes two fuel tanks, two boilers and two turbines (see Figure 6). The given data can be found at 7.4 in Tables 1-6. Both case studies assume the same data concerning fuels, equipment units and energy demands, but differ in the characteristics of the electricity purchased.

The initial demand of electricity is 29 MW/hr for both examples. The initial demand of steam (HP, MP and LP) is 2 ton/hr, 92 ton/hr and 98 ton/hr, respectively. A 5% increase of this demand is assumed in every time period. The model covers 7 periods of time of 48 hours each. The parameters and energy requirements for the fuels are given in Tables 1 and 2 7.4. The parameters associated with boilers and turbines are displayed in Tables 3 and 4 in 7.4. The capacity of tanks 1 and 2 are 120 and 50 tons, respectively. The maximum electricity power provided by each turbine is 70 MW. The LCI data of the emission inventories associated with the production of the different fuels are presented in Table 5 in 7.4, while the impacts associated with the external electricity are displayed in Table 6 7.4. The parameters of the damage model were taken from the Ecoinvent 2.2 database. The mathematical formulation of the model can be found in 7.4, Section 2.

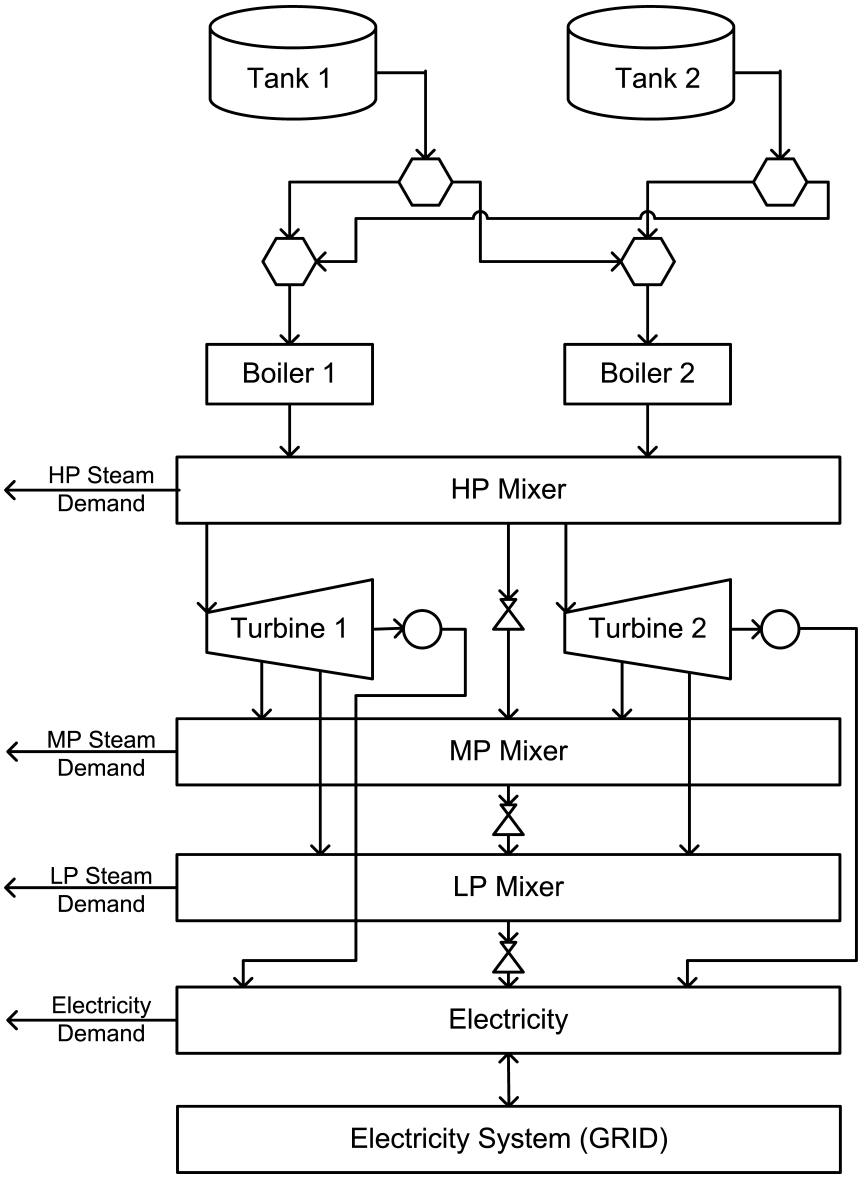

Figure 6: Superstructure of case study.

1.2.4 Identifying design principles in metabolic networks.

This problem belongs to the area of systems biology. Given a set of experimental fluxes obtained under different conditions, the goal of the analysis is to determine a set of meaningful biological objectives that drive the cell's machinery. To the approach described later in this document, we consider a previously reconstructed flux balance analysis model of the Escherichia coli central carbon metabolism [66]. The metabolic network includes 102 reactions and 62 metabolites that represent the major carbon flows through the cell. We consider as potential biological objectives, all reaction fluxes associated with an energy dissipation (Adenosine triphosphate, ATP, consumed), or redox potential dissipation (Nicotinamide adenine dinucleotide, NADH, consumed), biomass growth and total ATP production (which includes 21 different reaction rates that can generate ATP).

13C-detected in vivo flux distributions from four growth aerobic conditions were considered in the analysis. Experiment A: batch growth on glucose under aerobic conditions with fast growth (0.6 h-1); experiment B: chemostat growth 0.02 h-1; experiment C: chemostat growth 0.4 h-1; experiment D: chemostat growth (0.4 h-1) under ammonium limitation [66]. Given these experimental results, the main goal of the study is to identify the set of biological objective functions that better describes the operation of metabolic networks (see 7.5, Problem Statement Section).

2 Materials and methods

2.1 Mathematical programming

Mathematical programming deals with the problems of maximizing or minimizing objective functions in the presence of inequality ($g_n(x)$) and equality ($h_{n'}(x)$) constraints. Consider the following single objective (SO) minimization problem (Equation 1) :

$$SO(X) = \min_{x \in X}(f(x))$$

subject to

$$\begin{aligned} g_n(x) &\leq 0, \quad n = 1, 2, \ldots, N \\ h_{n'}(x) &= 0, \quad n' = 1, 2, \ldots, N' \end{aligned} \tag{1}$$

where $f(x)$ is the objective function. N is the number of inequality constraints, and N' is the number of equality constraints. X is the search space, while x is the vector of decision variables. Different types of models arise depending on the structure of the objective function and the constraints. Linear programming (LP) problems have a linear objective function and linear equality and inequality constraints. Nonlinear programming problems (NLP) contain at least one nonlinear equation, either in the objective function or the constraints. Mixed integer linear programming (MILP) and mixed integer non-linear programming (MINLP) contain are LPs and NLPs, respectively, that contain at least one binary variable. The models presented in this thesis are MINLPs and MILPs, which are the most complex ones to solve . These models can be found in Section 3 in 7.1, in Section 3 and 4 in 7.2, in 7.3 Section 3, in 7.4 Section 3 and 7.5 Materials and Methods Section.

2.2 Tool and Solvers for solving MINLP and MILP problems.

The MILP and MINLP models presented in this thesis were implemented in the General Algebraic Modeling System (GAMS) [68] version 22. GAMS is a high-level modeling system for mathematical optimization. It is designed for modeling and solving linear, nonlinear, and mixed-integer optimization problems. The system, which is tailored for complex, large-scale modeling applications, allows to build large maintainable models that can be adapted to differ-

ent situations. It is based on an integrated development environment (IDE) that allows the user to express optimization models in a special programming language called Algebraic Modeling Language (AML). GAMS interfaces with appropriate solvers that identify the optimal solution of a model within a given accuracy. MILPs were solved with CPLEX v9, while MINLP models were solved by DICOPT v1 and SBB v1.

2.3 Multi-objective optimization and Pareto front.

A standard multi-objective optimization problem (MOO), denoted by MO(X), can be expressed as follows (Equation 2):

$$MO(X) = \min_{x \in X}(F(x) = \{f_1(x), \ldots, f_k(x), \ldots, f_O(x)\})$$

subject to

$$\begin{aligned} g_n(x) &\leq 0, \quad n = 1, 2, \ldots, N \\ h_{n'}(x) &= 0, \quad n' = 1, 2, \ldots, N' \end{aligned} \tag{2}$$

where O are the objective functions to be optimized, while $F(x)$ denotes the vector of objective functions $f_k(x)$. The set of values taken by the objective functions $f_k(x)$ in the feasible solutions of MO(X) constitutes the feasible objective space Z. For example, in the context of sustainable engineering, one objectives f_k represents the economic performance (cost), whereas the others quantify a set of environmental impacts.

In 7.1, Section 2 the concept of Pareto optimality is presented. The Pareto optimal alternatives (which constitute the Pareto front or Pareto frontier) show the property that it is impossible to improve them in one objective without necessarily worsening at least another criterion. Figure 7 illustrates the concept of Pareto optimality for a case with two objectives (cost and suitability) taken from the sewage sludge amendment problem. Points lying above the curve are sub-optimal, since they are improved in both criteria simultaneously by the points lying in the Pareto front. The region bellow the curve is infeasible, since no alternative shows better (lower) cost and (higher) suitability simultaneously than the Pareto solutions. The final goal is to select a solution from the ones in the curve. The shape of curve plays an important role in the selection of the final solution. For example, from point A to point B in Figure 7, the slope of the curve

increases sharply. In contrast, from B to C, the slope is rather smooth, so in this region marginal increments in suitability are attained at the expense of a large increase in cost. Hence, the former part of the curve is more appealing for decision-makers. Examples of other multi-objective optimization approaches applied to environmental multi-criteria problems can be found elsewhere [26], [32].

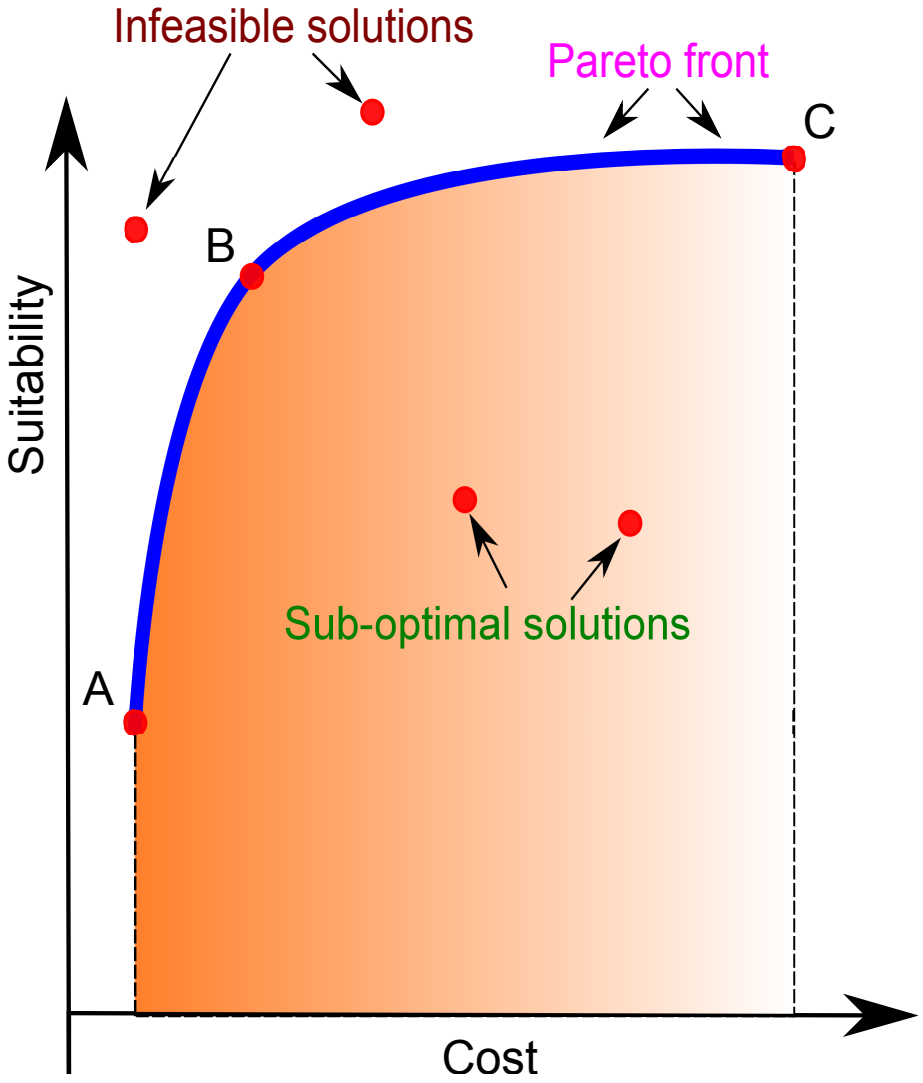

Figure 7: Description of Pareto front.

2.3.1 ε-CONSTRAINT METHOD

There are two main methods for solving MOO problems. These are the weighted-sum and the ε-constraint methods. Specifically, both of them are based on formulating a single-objective problem from the original multi-objective one. This problem is then solved repeatedly for different values of some auxiliary parameters introduced in the auxiliary model. In the weighted-sum

method, which is only rigorous for the case of convex problems, these parameters take the form of a vector of weighs that multiplies the vector of objectives. In the ε-constraint method, which is rigorous for both cases, convex and nonconvex Pareto fronts, they represent the limits imposed on the objectives that are transferred to the auxiliary constraints. Each single-objective problem provides a weakly efficient point, which might be as well strongly efficient. This condition is evaluated after exploring the whole space of auxiliary parameters [28].

In this work, the Pareto-optimal solutions are obtained by means of the ε-constraint method [69]. The ε-constraint method entails solving a set of single objective problems $SO_e(X)$, in which one objective is kept as the objective function (e.g., f_1) while the rest are transferred to auxiliary constraints in which upper bounds are imposed on them using a set of ε-parameters (Equation 3):

$$\begin{aligned} SO_e(X) = & \min_{x \in X}(f_1(x)) \\ \text{subject to } & g_n(x) \leq 0, \quad n = 1, 2, \ldots, N \\ & h_{n'}(x) = 0, \quad n' = 1, 2, \ldots, N' \\ & f_k(x) \leq \varepsilon_{k,e} \quad k = 2, \ldots, O \\ & \underline{\varepsilon_k} \leq \varepsilon_{k,e} \leq \overline{\varepsilon_k} \quad k = 2, \ldots, O \end{aligned} \tag{3}$$

Different Pareto solutions are obtained by solving repeatedly problem $SO_e(X)$ for different values of $\varepsilon_{k,e}$. In environmental engineering problems, we typically retain the cost ($k = 1$) as main objective and transfer the environmental indicators ($k \neq 1$) to the auxiliary constraints. The lower and upper limits of each ε-parameter are obtained from the minimization of each individual objective (e.g., in environmental engineering, the individual environmental objectives refer to climate change, minerals extractions, ionizing radiations etc.), as shown in Equation 4.

$$\begin{aligned} \underline{s_k} =& \arg\min_{x \in X}(f_k(x)),\ k \neq 1 \\ \text{subject to } & g_n(x) \leq 0, \quad n = 1, 2, \ldots, N \\ & h_{n'}(x) = 0, \quad n' = 1, 2, \ldots, N' \end{aligned} \tag{4}$$

Equation 4 defines $\underline{\varepsilon_k} = f_k(\underline{s_k}), k \neq 1$. The maximum values of every objective f_k among the solutions $\underline{s_k}$ provide the upper bounds for ε-parameters.

Next, the intervals $[\underline{\varepsilon_k}, \overline{\varepsilon_k}]$ are subdivided into $|E_k|$ sub-intervals, and model $SO_e(X)$ is solved for each of the limits of these sub-intervals, generating a different Pareto solution in each run. The detailed explanation of the algorithm can be found in [69]. Application of this method to other problems can be found in 7.1, 7.3, 7.4.

2.3.2 Objective reduction in MOO problems

The complexity of MOO increases drastically with the number of objectives considered in the problem from the viewpoints of generation and analysis of the Pareto solutions. [70]. One possible manner to overcome these difficulties is to eliminate redundant or non-essential objectives from the analysis. This simplifies the calculations while at the same time preserving the dominance structure of the problem. The concept of redundant objectives, and a measure for quantifying changes in the original dominance structure of a problem taking place after removing them are presented in 7.3, Section 4.2 and 7.4 Section 5.2.

2.3.3 Objective reduction methods

Dimensionality reduction methods are widely used in many areas like statistics and data mining. Unfortunately, these techniques are not directly applicable to MOO. Deb and Saxena [71] proposed a method based on Principal Component Analysis (PCA) for decreasing the number of objectives in MOO. Their approach identifies redundant objectives from the analysis of the eigenvectors of the correlation matrix.

Brockhoff-Zitzler [72, 73] proposed an alternative approach for reducing the number of objectives that aims at preserving the initial dominance structure. The main idea is to replace the

original set of objectives by a reduced set that is not conflicting with the original one. An approximation error was defined by the authors to quantify the extent to which the dominance structure of the problem changes when omitting objectives. They defined two different problems: computing the minimum subset of objectives with a given delta value (i.e., approximation error) and determining the minimum error for an objective subset of given size. Two algorithms, a greedy and an exact one, were proposed to solve the aforementioned problems. Based on similar ideas, Guillén-Gosálbez [1] developed a MILP-based objective reduction method to tackle these problems. The details of these strategies are presented in 7.3, Section 4.2 and 7.4, Section 5.2.

2.4 Bi-level optimization (KKT reformulation)

Bi-level optimization is a special kind of optimization where one problem is embedded (nested) within another. The outer optimization task is commonly referred to as the upper-level optimization task, and the inner optimization task is commonly referred to as the lower-level optimization task. These problems involve two kinds of variables, referred to as the upper-level variables and the lower-level variables. There are several methods to handle such type of problems. One way is to optimize every level step by step considering the results obtained in previous levels as a constraint for the current level [60].

Another solution methods consists of reformulating the bi-level problem as a single-level optimization problem via the Karush–Kuhn–Tucker (KKT) conditions [74]. For example, consider the following two nested single objective optimization problems $SO1(Y)$ and $SO2(X)$, where $SO2(X)$ is the special condition to $SO1(Y)$.

$$
\begin{aligned}
&SO1(Y) = \min(f_1(y)) \\
&\quad \text{s. t.} \\
&\qquad SO2(X) = \min(f_2(x)) \\
&\qquad \text{s. t.} \\
&\qquad g_n(x) \leq 0, \quad n = 1, 2, \ldots, N \\
&\qquad h_{n'}(x) = 0, \quad n' = 1, 2, \ldots, N'
\end{aligned} \tag{5}
$$

Where $f1(y)$ and $f2(x)$ are the objective functions, N is the number of inequality constraints, and N' is the number of equality constraints. X and Y are the search spaces, and x and y are vectors of decision variables. Problem $SO1(Y)$ is called outer problem, while $SO2(X)$ is the inner problem. In order to make this bi-level optimization problem computationally tractable, we reformulate it as a single-level optimization problem via the Karush Kuhn Tucker (KKT) conditions. The idea is to substitute the inner problems by their KKT conditions and solve the outer problem subject to the KKT conditions of the inner models. The reformulated problem takes the following form:

$$
\begin{aligned}
&SO1(Y) = \min(f_1(y)) \\
&\quad \text{s. t.} \\
&\qquad \bigtriangledown f_2(x) + \sum_{j=1}^{N'} \lambda_{n'} \bigtriangledown h_{n'}(x) + \sum_{j=1}^{N} \mu_n \bigtriangledown g_n(x) = 0 \\
&\qquad g_n(x) \leq 0, \quad n = 1, 2, \ldots, N \\
&\qquad h_{n'}(x) = 0, \quad n' = 1, 2, \ldots, N' \\
&\qquad \mu_n g_n(x) = 0, \quad n = 1, 2, \ldots, N \\
&\qquad \mu_n \geq 0, \quad n = 1, 2, \ldots, N
\end{aligned} \tag{6}
$$

Where $\lambda_{n'}$ and μ_n are the Lagrangean multipliers associated with the equality and inequality

constraints, respectively. Thus, the single level optimization problem seeks to minimize $f1(y)$ subject to the solution being in turn minimum in $f2(x)$. Further details of this method are described in 7.5, Materials and Methods Section.

2.5 Environmental assessment methods

In this thesis, the assessment of the environmental damage caused to lands receiving sewage sludge was performed using the "Suitabity Index" (SUI) proposed by [7]. The SUI quantifies the ability of land to receive the sewage sludge. Its value ranges between 0 (worst) and 1 (best). The SUI assesses the potential impacts or alterations in the environmental matrices (soil, food and water quality) and in human health. The SUI is determined from two main indexes: human exposure and environmental criteria. Human exposure quantifies the likelihood of causing damage to human health, and considers "distance to urban areas", and "crop type" as main criteria. The environmental criteria index measurea the likelihood of contaminating soils, surface water and groundwater, when soils are amended with SS. The aggregation tree of the selected criteria is depicted in Figure 8. Further details of this method can be found in [7] and 7.1, Section 3.2.2.

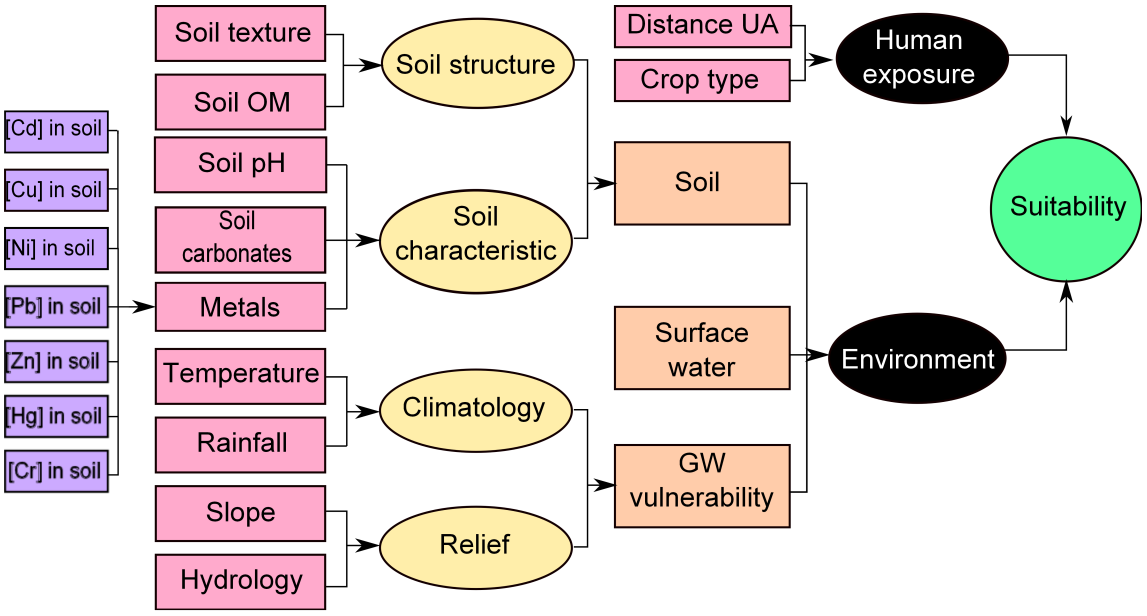

Figure 8: Schematic representation of the model implementation.

The assessment of the environmental performance of heat exchanger networks (HEN) and utility plants was conducted using life cycle assessment (LCA) principles. LCA is a methodology

for evaluating the environmental loads associated with a product, process or activity over its entire life cycle. Details on the application of LCA to our problems can be found in 7.3, Section 3.2. LCA calculations are performed following a four step procedure:

1. Goal and scope definition. This phase defines the goal of the study, system boundaries, allocation methods, and impact categories. We perform a "cradle-to-gate" analysis that embraces all the activities associated with the construction and operation of the systems. Ten impact categories, as defined by the Eco-indicator 99, are considered in our work:

   1. Carcinogenic effects on humans.
   2. Respiratory effects on humans caused by organic substances.
   3. Damage to human health caused by climate change.
   4. Human health effects caused by ionizing radiations.
   5. Human health effects caused by ozone layer depletion.
   6. Damage to ecosystem quality caused by ecosystem toxic emissions.
   7. Damage to ecosystem quality caused by the combined effect of acidification and eutrophication.
   8. Damage to ecosystem quality caused by land occupation and land conversion.
   9. Damage to resources caused by extraction of minerals.
   10. Damage to resources caused by extraction of fossil fuels.

2. Inventory analysis. The second stage determines the most relevant inputs and outputs flows of materials and energy associated with the main process. This information will be further translated into environmental impacts. For the HEN example, the environmental burdens are given by the production of the amount of stainless steel contained in the heat exchangers and the generation of cold and hot utilities. The life cycle inventory (LCI) of inputs and outputs is determined from the mass of stainless steel (continuous variable mass), and the amount of cold (continuous variable qcu) and hot utilities (continuous variable qhu) consumed as follows:

$$LCI_b = \sum_j qhu_j \, \omega_b^{HU} + \sum_i qcu_i \, \omega_b^{CU} + mass \, \omega_b^{M} \tag{7}$$

In this equation, ω_b^{HU}, ω_b^{CU}, ω_b^{M} denote the life cycle inventory entries (i.e., emissions released to the environment or resources taken from the ecosphere) associated with chemical b per reference flow of activity (i.e., mass of steam, cooling water and steel generated). These parameters are retrieved from environmental databases Ecoinvent 2.2.

3. Impact assessment. This stage quantifies the impact in a set of damage assessment categories. Following the ECO99 methodology, the damages in each impact category c (denoted by IM_c) are evaluated as follows:

$$IM_c = \sum_b LCI_b \, \theta_{bc} \tag{8}$$

Where θ_{bc} is a damage factor that translates the results of the inventory phase into a set of damages.

4. Interpretation. Here, the results of the LCA are analyzed and a set of conclusions and recommendations for the system are formulated. In our work, the preferences are articulated in the post optimal analysis of the Pareto optimal solutions.

The details of this method can be found at 7.3, Section 3.2 and 7.4, Section 3.5.2.

3 Results

A brief summary of the results obtained is next provided. Further details can be found in the original publications attached to this document in 7.1, 7.2, 7.3, 7.4, 7.5 Chapters.

3.1 Combined use of GIS and MILP for sustainable design of sewage sludge amendment

We developed a multi-objective optimization model that combines GIS and mixed-integer linear programming for identifying optimal agricultural areas for sewage sludge amendment. The MILP model was tested through its application to a real case study based on Catalonia. The MILP included two objective functions: total annual cost and index of suitability (see 2.5).

We obtained a set of Pareto solutions using the epsilon-constraint method (see 2.3 of this Thesis). Every solution represents a different distribution alternative of SS coming from the waste water plants and distributed among the set of agricultural fields (i.e., a different transportation plan, as shown in Figure 7 at 7.1 and explained in Section 4 of 7.1). The results show that significant environmental improvements can be attained at a marginal increase in cost, as observed in Figure 6 in Section 4 of the paper in 7.1. One of the main advantages of our approach is that it produces solutions that reflect precisely the default preferences of the decision-makers involved in the problem. Furthermore, it relies on a rigorous and systematic mathematical approach that avoids falling in sub-optimal solutions, something that might happen when applying heuristics or rules of thumb (Section 4 of the paper at 7.1).

The model led to a copmlext MILP. As an illustrative example, for a GIS map with 13 984 pixels, we define an MILP containing 69,920 continuous variables, 125,860 binary variables, and 153,832 equations (see 7.2, Section 4). The model size is hence quite sensitive to the number of pixels, which grows rapidly as we increase the map resolution. Therefore in the next work, we devised a decomposition strategy for this special class of mixed-integer linear programming (MILP) models. The bilevel decomposition algorithm used to solve such a complex MILP is summarized in Figure 2, 7.2. Numerical results show that our approach achieves reductions of orders of magnitude in CPU time (as compared to the full space GIS-based MILP) while still yielding near optimal solutions (Tables 1, 2 and 3, at Chapter 7.2). Our approach allows for the

solution of complex and realistic problems that might be found in practice.

3.2 Sustainable design of heat exchanger networks

We proposed a multi objective optimization model for the sustainable design of heat exchanger networks (HEN) considering simultaneously economic and environmental concerns. The design task is posed in mathematical terms as a multi-objective mixed integer non-linear programming (MINLP) problem, in which life cycle assessment (LCA) principles are used to quantify the environmental performance.

The capabilities of our approach are tested through two examples. We clearly illustrate how the use of a single overall aggregated environmental metric is inadequate in the design of HENs, since it may leave some solutions that are appealing for decision-makers out of the analysis (see Figure 5, Figure 11 and Section 5 at 7.3). We find that some individual LCA metrics are conflicting and can be aggregated into three main groups according to their behavior. The analysis of the pair cost vs. overall an aggregated environmental metric (i.e., Eco-indicator 99) does not preserve the whole dominance structure of the problem (Figures 6, 7, 8 and Figures 12, 13, 14 in 7.3).

To simplify the visualization and analysis of the Pareto solution, we investigated the use of a rigorous dimensionality reduction method in the post-optimal analysis of the trade-off designs. This technique enables the identification of redundant objectives that can be eliminated while still keeping the problem structure to the extent possible. The results show that there are several redundant environmental objectives that can be eliminated. The combination of total cost and extraction of minerals preserves the initial structure to the maximum extent possible. (see Figure 14, Figure 8 and Section 5 at 7.3).

3.3 Sustainable design of utility plant

A systematic method based on mathematical programming was introduced to tackle the design of an utility plant with economic and environmental concerns. The design task was formulated as a bi-criteria MILP problem. We employ for the analysis several environmental impacts which were calculated according to the LCA methodology.

The capabilities of the proposed method are illustrated through two cases studies. We ob-

tained a set of Pareto alternatives using the epsilon-constraint method, and identified operating regions where significant environmental improvements can be attained at a marginal increase in cost (see Figure 8 and Subsection 6.1 in 7.4). To facilitate the calculations, we employ an MILP-based dimensionality reduction approach that allows identifying key environmental metrics that exhibit the property that their optimization automatically results in the improvement of the system in all the remaining damage categories.

Numerical results show that in the first example all the environmental impacts behave similarly, while the cost is conflictive with them. Hence, the original multi-objective problem can be replaced by a bi-criteria one (cost against any environmental impact) without significant changes in the problem structure (see Figure 7, Table 7 and Section 6.1 in 7.4). In the second example, there is a conflict between environmental metrics (see Figure 11 in 7.4). Comparing with the previous case, we notice that some solutions would be lost when optimizing in the space of cost and Eco-indicator 99 are unique objectives (see Figure 12 at 7.4. The rigorous dimensionality reduction method shows that the problem structure can be kept by optimizing three objectives: cost, respiratory effects (inorganic) and climate change, which simplifies the overall procedure (see Table 9 at 7.4).

3.4 Identifying design principles in metabolic networks

We developed an MINLP method based on bi-level optimization for identifying in a rigorous and systematic manner the most probable biological objective functions driving the cell's metabolic machinery. To solve the bi-level problem efficiently, we reformulate it into a standard mixed-integer nonlinear program (MINLP) by replacing the inner problems by their Karush Kuhn Tucker conditions [75].

We benchmark the method by analyzing which combination of objective functions better explains a set of metabolic fluxes experimentally determined *invivo*. Our analysis confirms that biomass maximization is a fundamental objective function under the experimental conditions of the benchmark (see Figure 3, 4 and 5, Results and Discussion Section in 7.5). In addition, our optimization method identifies additional sets of functional criteria that, taken together with the optimization of the growth rate, improve the model fitting to the experimental data. The fitting of FBA models to the experimental data improves with the number of objectives considered in

the analysis, firstly sharply and then marginally after a certain number of criteria (Figures 3 and 4, Results and Discussion Section at 7.5).

We show also that there are several groups of objectives that behave similarly, which suggests the existence of redundant biological criteria (see Table 1, Results and Discussion, 7.5). Our tool can identify meaningful objective functions under various experiments simultaneously (Figures 6 and 7, Results and Discussion, 7.5).

4 Conclusions

In this thesis, we draw the following conclusions:

- The combined use of GIS and mathematical programming provides a comprehensive framework to address the sustainable distribution of SS on agricultural areas.
- The sets of solutions obtained using the GIS-based MILP approach are guaranteed to be optimal and reflect precisely the default preferences of the decision-makers (Section 5 at 7.1).
- It is possible to improve the environmental performance of SS allocation by compromising the associated cost (Figure 7 at 7.1).
- The bi-level decomposition method for GIS-based MILPs provides near optimal solutions in a fraction of the CPU time required by the full space model (Tables 1, 2 and 3, 7.2).
- The systematic spatial decision-making tool based on the combined use of GIS, MILP and, if necessary, coupled with the bi-level decomposition technique is general enough to be applied to various regions, especially in the European Mediterranean area.
- The MINLP model for the sustainable design of HENs, which incorporates several environmental LCA metrics, identifies design alternatives leading to significant environmental improvements.
- The MILP model of the utility plant (UP) that includes several LCA environmental metrics is an efficient approach for the sustainable design of energy production systems.
- The use of an aggregated indicator (i.e., Eco-indicator 99) is inadequate in the design of HENs (see Figure 5, Figure 11 and Section 5 in 7.3) and UP (see Figure 12 at 7.4), since it leaves solutions that may be appealing for decision makers out of the analysis.
- The use of dimensionality reduction techniques in the design of HENs and UPs shows that some environmental objectives might be redundant and can be therefore left out of the analysis without modifying significantly the problem structure (see Figure 14, Figure 8 and Section 5 at 7.3) and Table 9 , Section 6.2 at 7.4).

- Our approach can be applied to various types of energy systems (e.g., solar, wind, etc.) in order to facilitate decision-making with environmental impact considerations.
- Our approach based on bi-level optimization coupled with mixed-integer nonlinear programming (MINLP) identifies, in a rigorous and systematic manner, the most likely objective functions for a given set of experimental conditions.
- We find that biomass maximization is a fundamental objective function in cell metabolism. Numerical results show also that the inclusion of additional sets of functional criteria, along with growth rate maximization, improve the model fitting to experimental data (see Figure 3, 4 and 5, Results and Discussion Section in 7.5).

5 Future work

A set of potential research lines related to the material presented in this thesis is presented below:

- Introduce uncertainty in the models using stochastic programming techniques. This will increases their robustness and produce more realistic results.
- Apply GIS-based multi-objective optimization to other spatial decision-making problems, like the optimal allocation of crops in Spain, in order to reduce the amount of water used for irrigation (i.e., water blue).
- Apply dimensionality reduction to other environmental problems, like the design of compressors.
- Despite recent advances in the design of heat exchanger networks, we cannot guarantee that the solutions found with the MINLP model are globally optimal. Hence, we will explore the use of global optimization algorithms that will guarantee convergence to the global optimum of the problem.
- In systems biology, we are planning to apply our MINLP-based bi-level optimization approach to identify meaningful biological objective functions in other kinetic metabolic models.

6 Nomenclature

Abbreviations

AML	algebraic modeling language
EI99	eco-indicator 99
GAMS	general algebraic modeling system
FBA	flux balance analysis
HEN	heat exchanger network
IDE	integrated development environment
KKT	Karush–Kuhn–Tucker
LCA	life cycle assessment
LP	linear programming
NLP	nonlinear programming
MILP	mixed-integer linear programming
MINLP	mixed-integer nonlinear programming
SS	sewage sludge
WWTP	waste water treatment plant

Indices

e	epsilon iterations
k	objectives
n	inequality constraints
n’	equality constraints

Sets

F	set of objectives
g	set of inequality constraints
h	set of equality constraints

Parameters

N	number of inequality constraints
N’	number of equality constraints
O	number of objectives

References

[1] G. Guillén-Gosálbez, A novel milp-based objective reduction method for multi-objective optimization: Application to environmental problems, Computers & Chemical Engineering 35 (8) (2011) 1469–1477.

[2] M. Nadal, V. Kumar, M. Schuhmacher, J. L. Domingo, Definition and GIS-based characterization of an integral risk index applied to a chemical/petrochemical area, Chemosphere 64 (9) (2006) 1526–1535.

[3] L. Poggio, B. Vrščaj, A GIS-based human health risk assessment for urban green space planning—an example from grugliasco (italy), Science of the total environment 407 (23) (2009) 5961–5970.

[4] C. A. Schriever, M. Liess, Mapping ecological risk of agricultural pesticide runoff, Science of the Total Environment 384 (1) (2007) 264–279.

[5] M. S. Johnson, M. Korcz, K. von Stackelberg, B. K. Hope, Spatial analytical techniques for risk based decision support systems, in: Decision Support Systems for Risk-Based Management of Contaminated Sites, Springer, 2009, 1–19.

[6] J. Malczewski, GIS-based land-use suitability analysis: a critical overview, Progress in planning 62 (1) (2004) 3–65.

[7] A. Passuello, O. Cadiach, Y. Perez, M. Schuhmacher, A spatial multicriteria decision making tool to define the best agricultural areas for sewage sludge amendment, Environment international 38 (1) (2012) 1–9.

[8] J. Malczewski, GIS-based multicriteria decision analysis: a survey of the literature, International Journal of Geographical Information Science 20 (7) (2006) 703–726.

[9] R. Grabaum, B. C. Meyer, Multicriteria optimization of landscapes using GIS-based functional assessments, Landscape and Urban Planning 43 (1) (1998) 21–34.

[10] X. Wang, S. Yu, G. Huang, Land allocation based on integrated GIS-optimization modeling at a watershed level, Landscape and Urban Planning 66 (2) (2004) 61–74.

[11] S. M. S. Mapa, R. d. S. Lima, J. F. Mendes, Combining geographica information systemas (GIS) and mathematical modeling to location-allocation problems in education facilities management, CUPUM 2007, (2007)

[12] H. Jung, K. Lee, W. Chun, Integration of GIS, GPS, and optimization technologies for the effective control of parcel delivery service, Computers & Industrial Engineering 51 (1) (2006) 154–162.

[13] E. C. Marcoulaki, I. A. Papazoglou, N. Pixopoulou, Integrated framework for the design of pipeline systems using stochastic optimisation and GIS tools, Chemical Engineering Research and Design 90 (12) (2012) 2209–2222.

[14] M. van den Broek, E. Brederode, A. Ramírez, L. Kramers, M. van der Kuip, T. Wildenborg, W. Turkenburg, A. Faaij, Designing a cost-effective co2 storage infrastructure using a GIS based linear optimization energy model, Environmental Modelling & Software 25 (12) (2010) 1754–1768.

[15] A. Passuello, M. Schuhmacher, M. Mari, O. Cadiach, M. Nadal, A spatial multicriteria decision analysis to manage sewage sludge application on agricultural soils, Environmental Modeling for Sustainable Regional Development: System Approaches and Advanced Methods 221 (2010) 54–68.

[16] J. Cano-Ruiz, G. McRae, Environmentally conscious chemical process design, Annual Review of Energy and the Environment 23 (1) (1998) 499–536.

[17] C.-T. Chang, J.-R. Hwang, A multiobjective programming approach to waste minimization in the utility systems of chemical processes, Chemical Engineering Science 51 (16) (1996) 3951–3965.

[18] A. K. Hilaly, S. K. Sikdar, Pollution balance method and the demonstration of its application to minimizing waste in a biochemical process, Industrial & engineering chemistry research 34 (6) (1995) 2051–2059.

[19] I. E Grossmann, R. Drabbant, R. K. Jain, Incorporating toxicology in the synthesis of industrial chemical complexes, Chemical Engineering Communications 17 (1-6) (1982) 151–170.

[20] H. Cabezas, J. C. Bare, S. K. Mallick, Pollution prevention with chemical process simulators: the generalized waste reduction (war) algorithm, Computers & chemical engineering 21 (1997) S305–S310.

[21] J. B. Guinée, Handbook on life cycle assessment operational guide to the iso standards, The international journal of life cycle assessment 7 (5) (2002) 311–313.

[22] S. Stefanis, A. Buxton, A. Livingston, E. Pistikopoulos, A methodology for environmental impact minimization: Solvent design and reaction path synthesis issues, Computers & chemical engineering 20 (1996) S1419–S1424.

[23] S. Stefanis, A. Livingston, E. Pistikopoulos, Minimizing the environmental impact of process plants: a process systems methodology, Computers & chemical engineering 19 (1995) 39–44.

[24] A. Azapagic, R. Clift, Application of life cycle assessment to process optimization, Computers & Chemical Engineering 23 (10) (1999) 1509–1526.

[25] G. Guillen-Gosalbez, J. A. Caballero, L. Jimenez, Application of life cycle assessment to the structural optimization of process flowsheets, Industrial & Engineering Chemistry Research 47 (3) (2008) 777–789.

[26] R. Brunet, D. Cortés, G. Guillén-Gosálbez, L. Jiménez, D. Boer, Minimization of the lca impact of thermodynamic cycles using a combined simulation-optimization approach, Applied Thermal Engineering 48 (2012) 367–377.

[27] A. Hugo, E. Pistikopoulos, Environmentally conscious long-range planning and design of supply chain networks, Journal of Cleaner Production 13 (15) (2005) 1471–1491.

[28] G. Guillén-Gosálbez, I. E. Grossmann, Optimal design and planning of sustainable chemical supply chains under uncertainty, AIChE Journal 55 (1) (2009) 99–121.

[29] G. Guillén-Gosálbez, I. Grossmann, A global optimization strategy for the environmentally conscious design of chemical supply chains under uncertainty in the damage assessment model, Computers & chemical engineering 34 (1) (2010) 42–58.

[30] L. Puigjaner, G. Guillén-Gosálbez, Towards an integrated framework for supply chain management in the batch chemical process industry, Computers & Chemical Engineering 32 (4-5) (2008) 650–670.

[31] P. Vaskan, G. Guillén-Gosálbez, L. Jiménez, Multi-objective design of heat-exchanger networks considering several life cycle impacts using a rigorous milp-based dimensionality reduction technique, Applied Energy 98 (2012) 149–161.

[32] R. Salcedo, E. Antipova, D. Boer, L. Jiménez, G. Guillén-Gosálbez, Multi-objective optimization of solar rankine cycles coupled with reverse osmosis desalination considering economic and life cycle environmental concerns, Desalination 286 (2012) 358–371.

[33] G. Guillén-Gosálbez, F. D. Mele, I. E. Grossmann, A bi-criterion optimization approach for the design and planning of hydrogen supply chains for vehicle use, AIChE Journal 56 (3) (2010) 650–667.

[34] N. Sabio, A. Kostin, G. Guillén-Gosálbez, L. Jiménez, Holistic minimization of the life cycle environmental impact of hydrogen infrastructures using multi-objective optimization and principal component analysis, International Journal of Hydrogen Energy 37 (6) (2012) 5385–5405.

[35] K. C. Furman, N. V. Sahinidis, A critical review and annotated bibliography for heat exchanger network synthesis in the 20th century, Industrial & Engineering Chemistry Research 41 (10) (2002) 2335–2370.

[36] B. Linnhoff, S. Ahmad, Cost optimum heat exchanger networks—1. minimum energy and capital using simple models for capital cost, Computers & Chemical Engineering 14 (7) (1990) 729–750.

[37] S. Ahmad, B. Linnhoff, R. Smith, Cost optimum heat exchanger networks—2. targets and design for detailed capital cost models, Computers & Chemical Engineering 14 (7) (1990) 751–767.

[38] B. Linnhoff, E. Hindmarsh, The pinch design method for heat exchanger networks, Chemical Engineering Science 38 (5) (1983) 745–763.

[39] K. Trivedi, B. O'Neill, J. Roach, Synthesis of heat exchanger networks featuring multiple pinch points, Computers & chemical engineering 13 (3) (1989) 291–294.

[40] K. Trivedi, B. O'Neill, J. Roach, R. Wood, A new dual-temperature design method for the synthesis of heat exchanger networks, Computers & chemical engineering 13 (6) (1989) 667–685.

[41] J. Cerda, A. W. Westerberg, D. Mason, B. Linnhoff, Minimum utility usage in heat exchanger network synthesis a transportation problem, Chemical Engineering Science 38 (3) (1983) 373–387.

[42] S. A. Papoulias, I. E. Grossmann, A structural optimization approach in process synthesis—ii: Heat recovery networks, Computers & Chemical Engineering 7 (6) (1983) 707–721.

[43] C. A. Floudas, A. R. Ciric, I. E. Grossmann, Automatic synthesis of optimum heat exchanger network configurations, AIChE Journal 32 (2) (1986) 276–290.

[44] X. Yuan, L. Pibouleau, S. Domenech, Experiments in process synthesis via mixed-integer programming, Chemical Engineering and Processing: Process Intensification 25 (2) (1989) 99–116.

[45] T. F. Yee, I. E. Grossmann, Simultaneous optimization models for heat integration—ii. heat exchanger network synthesis, Computers & Chemical Engineering 14 (10) (1990) 1165–1184.

[46] A. Eliceche, S. Corvalan, P. Martinez, Environmental life cycle impact as a tool for process optimisation of a utility plant, Computers & chemical engineering 31 (5-6) (2007) 648–656.

[47] C. Chou, Y. Shih, A thermodynamic approach to the design and synthesis of plant utility systems, Industrial & engineering chemistry research 26 (6) (1987) 1100–1108.

[48] M. Nishio, J. Itoh, K. Shiroko, T. Umeda, A thermodynamic approach to steam-power system design, Industrial & Engineering Chemistry Process Design and Development 19 (2) (1980) 306–312.

[49] J. Bruno, F. Fernandez, F. Castells, I. Grossmann, A rigorous minlp model for the optimal synthesis and operation of utility plants, Chemical Engineering Research and Design 76 (3) (1998) 246–258.

[50] M. Nishio, A. Johnson, Strategy for energy system expansion, Chemical Engineering Progress (1977) 73–79.

[51] T. Petroulas, G. Reklaitis, Computer-aided synthesis and design of plant utility systems, AIChE journal 30 (1) (1984) 69–78.

[52] C. Hui, Y. Natori, An industrial application using mixed-integer programming technique: A multi-period utility system model, Computers & chemical engineering 20 (1996) S1577–S1582.

[53] R. Iyer, I. Grossmann, Optimal multiperiod operational planning for utility systems, Computers & chemical engineering 21 (8) (1997) 787–800.

[54] S. Micheletto, M. Carvalho, J. Pinto, Operational optimization of the utility system of an oil refinery, Computers & Chemical Engineering 32 (1-2) (2008) 170–185.

[55] M. A. Savageau, R. Rosen, Biochemical systems analysis: a study of function and design in molecular biology, Vol. 725, Addison-Wesley Reading, MA, 1976.

[56] J. S. Edwards, R. U. Ibarra, B. O. Palsson, In silico predictions of escherichia coli metabolic capabilities are consistent with experimental data, Nature biotechnology 19 (2) (2001) 125–130.

[57] M. T. Borisuk, J. J. Tyson, Bifurcation analysis of a model of mitotic control in frog eggs, Journal of theoretical biology 195 (1) (1998) 69–85.

[58] K. C. Chen, A. Csikasz-Nagy, B. Gyorffy, J. Val, B. Novak, J. J. Tyson, Kinetic analysis of a molecular model of the budding yeast cell cycle, Molecular biology of the cell 11 (1) (2000) 369–391.

[59] A. M. Feist, B. O. Palsson, The biomass objective function, Current opinion in microbiology 13 (3) (2010) 344–349.

[60] A. P. Burgard, C. D. Maranas, Optimization-based framework for inferring and testing hypothesized metabolic objective functions, Biotechnology and bioengineering 82 (6) (2003) 670–677.

[61] E. P. Gianchandani, M. A. Oberhardt, A. P. Burgard, C. D. Maranas, J. A. Papin, Predicting biological system objectives de novo from internal state measurements, BMC bioinformatics 9 (1) (2008) 43.

[62] A. L. Knorr, R. Jain, R. Srivastava, Bayesian-based selection of metabolic objective functions, Bioinformatics 23 (3) (2007) 351–357.

[63] H. Bachmann, M. Fischlechner, I. Rabbers, N. Barfa, F. B. dos Santos, D. Molenaar, B. Teusink, Availability of public goods shapes the evolution of competing metabolic strategies, Proceedings of the National Academy of Sciences 110 (35) (2013) 14302–14307.

[64] R. Schuetz, N. Zamboni, M. Zampieri, M. Heinemann, U. Sauer, Multidimensional optimality of microbial metabolism, Science 336 (6081) (2012) 601–604.

[65] E. Fischer, N. Zamboni, U. Sauer, High-throughput metabolic flux analysis based on gas chromatography–mass spectrometry derived< sup> 13</sup> C constraints, Analytical biochemistry 325 (2) (2004) 308–316.

[66] R. Schuetz, L. Kuepfer, U. Sauer, Systematic evaluation of objective functions for predicting intracellular fluxes in escherichia coli, Molecular systems biology 3 (1) (2007) 1–15.

[67] H. Teotónio, M. R. Rose, Variation in the reversibility of evolution, Nature 408 (6811) (2000) 463–466.

[68] GAMS, http://www.gams.com/, Accesses in March 2014.

[69] M. Ehrgott, Multicriteria optimization, Vol. 491, Springer Verlag, 2005.

[70] I. Das, A preference ordering among various pareto optimal alternatives, Structural optimization 18 (1) (1999) 30–35.

[71] K. Deb, D. Saxena, On finding pareto-optimal solutions through dimensionality reduction for certain large-dimensional multi-objective optimization problems, Kangal report 2005011 (2005).

[72] D. Brockhoff, E. Zitzler, Are all objectives necessary? on dimensionality reduction in evolutionary multiobjective optimization, Parallel Problem Solving from Nature-PPSN IX (2006) 533–542.

[73] D. Brockhoff, E. Zitzler, Objective reduction in evolutionary multiobjective optimization: Theory and applications, Evolutionary Computation 17 (2) (2009) 135–166.

[74] L. Biegler, I. Grossmann, A. Westerberg, Systematic methods for chemical process design, Prentice Hall, Old Tappan, NJ (United States), 1997.

[75] O. Ben-Ayed, Bilevel linear programming, Computers & operations research 20 (5) (1993) 485–501.

7 Research articles

The results of this research were published in three journal articles and two articles are pending submission. Articles are presented below.

7.1 Combined use of GIS and mixed-integer linear programming for identifying optimal agricultural areas for sewage sludge amendment: A case study of Catalonia.

Vaskan P., Passuello A., Guillén-Gosálbez G., Schuhmacher M., Jiménez L. Combined use of GIS and mixed-integer linear programming for identifying optimal agricultural areas for sewage sludge amendment: A case study of Catalonia. *Environmental Modelling & Software* 48, 163–169, 2013.

Environmental Modelling & Software 46 (2013) 163–169

Contents lists available at SciVerse ScienceDirect

Environmental Modelling & Software

journal homepage: www.elsevier.com/locate/envsoft

Combined use of GIS and mixed-integer linear programming for identifying optimal agricultural areas for sewage sludge amendment: A case study of Catalonia

Pavel Vaskan, Ana Passuello, Gonzalo Guillén-Gosálbez*, Marta Schuhmacher, Laureano Jiménez

Departament d'Enginyeria Quimica, Universitat Rovira i Virgili, Avinguda Països Catalans 26, 43007 Tarragona, Spain

ARTICLE INFO

Article history:
Received 6 March 2012
Received in revised form
7 March 2013
Accepted 10 March 2013
Available online 4 May 2013

Keywords:
GIS
MILP
MCDA
Environmental management
Decision making
Land classification

ABSTRACT

This work proposes a systematic decision-making tool for identifying the best geographical areas for sewage sludge (*SS*) amendment in terms of economic and environmental criteria. Our approach integrates GIS and multi-objective mixed-integer linear programming (MILP) within a unified framework that allows exploring in a rigorous and systematic manner a large number of alternatives for sewage sludge amendment from which the best ones (according to the decision-makers' preferences) are finally identified. The capabilities of our methodology are illustrated through its application to a case study based on Catalonia (NE of Spain). The tool presented provides as output a set of optimal alternatives for sewage sludge distribution, each one achieving a unique combination of economic and environmental performance. Our ultimate goal is to guide decision-makers toward the adoption of more sustainable patterns for sewage sludge amendment.

1. Introduction

Wastewater treatment plants generate several contaminants, such as grit, screenings and sludge (Fytili and Zabaniotou, 2008). The production of sewage sludge (*SS*) has recently increased in several countries due to the population growth, which has posed an important environmental problem. In this general context, there is a strong motivation for developing systematic tools to provide decision-support for the management of sewage sludge, a topic that has recently gained an increasing attention in the research community (Passuello et al., 2010).

Several methods currently exist to dispose the residue of wastewater plants: combustion, wet oxidation, pyrolysis, gasification and co-combustion of sewage sludge with other materials for further use as energy source. In addition, the reuse of *SS* as an agricultural fertilizer has traditionally received increasing interest. This last practice is environmentally appealing, as it recycles organic matter and nutrients to soils (Werle and Wilk, 2010). Unfortunately, the *SS* matrix contains harm emissions, such as heavy metals and persistent organic pollutants (POPs) that can contaminate the soil, crops, groundwater, open waters, and eventually reach the human food chain. The probability of contamination depends on the local characteristics of the field. Spatial decision-making tools for land classification are well suited for this problem, as they allow identifying the best regions for *SS* amendment from information available in spatial databases (Passuello et al., 2012).

One of the most widely applied tools for handling geographic data is the Geographic Information Systems (GIS). GIS have been extensively employed in several environmental fields, such as vulnerability (Kattaa et al., 2010), and human health assessment (Nadal et al., 2006; Poggio and Vrscaj, 2009), as well as ecological exposure, and risk assessment (Johnson et al., 2009; Schriever and Liess, 2007). The concept of Spatial Multicriteria Decision Analysis (SMCA) refers to the combined use of Multicriteria Decision Analysis (MCDA) tools and GIS to solve spatial decision-making problems. MCDA allows the combination of quantitative and qualitative inputs, like risks, costs, benefits, and stakeholders views. This general approach has been applied to a wide variety of environmental management problems, such as agriculture application (Malczewski, 2004) and management of sewage sludge (Passuello et al., 2012).

* Corresponding author.
E-mail addresses: pavel.vaskan@urv.cat (P. Vaskan), ana.passuello@urv.cat (A. Passuello), gonzalo.guillen@urv.cat (G. Guillén-Gosálbez), marta.schuhmacher@urv.cat (M. Schuhmacher), laureano.jimenez@urv.cat (L. Jiménez).

1364-8152/$ – see front matter © 2013 Elsevier Ltd. All rights reserved.
http://dx.doi.org/10.1016/j.envsoft.2013.03.007

The capabilities of GIS can be further enhanced through its integration with optimization tools. Grabaum and Meyer (1998) investigated the use of GIS in the multi-criteria optimization of landscapes. Wang et al. (2004) employed a GIS model to allocate future land uses based on the results of an inexact-fuzzy multi-objective linear programming (IFMOP) model. Ducheyne et al. (2006) combined genetic algorithms and GIS for forest-management optimization. van den Broek et al. (2010) integrated ArcGIS, a geographical information system with spatial and routing functions, with MARKAL, an energy bottom-up model based on linear optimization for designing a cost-effective CO_2 storage infrastructure in the Netherlands.

Despite these recent advances, the literature on the combined use of GIS and optimization techniques is quite scarce. In this work we propose a systematic tool based on mathematical programming and spatial analysis techniques (i.e., GIS) to support decision-making in the management of sewage sludge. To the best of our knowledge, this is the first contribution of this type in the area of *SS* amendment. Given a certain amount of sludge to be treated and a set of available agricultural areas, the goal of the analysis is to identify the optimal agricultural fields for sewage sludge amendment according to some economic and environmental criteria. The capabilities of our tool are illustrated through its application to a case study based on Catalonia (Northeast of Spain). The article is organized as follows. Section 2 describes a case study in Catalonia that is taken as a test bed to illustrate the capabilities of our approach, while Section 3 describes our proposed methodology. The numerical results are presented and discussed in Section 4, while the conclusions of the work are finally drawn in Section 5.

2. Case study

Catalonia is a region in the Northeastern part of Spain that covers an area of 32,114 km^2 (Fig. 1). It extends from the Pyrenees southward along the Mediterranean. The relief of Catalonia (NE of Spain) is characterized by a diverse morphology, being mostly mountainous in the north (Pyrenees) and flat at the center and the coast (see Fig. 1). The region is also characterized by the presence of a littoral mountain system, between the central depression and the coast. In the central and cost areas summer is hot and winter is warm with an annual average temperature of around 17 °C, whereas in the Pyrenees region the annual temperature is around 5 °C.

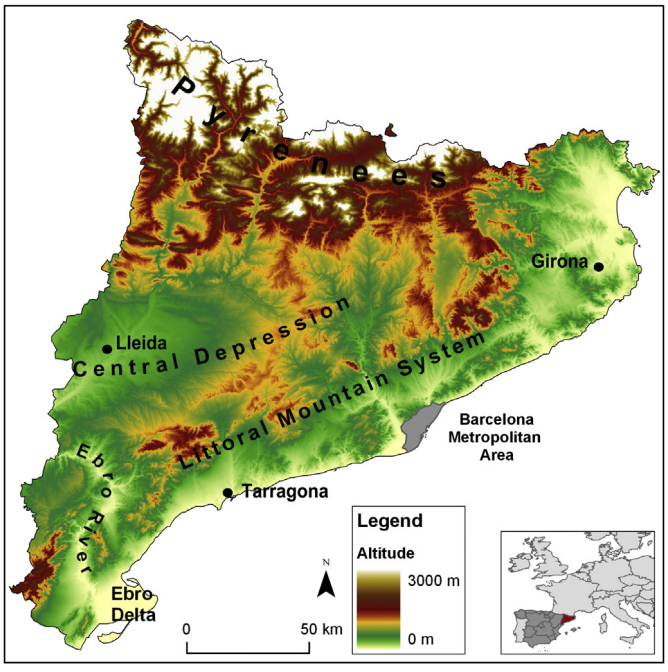

Fig. 1. The map of Catalonia.

The precipitation levels vary along the territory. The northern and mountainous regions show the higher mean precipitation levels (between 700 and 1250 mm year^{-1}), while the southern and the coastal regions are characterized by lower rainfall levels (between 450 and 700 mm year^{-1}). The main basin of Catalonia is the Ebro catchment. Catalonia has a diversity of soil types, mostly calcareous sediments mixed with alluvium and clay. Catalonia's agriculture was centered on the production of wine, wheat, rice, barley, olive, grapes, fruits, nuts and vegetables. The agricultural area currently available has more than 1 million ha. The largest area is located in the central depression zone and the delta of the Ebro river. More than 85% of this area is covered by fruit and cereal fields (IDESCAT, 2009).

The official population of Catalonia is 7,354,411. It is administratively divided in four provinces: Barcelona, Tarragona, Girona, and Lleida, with a population of 5,416,447; 788,895; 731,864; and 426,872 people, respectively. Sewage sludge amendment is a common practice in Catalonia. Reported data for 2007 showed that 140,000 tons of dry weight (dw) sludge were produced in Catalonia, 83% of which (114,000 tons dw) were applied on agricultural soils (ACA, 2008).

Deciding the best agricultural soils for *SS* amendment is not a trivial task. Several environmental aspects, such as groundwater contamination by nitrates, open waters and soil protection, as well as human exposure to the contaminants present in the sludge matrix must be considered along with economic aspects, making this task quite challenging. This is because the management of this residue concerns different stakeholders, with different views of the problem and conflicting interests. In addition, they may find that their interests are not reached, fact that leads to a low acceptance of the practice. Fig. 2 briefly describes the objectives of each stakeholder.

The environment agency is interested on managing the increased amount of residues produced, considering that safe levels are maintained for humans and as well as for the environment. In this regard, the agency is concerned not only in having low contamination levels on food but also in protecting soil and water bodies from contamination, while at the same time keeping the overall economic expenditures below an affordable level. To cut down the management costs, external private companies are hired. These companies shall transport the sewage sludge (*SS*) from the wastewater treatment plants (WWTP) to the agricultural fields, and apply the *SS* to the fields in appropriate levels. These companies aim to make the maximum profit.

For the farmer, the amendment of soils with *SS* may represent a profitable practice, as the land is fertilized with no extra costs. In this regard, the farmer does not pay for fertilizers, or transport and application costs, as the last two are covered by the hired company. In this context, there is a strong concern about food quality, as farmers must fulfill specific quality requirements determined by the industry to prevent a reduction on their market share. Furthermore, farmers should be aware about the risks related to the practice. Soil quality has a strong connection with food quality and must be thus carefully preserved.

Reaching a final solution satisfying all the decision-makers involved is indeed very challenging. Systematic tools based on multi-objective mathematical programming are well suited to tackle this type of problems, as they allow screening in a rigorous and systematic manner a large number of alternatives from which the best ones are identified. The final goal is to calculate a set of

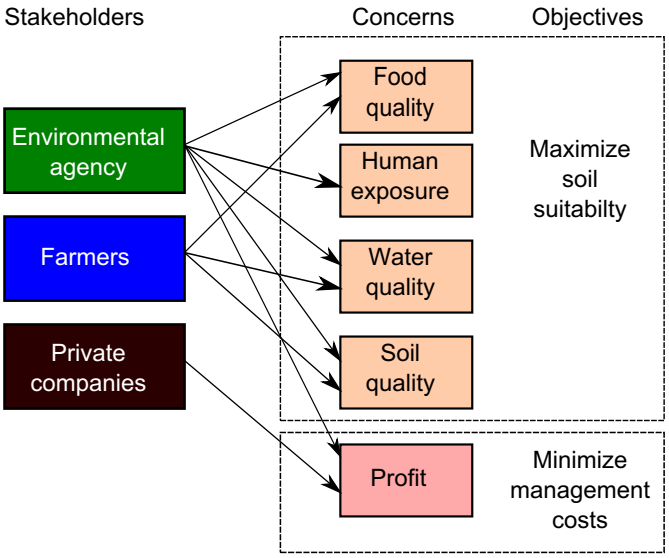

Fig. 2. Relationship between the stakeholders and objectives.

Pareto optimal alternatives, that is, a set of solutions with the property that it is impossible to improve them in one of the objectives without necessarily worsening at least another criterion. Fig. 3 illustrates the concept of Pareto optimality for a simple case with two objectives (cost and suitability). Points lying below the curve are sub-optimal, since they can be improved in both criteria simultaneously. The region above the curve is infeasible, since no alternative shows better profit and suitability simultaneously than the Pareto solutions. The final goal is to select a solution on the curves. Examples of other multi-objective optimization approaches applied to environmental multicriterial problems can be found elsewhere (Fu et al., 2008; Kollat and Reed, 2007; Bourmistrova et al., 2005). In the sections that follow, we introduce a systematic tool based on these principles that provides decision-support for *SS* amendment.

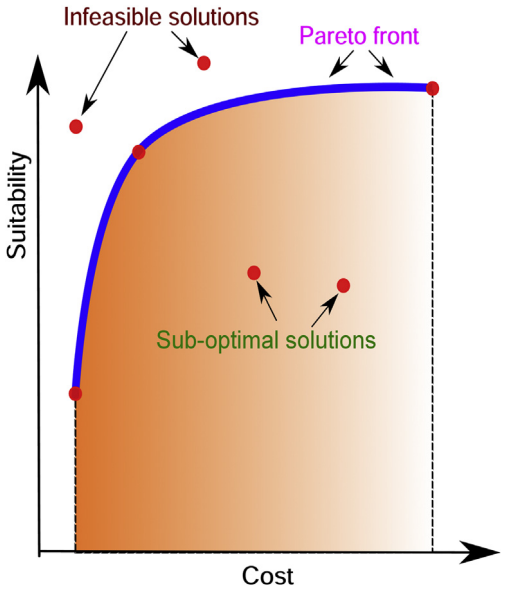

Fig. 3. Description of Pareto front.

3. Proposed approach: mixed-integer linear programming model

In this section, we first formally state the problem of interest, and then present a mathematical formulation that provides as output the optimal distribution of *SS*.

3.1. Problem statement

SS amendment on agricultural soils is an activity that affects several groups of interests, such as farmers, environmental agencies, the general population, and wastewater treatment plants (WWTPs), among others. Each of these groups of stakeholders presents different concerns. For example, WWTPs are interested in cheap procedures of disposal. The environmental agencies want to keep good environmental levels on the different matrices (soil, open waters, groundwater), while the general population expects not to be exposed to contamination as well as to the bad odors caused by the amendment. In order to respect all the stakeholders' concerns, two groups of criteria were defined: suitability (that comprises environmental and human exposure factors) and total cost.

We consider a region of interest (i.e., the whole area of Catalonia) that is subdivided into a certain number of fields (12,536 in our case). Each of these fields is defined by a set of coordinates in meters (x,y), an index of suitability, an acceptable capacity in tons per year of sludge, and an application cost (in euro ton^{-1} year^{-1}). We are also given a set of WWTPs (waste water treatment plants). In this study, and without loss of generality, we have considered the capitals of each provinces of Catalonia as the main producer in each province (i.e., Barcelona, Tarragona, Girona, and Lleida). Each of these cities is characterized by a pair of coordinates and total production of *SS* per year. The goal of the analysis is to determine the optimal distribution of *SS* production among the Catalonian agricultural areas that simultaneously optimizes the overall suitability and the total cost.

3.2. Mixed-integer linear programming (MILP) formulation

A MILP model is constructed for the efficient solution of the problem stated above. The formulation is derived based on the superstructure shown in Fig. 4. We consider a set I, WWTPs that generate *SS*, and a set J of agricultural areas that receive *SS*. Given a certain amount of *SS* generated in the plants, the MILP seeks to determine the optimal flows to be established between the plants and agricultural fields. The model comprises two main sets of equations: capacity constraints and objective function equations. We describe next these sets of constraints in detail.

3.2.1. Capacity limitations

All the amount of *SS* generated by the WWT plants (parameter $CAP(i)$) must be treated in the agricultural areas as shown in Eq. 1. Furthermore, the amount of *SS* sent to agricultural soil j should not exceed its capacity (parameter $CAPf(j)$).

$$\sum_j x(i,j) = CAP(i) \quad \forall i \tag{1}$$

$$\sum_i x(i,j) \le CAPf(j) \quad \forall j \tag{2}$$

Here $x(i,j)$ is a continuous variable that represents the amount of *SS* sent from plant i to agricultural soil j. The amount of *SS* transported from i to j is constrained within lower and upper bounds if a transportation link is established between them and must be zero otherwise:

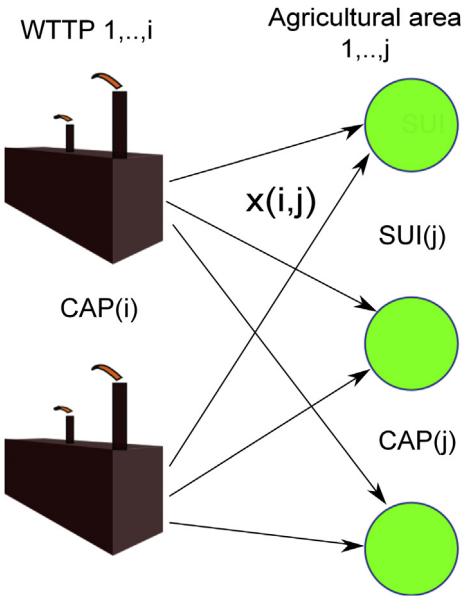

Fig. 4. Superstructure of the supply chain problem.

$$\underline{X(i,j)}\, z(i,j) \le x(i,j) \le \overline{X(i,j)} z(i,j) \quad \forall j,i \tag{3}$$

The existence of a transportation link between plant i and field j is represented by binary variable $z(i,j)$, which equals 1 if a transportation link is established and 0 otherwise. In the same equation, $\underline{X(i,j)}$ and $\overline{X(i,j)}$ denote the minimum and maximum allowable flows of *SS*, respectively, that can be transported between i and j. The total amount of *SS* sent to area j must lie within lower and upper limits:

$$\underline{Y(j)}\, y(j) \le \sum_i x(i,j) \le \overline{Y(j)} y(j) \quad \forall j \tag{4}$$

In this equation, $y(j)$ is a binary variable that takes the value of 1 if area j is used and 0 otherwise, while $\underline{Y(j)}$ and $\overline{Y(j)}$ are lower and upper bounds, respectively, on the total amount of *SS* disposed on field j.

3.2.2. Objective functions

The model considers two objective functions: suitability ($f1 = SF$) and economic performance ($f2$). The first is defined as the total suitability among the agricultural areas used for sewage sludge (*SS*) amendment.

$$f1 = SF = \sum_i \sum_j x(i,j) SUI(j) \tag{5}$$

where the suitability index associated with each field ($SUI(j)$) is multiplied by the amount of *SS* sent from plant i to agricultural soil j ($x(i,j)$). The parameter $SUI(j)$ is defined as proposed in Passuello et al. (2012) and ranges between 0 (worst) and 1 (best areas). This indicator considers a wide range of concerns related to the environmental agency and farmers' stakeholders (see Fig. 2). The *SF* assesses the potential impacts or alterations in the environmental matrices (soil, food and water quality) and the human exposure.

Following the work by Passuello et al. (2012), the suitability is determined from two main indexes: human exposure and environmental criteria. Human exposure quantifies the likelihood of causing damage to human health, and considers "distance to urban areas", and "crop type". The environmental criteria measure the likelihood of contaminating soils, surface water and groundwater, when soils are amended with *SS*. The tree of the selected criteria can be seen on Fig. 5.

For soil criteria, two subcriteria are considered: "soil structure" and "soil characteristics". The subcriterion "soil structure" quantifies the ability of the soils to receive *SS* (for instance, organic soils with a fine texture are preferred due to their buffer properties), while the "soil characteristics" consider metal concentration and mobility in soil (bioavailability and lower mobility for high pH and carbonate content). For the open waters criteria, two groups of subcriteria were considered: "climatology", which evaluates contaminant degradation and mobility due to the local temperature and precipitation values; and "relief", which quantifies the likelihood of the contaminant to reach open waters. For this criterion, two subcriteria are considered: the terrain "slope", and the proximity to open waters ("hydrology").

The suitability index is calculated for all the areas considered in the analysis following the decision rules and criteria weights proposed by Passuello et al. (2012), in which the reader can find further details.

The total cost, denoted by the continuous variable *TC*, accounts for the transportation cost from the *SS* plants to the fields (*TRC*), as

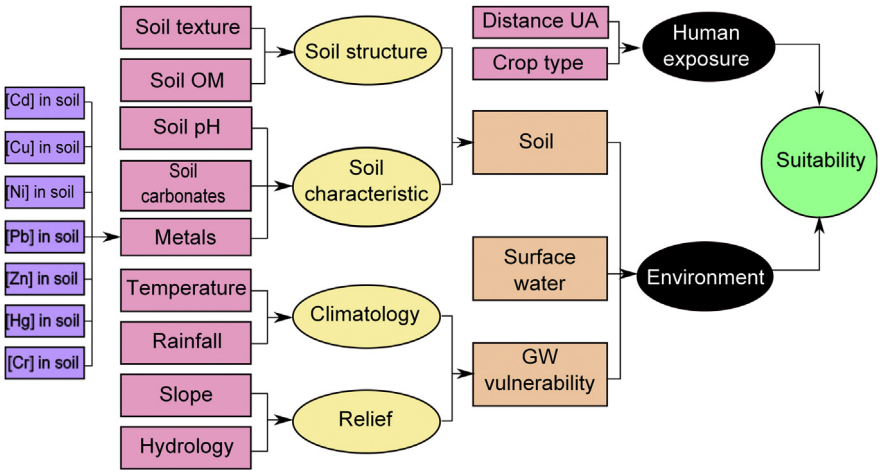

Fig. 5. Schematic representation of the model implementation.

well as the application cost (*AC*) associated with the disposal of *SS* on the fields.

$$f2 = TC = TRC + AC \tag{6}$$

The total cost (*TC*) is included in the model to reflect the preferences of the companies hired for managing the disposal of *SS*, which are interested in a cheap process. The transportation cost is calculated from the amount of *SS* sent from plants to soils and the associated distance:

$$TRC = \sum_i \sum_j tc\, x(i,j)\lambda(i,j) \tag{7}$$

where, $\lambda(i,j)$ represents the distance between plant i and field j in kilometers, tc is the cost of transporting 1 ton of *SS* per km of distance (euro ton^{-1} km^{-1}), and $x(i,j)$ denotes the amount of *SS* transported from i to j expressed in ton per year (ton year^{-1}).

The application cots are calculated from the amount of *SS* disposed as follows:

$$AC = \sum_i \sum_j ac(j)x(i,j) \tag{8}$$

where $ac(j)$ represents the application cost of 1 ton of *SS* per year (euro ton^{-1} year^{-1}).

3.3. Solution method

The overall MILP can be finally expressed in compact form as follows:

$$\min\{-f1(x,y,z),\ f2(x,y,z)\} \quad (OPTTS)$$
$$\text{s.t. constraints } 1-8$$
$$x \subset \mathbb{R} \quad y,z \subset \{0,1\}$$

where $f1$, $f2$ are the suitability and total cost, respectively (Section 3.2.2), constrains 1–8 correspond to Equations (1)–(8) (see Section 3.2.1), and x, y, z denote the continuous and binary variables, respectively, of the model. Model *OPTSS* can be solved by any multi-objective optimization method available in the literature (Raith and Ehrgott, 2009). Without loss of generality, we apply here the epsilon-constraint method (Ehrgott, 2005), which is based on formulating an auxiliary model in which one objective is kept as main objective and the remaining are transferred to auxiliary constraints that impose epsilon bounds on their values. These single-objective problems are solved for several epsilon values, generating in each run a different Pareto solution. Further details of this method can be found elsewhere (Ehrgott, 2005).

4. Results and discussion

The input data for the MILP were taken from Passuello et al. (2012). We consider an area of 451,296 ha (12,536 pixels, each one with a surface of 36 ha). All these areas show a suitability index above 0.7. The agricultural areas are of different types: cereals, fruits, vegetables, and pastures. Each MILP of the epsilon constraint method contains 125,371 equations, 112,830 continuous variables, and 62,680 binary variables. Fig. 6 shows the results of the Pareto analysis for the two criteria considered (Total Cost and Suitability). Ten Pareto points were generated following the procedure mentioned before. It took around 7.52 CPU seconds to solve each MILP on an AMD Athlon 2.99 GHz, 3.49 GB of RAM.

Note that each Pareto solution represents a different distribution alternative of *SS* from the water plants to the set of agricultural

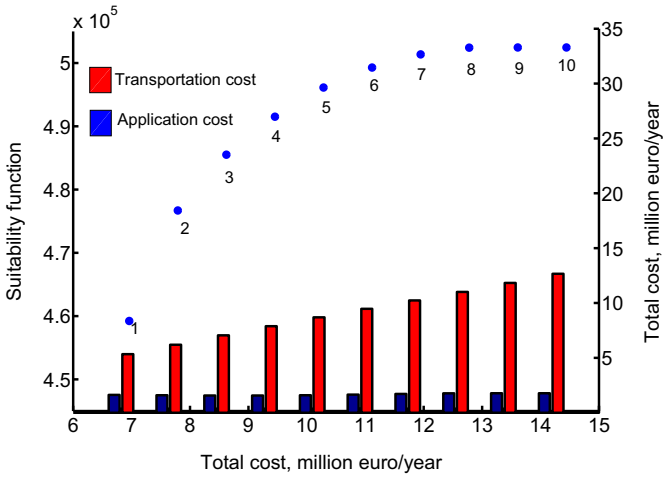

Fig. 6. Results obtained from solving the bi-criteria problem *TC* vs. *SF*.

fields (Fig. 6). As observed, there is a clear trade-off between overall suitability and cost, as an improvement in one criterion is only possible by worsening the other one. Two different zones can be identified in the Pareto set. From point 1 to point 6, the slope of the curve increases sharply. In contrast, from 6 to 10, the slope is rather smooth, so increments in suitability are attained at a large increase in cost. Fig. 6 shows also a breakdown of the cost for each Pareto solution. As can be seen, the transportation cost represents the largest contribution to the total cost (*TC*), and constantly increases along the Pareto set, while the application cost stays approximately constant.

Fig. 7 shows the solutions associated with points 1, 6 and 10 (a, b and c, respectively, in Fig. 7), which correspond to the extreme solutions and an intermediate alternative. The distribution of *SS* denoted by variables $x(i,j)$ (see Section 3.2.1) is given by the amount of *SS* sent from plant i to agricultural soil j in ton per year. Every agricultural soil used for sewage sludge amendment has its own color (red, green, blue and violet) that depends on the city from which it is receiving the *SS*. The intensity of the color depends on the amount of *SS* applied to the soil. For a better understanding of Fig. 7, please refer Fig. 1.

Fig. 7(a) shows the distribution for the minimum cost. As observed, the disposal areas are located relatively close to the water treatment plants, since this configuration reduces the transportation costs. It should be noticed that we only consider in our analysis those agriculture areas with a suitability index above 0.7, a minimum target value that is not fulfilled by many areas close to the water treatment plants. For example, in Girona, the only suitable areas for *SS* amendment are located far away from the capital, and close to the border with Barcelona.

Fig. 7(b) depicts the results for the intermediate point 6. As observed, the disposal areas for Barcelona and Tarragona are far away from the cities, and close to Lleida, a region with more suitable agricultural fields. Fig. 7(c) shows the results for the maximum suitability solution (point 10 in Fig. 3). Recall that in this case the cost does not play any role in the optimization. As a consequence, *SS* from all the provinces is distributed in the most suitable areas of Catalonia regardless of the distance from the treatment plants. These areas are located mainly in Lleida.

As observed, our systematic approach provides as output a set of candidate solutions from which the one to be implemented in practice should be identified. Identifying these alternatives is by no means a straightforward task, since many alternatives exist. The main advantage of our strategy is that it ensures that the final

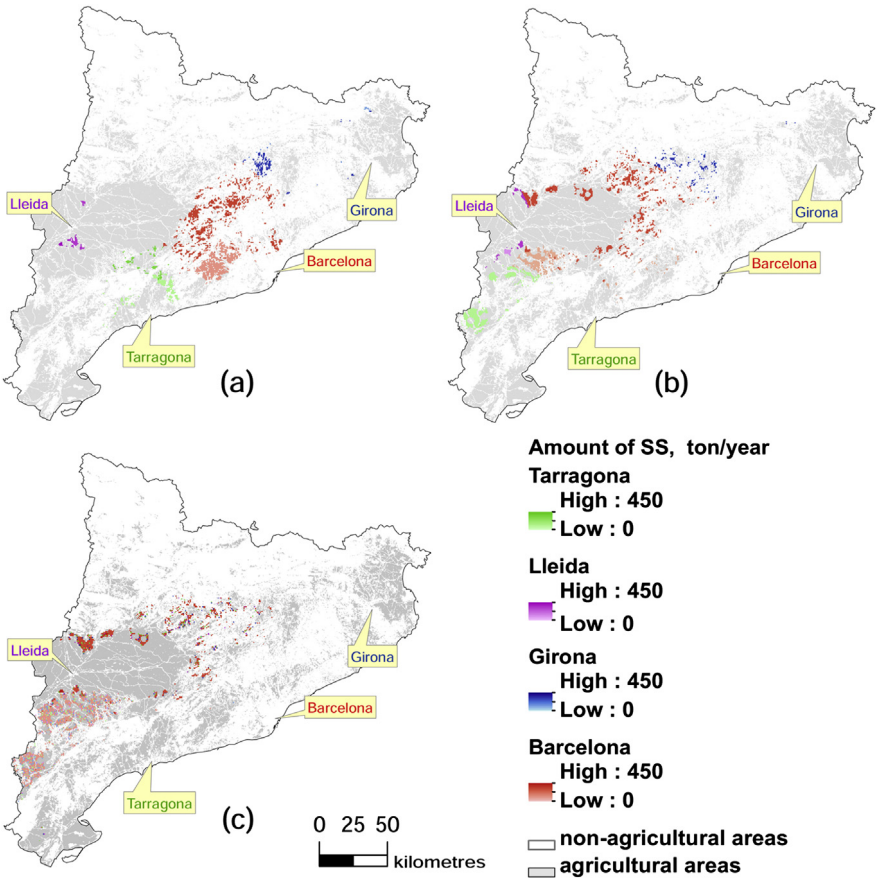

Fig. 7. Distribution of *SS* in agricultural soils for the (a) minimum cost solution, (b) an intermediate solution, (c) and the maximum suitability solution.

solution implemented in practice is Pareto optimal, that is, that it cannot be improved in all of the objectives simultaneously without necessarily worsening at least one of the interests of the decision-makers.

The question that arises at this point is how to choose the best alternative from the set of Pareto solutions. The final choice should be made by a panel of experts according to their experience, and should ideally represent the views of the society or a group of stakeholders. The main advantage of our tool is that it provides a set of solutions to be assessed by decision-makers, so they do not spend extra time (and money) in generating them. Furthermore, these alternatives are guaranteed to be optimal, so we avoid sub-optimal solutions whose economic and environmental performance can be improved simultaneously. Finally, including economic aspects in the model along with environmental concerns avoids potential conflicts between environmental agencies and industry. These advantageous characteristics make our approach quite appealing in this context.

5. Conclusion

This work has presented a systematic spatial decision-making tool for the optimal distribution of *SS* on agricultural areas based on the combined use of GIS and mathematical programming. The task of identifying the best agricultural soils for *SS* amendment was formulated as a mixed-integer linear programming (MILP) problem that seeks to optimize simultaneously the economic and environmental performance of the system. The multi-objective optimization model coupled with GIS data provides a comprehensive procedure to evaluate *SS* disposal options on agricultural areas for organic amendment.

The capabilities of our approach were tested through its application to a case study based on Catalonia. Numerical results show that it is possible to improve the environmental performance of the final solution by compromising the associated cost. Our methodology is intended to assist decision-makers in such a challenging task. The tool presented is general enough to be applied to other regions, especially in the European Mediterranean area, after performing a careful adaptation to the local features and knowledge of the region of interest.

One of the main advantages of our approach is that it produces solutions that reflect precisely the default preferences of the decision-makers involved in the problem. Furthermore, it relies on a rigorous and systematic mathematical approach that avoids falling in sub-optimal solutions, something that might happen when applying heuristics or rules of thumb. Finally, the approach presented may lead to significant savings in time and money when solving such a challenging environmental engineering problem.

References

ACA (Agncia Catalana de l'Aigua), 2008. Dades de produccio i gestio de fangs del any 2007. Departament de Medi Ambient i Habitatge de la Generalitat de Catalunya Barcelona.

Bourmistrova, L.V., Efremov, R.V., Bushenkov, V.A., Buber, A.L., Brainin, N.A., 2005. Experience of model integration and Pareto frontier visualization in the search for preferable water quality strategies. Environmental Modelling & Software 20 (2), 243–260.

Ducheyne, E., De Wulf, R., De Baets, B., 2006. A spatial approach to forest-management optimization: linking GIS and multiple objective genetic

algorithms. International Journal of Geographical Information Science 20 (8), 917–928.
Ehrgott, M., 2005. Multicriteria Optimization, vol. 491. Springer Verlag.
Fu, G., Butler, D., Khu, S.T., 2008. Multiple objective optimal control of integrated urban wastewater systems. Environmental Modelling & Software 23 (2), 225–234.
Fytili, D., Zabaniotou, A., 2008. Utilization of sewage sludge in eu application of old and new methods – a review. Renewable and Sustainable Energy Reviews 12 (1), 116–140.
Grabaum, R., Meyer, B., 1998. Multicriteria optimization of landscapes using GIS-based functional assessments. Landscape and Urban Planning 43 (1–3), 21–34.
IDESCAT (Institut d'Estadistica de Catalunya), 2009. Superfície agrcola. Per productes. Provncies, Barcelona.
Johnson, M., Korcz, M., von Stackelberg, K., Hope, B., 2009. Spatial Analytical Techniques for Risk Based Decision Support Systems. Decision Support Systems for Risk-based Management of Contaminated Sites. Springer, New York, USA, pp. 75–93.
Kattaa, B., Al-Fares, W., Al Charideh, A., 2010. Groundwater vulnerability assessment for the Banyas Catchment of the Syrian coastal area using GIS and the RISKE method. Journal of Environmental Management 91 (5), 1103–1110.
Kollat, J.B., Reed, P., 2007. A framework for visually interactive decision-making and design using evolutionary multi-objective optimization (VIDEO). Environmental Modelling & Software 22 (12), 1691–1704.
Malczewski, J., 2004. GIS-based land-use suitability analysis: a critical overview. Progress in Planning 62 (1), 3–65.
Nadal, M., Kumar, V., Schuhmacher, M., Domingo, J., 2006. Definition and GIS-based characterization of an integral risk index applied to a chemical/petrochemical area. Chemosphere 64 (9), 1526–1535.
Passuello, A., Schuhmacher, M., Mari, M., Cadiach, O., Nadal, M., 2010. A spatial multicriteria decision analysis to manage sewage sludge application on agricultural soils. Environmental Modeling for Sustainable Regional Development: System Approaches and Advanced Methods, 221.
Passuello, A., Cadiach, O., Perez, Y., Schuhmacher, M., 2012. A spatial multicriteria decision making tool to define the best agricultural areas for sewage sludge amendment. Environment International 38 (1), 1–9.
Poggio, L., Vrscaj, B., 2009. A GIS-based human health risk assessment for urban green space planning – an example from grugliasco (Italy). Science of the Total Environment 407 (23), 5961–5970.
Raith, A., Ehrgott, M., 2009. A comparison of solution strategies for biobjective shortest path problems. Computers & Operations Research 36 (4), 1299–1331.
Schriever, C., Liess, M., 2007. Mapping ecological risk of agricultural pesticide runoff. Science of the Total Environment 384 (1–3), 264–279.
van den Broek, M., Brederode, E., Ramírez, A., Kramers, L., van der Kuip, M., Wildenborg, T., Turkenburg, W., Faaij, A., 2010. Designing a cost-effective CO_2 storage infrastructure using a GIS based linear optimization energy model. Environmental Modelling & Software 25 (12), 1754–1768.
Wang, X., Yu, S., Huang, G., 2004. Land allocation based on integrated GIS-optimization modeling at a watershed level. Landscape and Urban Planning 66 (2), 61–74.
Werle, S., Wilk, R., 2010. A review of methods for the thermal utilization of sewage sludge: the polish perspective. Renewable Energy 35 (9), 1914–1919.

7.2 Decomposition Algorithm for Geographic Information System Based Mixed-Integer Linear Programming Models: Application to Sewage Sludge Amendment.

Vaskan P., Guillén-Gosálbez G., Kostin A., Jiménez L. Decomposition algorithm for geographic information system based mixed-integer linear programming models: application to sewage sludge amendment. *Industrial & Engineering Chemistry Research*, 52(49), 17640–17647, 2013.

I&EC research
Industrial & Engineering Chemistry Research

Article

pubs.acs.org/IECR

Decomposition Algorithm for Geographic Information System Based Mixed-Integer Linear Programming Models: Application to Sewage Sludge Amendment

P. Vaskan, G. Guillén-Gosálbez,* A. Kostin, and L. Jiménez

Departament d'Enginyeria Química (EQ), Escola Tècnica Superior d'Enginyeria Química (ETSEQ), Universitat Rovira i Virgili (URV), Campus Sescelades, Avinguda Països Catalans, 26, 43007 Tarragona, Spain

ABSTRACT: We present a decomposition strategy for mixed-integer linear programming (MILP) models that are formulated on the basis of geographic information system (GIS) data. Our algorithm relies on decomposing the MILP into two levels, a master problem and a slave problem between which we iterate until a termination criterion is satisfied. The former is constructed using a K-clustering statistical aggregation method that reduces the computational burden of the model. The solution of this level is used to guide the search in the slave model. A case study that addresses the optimal design of sewage sludge amendment in Catalonia (NE of Spain) is introduced to illustrate the capabilities of the proposed approach.

1. INTRODUCTION

Geographic informational systems (GIS) were initially developed as a tool for storing and displaying all forms of geographically referenced information. In the recent past, however, there has been a growing interest on the application of GIS in the solution of various social and economic problems. Particularly, GIS has been used in the context of spatial decision analysis for the assessment of potential locations for different types of systems considering various inputs simultaneously, with a recent growing interest placed on its application to environmental problems. As an example, Nadalet al.,[1] Poggio and Vrščaj[2] investigated the use of GIS for human health assessment, whereas Johnson et al.[3] Schriever and Liess[4] applied GIS in the assessment of the ecological exposure and environmental risk of several systems.

GIS can be combined with multicriteria decision analysis (GIS-MCDA) to address problems in which different (typically conflictive) criteria must be accounted for in the analysis. Malczewski[5] investigated the use of GIS-based tools in land-use suitability analysis, whereas Passuello et al.[6] applied GIS and MCDA to the management of sewage sludge.

The capabilities of GIS and spatial analysis can be further enhanced through its integration with optimization tools. Grabaum and Meyer[7] investigated the use of GIS to support decision making in planning problems. Wang et al.[8] developed a GIS model to identify the best location for future land uses in the Lake Erhai basin in China. Mapa et al.[9] combined GIS and mathematical modeling for the solution of location-allocation problems arising in the management of education facilities. Jung et al.[10] integrated GIS and optimization tools for the effective control of parcel delivery services. Marcoulaki et al.[11] developed an integrated framework based on stochastic optimization and GIS for the design of pipeline systems.

One problem in which the combined use of GIS and mathematical programming holds good promise is the treatment of sewage sludge in agricultural areas. The production of sewage sludge (SS) has grown rapidly during the last years, mainly due to the increase of the world population. Despite recent advances, the question on how to treat the SS still remains open. One effective method for this is to reuse it as a fertilizer in the agricultural sector, an alternative encouraged by the European Community, which promotes the recycling of organic matter and nutrients to soils.[12] Identifying the best agricultural areas for SS amendment is challenging because this strategy shows not only benefits to both soil and crops but also disadvantages due to the potential contamination of the fields.

GIS tools for land classification are well suited for this problem, as they allow identifying the best regions for SS amendment from information available in spatial databases.[6] These tools are mainly descriptive; that is, they provide valuable information about the system, but no guidelines on how to solve the underlying problem. In this general context, there is a strong motivation for developing systematic tools that integrate GIS and optimization to facilitate decision-support in this area.

Vaskan et al.[13] investigated the combined use of GIS and MILP (mixed-integer linear programming) for identifying optimal agricultural areas for sewage sludge amendment in the area of Catalonia. The combined use of GIS and optimization tools led to complex MILP models due to the spatially explicit nature of the problems addressed. In these MILPs, the decision variables are defined for every pixel of the GIS map, thereby giving rise to mathematical models with a very large number of variables and constraints. In our previous paper,[13] we overcame this limitation by considering a GIS map with low resolution. Although this strategy simplifies the calculations, it offers no guarantee of convergence to the global optimum of the original problem (i.e., the one defined for the original map with high resolution).

In work, we propose a rigorous decomposition algorithm for the efficient solution of GIS-based MILPs that exploits their

Received: July 30, 2013
Revised: October 10, 2013
Accepted: October 18, 2013
Published: October 18, 2013

particular structure. This strategy allows handling models based on GIS maps with high resolution. Our approach is based on decomposing the problem into two hierarchical levels between which the algorithm iterates until a termination criterion is satisfied. We illustrate the capabilities of our strategy via its application to the optimal location of agricultural areas for sewage sludge amendment. Numerical results show that our approach achieves reductions of orders of magnitude in CPU time (as compared to the full space GIS-based MILP) while still yielding near optimal solutions.

The article is organized as follows. Section 2 formally states the problem. Section 3 introduces a rigorous decomposition algorithm to tackle GIS-based MILP problems. Some numerical results are presented and discussed in section 4, and the conclusions of the work are finally drawn in section 5.

2. PROBLEM STATEMENT

We consider as a test bed to illustrate the capabilities of our approach the optimal allocation of agricultural areas for sewage sludge (SS) amendment. We next formally state the problem of interest before describing the MILP derived to solve it. To this end, we consider a superstructure like the one depicted in Figure 1. Given are a set of wastewater treatment plants

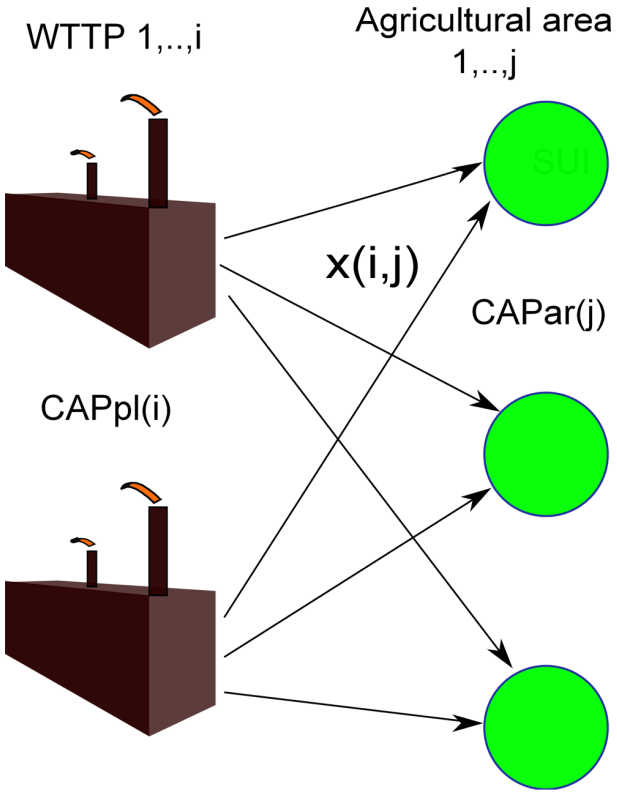

Figure 1. Superstructure of the supply chain problem.

(WWTP) and a set of agricultural areas that can receive the sludge sent by the plants. Each field is described by coordinates expressed in meters, and it features an acceptable capacity (CAPar(j)) in tons per year of sludge, and an application cost (in euro ton^{-1}year^{-1}). In addition, every plant is characterized by a pair of Cartesian coordinates and a total production of SS per year (CAPpl(i)). The goal of the analysis is to determine the optimal distribution of SS production among a set of agricultural areas so that the total cost is minimized.

3. MODEL FORMULATION

The MILP used in this work, which is taken from Vaskan et al.,[13] is based on the superstructure showed in Figure 1. The MILP seeks to determine the optimal flows to be established between the wastewater treatment plants and the agricultural fields considering the cost as unique criterion. This is a major difference with respect to the original bicriteria model that optimized the cost along with the environmental impact. For the sake of completeness of this work, we next describe the equations of the MILP. Further details can be found in our previous publication.

3.1. MILP Model. *3.1.1. Capacity Limitations.* We define the continuous variable $x(i,j)$, which denotes the amount of SS sent from plant i to agricultural soil j. The total amount of sludge sent from a plant to the fields is equal to the plant capacity (represented by the parameter CAPpl), as shown in the following equation:

$$\sum_j x(i,j) = \mathrm{CAPpl}(i) \qquad \forall\, i \tag{1}$$

$$\sum_j x(i,j) \le \mathrm{CAPar}(j) \qquad \forall\, j \tag{2}$$

Furthermore, the amount of SS sent to an agricultural field must not exceed its capacity (parameter CAPar(j)) The amount of SS sent from a plant to a field must lie within lower and upper bounds if a transportation link is established between them, and should be zero otherwise:

$$\underline{X(i,j)}\, z(i,j) \le x(i,j) \le \overline{X(i,j)}\, z(i,j) \qquad \forall\, j,\, i \tag{3}$$

In this equation $z(i,j)$ is a binary variable that represents the existence of a transportation link between plant i and field j. $z(i,j)$ equals 1 if a transportation link is established, and 0 otherwise. In the same equation, $\underline{X(i,j)}$ and $\overline{X(i,j)}$ denote the minimum and maximum allowable flows of SS, respectively, that can be transported between i and j. The total amount of SS sent to field j must lie within lower and upper limits, provided the field is used for SS amendment:

$$\underline{Y(j)}\, y(j) \le \sum_i x(i,j) \le \overline{Y(j)} y(j) \qquad \forall\, j \tag{4}$$

In this equation, $y(j)$ is a binary variable that takes the value of 1 if area j is used and 0 otherwise, and $\underline{Y(j)}$ and $\overline{Y(j)}$ are lower and upper bounds, respectively, on the total amount of SS disposed on field j.

3.1.2. Objective Functions. The model minimizes the total cost (TC), which is obtained as follows:

$$\mathrm{TC} = \mathrm{TRC} + \mathrm{AC} \tag{5}$$

Here TRC represents the transportation cost from the SS plants to the fields (TRC) and AC is the application cost associated with SS in the fields. The transportation cost is given by

$$\mathrm{TRC} = \sum_i \sum_j \mathrm{tc}\, x(i,j)\, \lambda(i,j) \tag{6}$$

where $\lambda(i,j)$ represents the distance between plant i and field j in kilometers, tc is the cost of transporting 1 ton of SS per km

of distance (euro ton^{-1} km^{-1}), and $x(i,j)$ denotes the amount of SS transported from i to j expressed in ton per year (ton year^{-1}).

The application cots are calculated from the amount of SS disposed as follows:

$$\mathrm{AC} = \sum_i \sum_j \mathrm{ac}(j)\, x(i,j) \tag{7}$$

where $\mathrm{ac}(j)$ represents the application cost of 1 ton of SS per year (euro ton^{-1} year^{-1}).

The overall MILP can be expressed in compact form as follows:

$$\min \mathrm{TC}\ (M)$$

$$\text{s.t.} \quad h(x,y) = 0$$

$$g(x,y) \le 0$$

$$x \subset \mathbb{R},\ y \subset 0,\ \mathbf{1}$$

where x are continuous variables and y binary ones. Functions $h(x,y)$ are equality constraints that model mass balances, whereas $g(x,y)$ are inequality constraints that define capacity limitations. This MILP tends to be large because decision variables need to be defined for every pixel of the GIS map. GIS maps typically show thousands of pixels (or even hundreds of thousands). Hence, they might lead to optimization models showing a large computational burden. In the section that follows, we introduce a method to expedite this type of GIS-based MILPs.

4. BILEVEL DECOMPOSITION

In the MILP model presented above, the number of potential areas for SS amendment depends on the number of pixels in the GIS map. In other words, we consider the option of sending the SS to as many different locations as pixels contained in the GIS map. As an example, for a GIS map with 13 984 pixels, we would define an MILP containing 55 940 continuous variables, 69 920 binary variables, and 153 832 equations. The model size is hence quite sensitive to the number of pixels, which can grow rapidly as we increase the map resolution. More precisely, the total number of binary variables (BV) can be expressed as follows:

$$\mathrm{BV} = |I| + |IJ| \tag{8}$$

where $|I|$ is the cardinality of the set of plants and $|J|$ is the cardinality of the set of fields.

To expedite the solution of this GIS-based MILP, we propose an algorithm that decomposes the model into two hierarchical levels, a master and a slave level, between which we iterate until a stopping criterion is reached. The scheme of the bilevel algorithm is shown in Figure 2. The master MILP contains the same equations of the original MILP, but it is defined for a smaller number of (aggregated) pixels. This MILP identifies the aggregated regions where SS should be sent and provides in turn a lower bound on the cost (LB problem). In the lower lever, we disaggregate the aggregated pixels and remove those regions discarded by the master MILP. This slave MILP provides an upper bound on the cost (UB problem). After the slave MILP is solved, an integer cut is added to the master MILP to remove those solutions explored so far in previous iterations. The master and slave MILPs are then solved iteratively until a termination criterion is reached. We

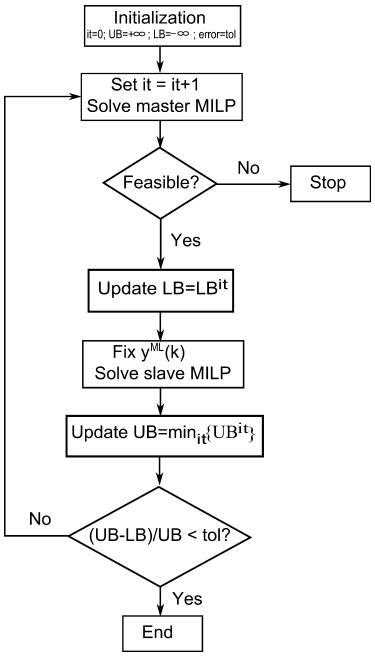

Figure 2. Flow chart for the bilevel decomposition algorithm.

describe in detail the two levels of the algorithm in the ensuing sections.

4.1. Master MILP: k-Means Clustering Method. As already mentioned, the master MILP is constructed by aggregating pixels in the original model. To this end, we use a k-means clustering method. The k-means clustering is a partitioning method that aggregates data into clusters such that observations within each cluster are as close to each other as possible and as far from observations in other clusters as possible. In the context of our application, each observation corresponds to a pixel with a given location in the space of coordinates. This makes such a clustering aggregation very useful for spatially explicit problems.

Each cluster is defined by the centroid or center and its member objects (pixels). The goal is to determine the centroid with the minimum sum of distances from all objects in that cluster. k-means uses an iterative algorithm that minimizes the sum of distances from each object to its cluster centroid, over all the clusters. This algorithm moves objects between clusters until the sum cannot be decreased any further. The result is a set of clusters that are as compact and as well-separated as possible.

To clarify this technique we consider a simple example with 15 fields, each one defined by given coordinates. These fields are aggregated into three clusters with minimum total sum of distances between centroids and fields. After applying the k-means strategy, we identify three clusters containing different numbers of pixels (Figure 3). Further details on this method can be found in Hartigan and Wong[14] and Kanungo et al.,[15] and implementation details are available in Matlab.[16]

After performing the aggregation, we slightly modify the original MILP to accommodate the new aggregated clusters. Let $JK(k)$ be the set of pixels j contained in the aggregated cluster k. To this end, we use the following equations:

$$\mathrm{ac}^{\mathrm{ML}}(k) = \min_{j \subset JK} \mathrm{ac}(j) \tag{9}$$

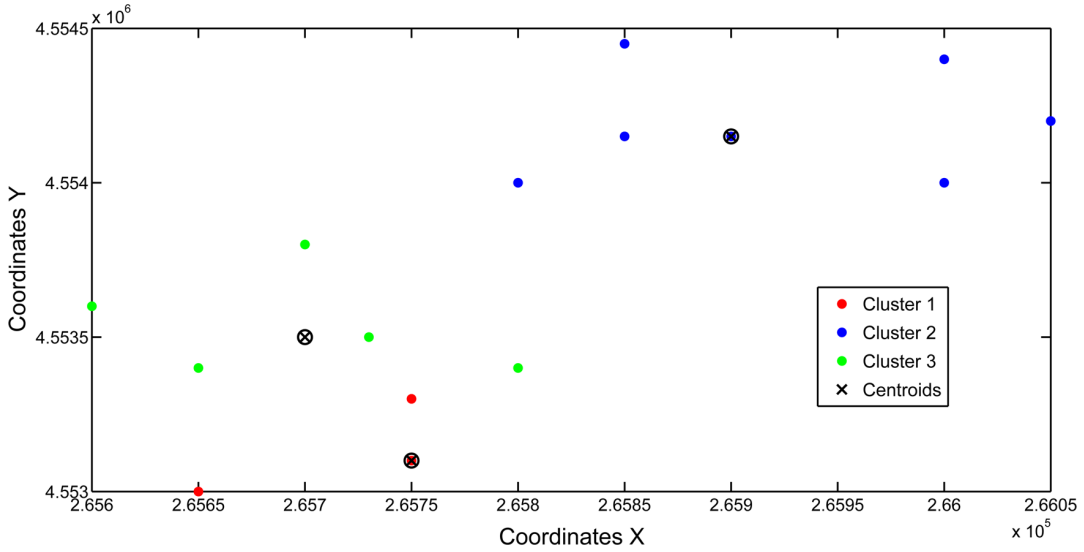

Figure 3. k-means aggregation example.

$$\lambda^{ML}(i,k) = \min_{j \subset JK} \lambda(i,j) \tag{10}$$

$$CAPar^{ML}(k) = \sum_{j \subset JK} CAPar(j) \tag{11}$$

Hence, the values of the application cost ($ac^{ML}(k)$) and distance ($\lambda^{ML}(i,k)$) of an aggregated pixel (i.e., k clusters) in the master MILP correspond to the minimum values among the pixels contained in the cluster (note that in this notation ML stands for master level). Furthermore, the capacity of the aggregated pixel ($CAPar^{ML}(i,k)$) is given by the sum of capacities of all of the pixels of the cluster. Because of the manner in which it is constructed, the master MILP is guaranteed to provide a rigorous lower bound on the total cost. The master MILP identifies in a systematic and rigorous manner the aggregated pixels that will receive the sludge from the treatment plants. As will be shown in the next section, this information is used to reduce the number of variables and constraints of the slave MILP.

Note that the master MILP is defined for the k aggregated clusters, rather than for the j fields. Apart from this, the master MILP is identical to the MILP model described above. It therefore includes the following equations:

$$\sum_k x^{ML}(i,k) = CAPpl(i) \qquad \forall\, i \tag{12}$$

$$\sum_i x^{ML}(i,k) \le CAPar^{ML}(k) \qquad \forall\, k \tag{13}$$

$$\underline{X^{ML}(i,k)}\, z^{ML}(i,k) \le x^{ML}(i,k) \le \overline{X^{ML}(i,k)}\, z(i,k) \qquad \forall\, k, i \tag{14}$$

$$\underline{Y^{ML}(k)}\, y^{ML}(k) \le \sum_i x^{ML}(i,k) \le \overline{Y^{ML}(k)}\, y^{ML}(k) \qquad \forall\, k \tag{15}$$

The model minimizes the total cost (TC^{ML}), which is obtained as follows:

$$TC^{ML} = TRC^{ML} + AC^{ML} \tag{16}$$

$$TRC^{ML} = \sum_i \sum_k tc x^{ML}(i,k)\, \lambda^{ML}(i,k) \tag{17}$$

$$AC^{ML} = \sum_i \sum_k ac^{ML}(k)\, x^{ML}(i,k) \tag{18}$$

4.2. Slave MILP. As already mentioned, the master problem identifies the aggregated pixels where SS should be disposed. In the slave problem, we disaggregate this information assuming that the pixels belonging to the active clusters of the master MILP (i.e., those for which $y^{ML}(k)$ equals 1 in the master MILP) can be utilized for SS amendment. In contrast, if a pixel defined in the slave MILP does not belong to any of the aggregated pixels selected in the master problem, then it is removed from the slave model. The slave MILP contains therefore the same equations of the original MILP, but fewer constraints and variables, because pixels that are not selected in the master MILP are omitted in the formulation. Let JAK^{it} be the set of pixels j contained in the aggregated clusters k that are active in the solution of the mater MILP (those for which $y^{ML}(k)$ takes a value of one) in iteration it of the algorithm. With this notation, the slave MILP includes the following constraints:

$$\sum_{j \subset JAK} x(i,j) = CAPpl(i) \qquad \forall\, i \tag{19}$$

$$\sum_{j \subset JAK} x(i,j) \le CAPar(j) \qquad \forall\, j \tag{20}$$

$$\underline{X(i,j)}\, z(i,j) \le x(i,j) \le \overline{X(i,j)}\, z(i,j) \qquad \forall\, j \subset JAK, i \tag{21}$$

$$\underline{Y(j)}\, y^{ML}(j) \le \sum_i x(i,j) \le \overline{Y(j)}\, y^{ML}(j) \qquad \forall\, j \subset JAK \tag{22}$$

The model minimizes the total cost (TC), which is obtained as follows:

$$TC = TRC + AC \tag{23}$$

dx.doi.org/10.1021/ie402471w | Ind. Eng. Chem. Res. 2013, 52, 17640−17647

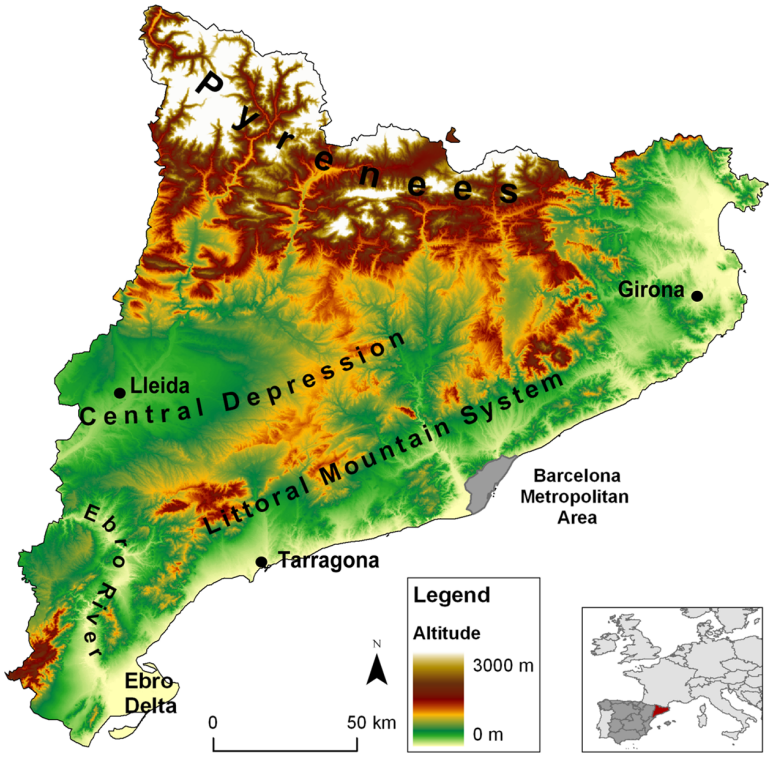

Figure 4. Map of Catalonia.

$$\mathrm{TRC} = \sum_{i} \sum_{j \subset \mathrm{JAK}} \mathrm{tc}x(i,j)\,\lambda(i,j) \tag{24}$$

$$\mathrm{AC} = \sum_{i} \sum_{j \subset \mathrm{JAK}} \mathrm{ac}(j)\,x(i,j) \tag{25}$$

After calculating the master MILP, we next solve the slave MILP minimizing the total cost and fixing the values of $y(j)$ to the values provided by the master problem (thereby disaggregating the information obtained therein). Note that the slave subproblem provides an upper bound on the cost. This is because the slave MILP contains the same equations of the original MILP, but it is solved in a reduced domain with a smaller feasible space. Finally, after solving the slave MILP, we derive an integer cut to exclude solutions identified so far in previous iterations.

Hence, the master model works with data from the k-means clustering aggregation, whereas the slave model works with disaggregated clusters obtained from the solution of the master model. Both problems (slave and master) are solved iteratively until a termination criterion is satisfied.

In summary, the steps of the bilevel decomposition algorithm are the following:

1. Aggregate the data into the desired number of clusters using the k-means clustering aggregation.
2. Set iteration count it = 0, upper bound UB = $+\infty$, lower bound LB = $-\infty$, and tolerance error = tol.
3. Set it = it + 1. Solve the MILP master problem (LP):
   If problem (LP) is infeasible, then stop.
   Otherwise, set the current lower bound to LB = $\mathrm{LB}^{\mathrm{it}}$
4. Disaggregate the pixels of the master MILP and fix variables $y^{\mathrm{ML}}(k)$ (eq 14) obtained from step 2, in the slave problem and solve it.
5. Update the upper bound (UB) to UB = $\min_{\mathrm{it}}\{\mathrm{UB}^{\mathrm{it}}\}$ where $\mathrm{UB}^{\mathrm{it}}$ represents the objective function value associated with the optimal solution in iteration it.
6. Check the convergence criteria:
   a. If (UB − LB)/UB < tol, then stop. The solution corresponding to UB (i.e., the solution of the slave model in the iteration with minimum cost) satisfies the termination criterion (i.e., it can be regarded as optimal within the predefined optimality gap).
   b. Otherwise, go to step 3.

5. CASE STUDY: CATALONIA

We apply our method to a case study based on Catalonia. Catalonia is a province of Spain located in the Northeastern part of the Iberian Peninsula. The total area of Catalonia is 32 114 km^2, with an agricultural area available for cultivation of near 5000 km^2. The relief is very different from the mountains on the north, to the flat at the center and the coast (Figure 4). The Mediterranean climate and precipitation levels favors the existence of agricultural sectors. The Catalonian agriculture is mainly based on the production of wine, wheat, rice, barley, olive, grapes, fruits, nuts, and vegetables. The total population of Catalonia is near 7 350 000 people. It is divided into four provinces: Barcelona, Tarragona, Girona, and Lleida, with a population of 5 416 447, 788 895, 731 864, and 426 872 people, respectively. The production of sewage sludge (SS) has been growing in the recent past and near 83% of the total production of SS was applied on agricultural soils.[6]

6. RESULTS AND DISCUSSION

We illustrate the capabilities of our approach through its application to a case study based on Catalonia. The input data for the MILP were taken from ref 6. We consider three different

levels of aggregation in the problem (all of them for the same agricultural area of 505 176 ha): 126 294, 31 517, and 13 984 pixels, each one with a surface of 4, 16, and 36 ha, respectively. The MILP model and the bilevel algorithm were both implemented in GAMS and solved with CPLEX on an AMD Athlon 2.99 GHz, 3.49 GB of RAM machine. The optimality gap set for CPLEX was 3%, whereas the bilevel algorithm was executed considering a tolerance (relative error between the lower and upper bounds) of 3%.

We should make a remark concerning the use of models with a large number of pixels. In general, it is desirable to include as many pixels as possible in the analysis, because the decisions involved might be rather sensitive to the scale of the map. Moreover, the main characteristics of the map areas are in some cases very sensitive to the scale, which motivates the need to define a large number of pixels for a better assessment of the performance of each alternative. Hence, back to our example, it is more convenient for an adequate analysis to consider 4 ha for every pixel (126 294 pixels in total) rather then 36 ha (13 984 pixels in total). Unfortunately, this leads to more complex problems.

Particularly, we solved a set of problems of increasing complexity involving a different number of cities in Catalonia. We consider first the location of WWTPs in four main cities: Barcelona, Girona, Tarragona, and Lleida, and then solve the same problem considering additional locations (i.e., Terrasa, Vic, Amposta, and Montblanc).

Numerical results for different levels of complexity are presented in Tables 1−3. The goal is to illustrate the performance of the algorithm as compared to the full-space method. The objective in these problems was to minimize the cost as single objective function. In all of the cases, the optimality gap set for the bilevel algorithm (i.e., 3%) was reached in one single iteration.

Table 1. Computational Results for 13 984 Pixels with GAP 3% (CPLEX)

	binary variables	continuous variables	equations	time (s)	cost (euro)
		Four Plants			
full space	69 920	55 940	153 832	5.58	6 425 371
bilevel (UB)	12 980	10 386	28 562	0.81	6 436 821
LB	6 995	5 598	15 395	0.42	6 257 572
		Five Plants			
full space	83 904	69 924	181 801	7.66	5 381 347
bilevel (UB)	15 540	12 952	33 677	1.2	5 393 824
LB	8 394	6 997	18 194	0.55	5 214 386
		Six Plants			
full space	97 888	83 908	209 770	9.64	5 138 030
bilevel (UB)	18 102	15 518	38 798	1.23	5 149 251
LB	9 793	8 396	20 993	0.69	4 971 599
		Seven Plants			
full space	111 872	97 892	237 739	10.56	5 055 427
bilevel (UB)	20 824	18 223	44 260	1.64	5 070 094
LB	11 192	9 795	23 792	0.8	4 889 444
		Eight Plants			
full space	125 856	111 876	265 708	11.2	5 000 648
bilevel (UB)	23 652	21 026	49 942	1.8	5 015 416
LB	12 591	11 194	26 591	0.88	4 828 968

Table 2. Computational Results for 31 517 Pixels with GAP 3% (CPLEX)

	binary variables	continuous variables	equations	time (s)	cost (euro)
		Four Plants			
full space	157 585	126 072	346 695	14.44	6 392 357
bilevel (UB)	28 795	23 038	63 355	1.91	6 399 849
LB	15 760	12 610	34 678	1.14	6 268 917
		Five Plants			
Full space	189 102	157 589	409 730	18.19	5 350 280
bilevel (UB)	43 278	36 067	93 776	2.94	5 358 057
LB	18 912	15 762	40 983	1.2	5 227 879
		Six Plants			
full space	220 619	189 106	472 765	22.03	5 107 400
bilevel (UB)	40 152	34 418	86 048	3.5	5 115 116
LB	22 064	18 914	47 288	1.63	4 985 148
		Seven Plants			
full space	252 136	220 623	535 800	24.97	5 021 803
bilevel (UB)	46 248	40 469	98 286	4.36	5 031 313
LB	25 216	22 066	53 593	3.38	4 898 018
		Eight Plants			
full space	283 653	252 140	598 835	29.55	4 965 311
bilevel (UB)	52 533	46 698	110 913	4.59	4 978 131
LB	28 368	25 218	59 898	1.86	4 839 344

We start by generating results for the lowest resolution (i.e., 13 984 pixels). As observed in Table 1, the proposed approach shows better numerical performance than the full-space method. First, the computational time is less for our bilevel strategy because in every level of the algorithm we have less number of equations and variables than in the full space problem. Second, the value of the objective function obtained from the bilevel strategy is very close to the value generated by the full space problem. Note that although we fixed an optimality gap of 3% for CPLEX, we obtain indeed the global optimum in all the runs (i.e., we solved again fixing a 0% gap, and we got the same results). On average, our bilevel algorithm reduces the CPU time by a factor of almost 1 when compared to the full space approach.

We next increase the map resolution and repeat the calculations (Table 2). As seen, we get very similar results as in the previous case. The CPU times of both methods increase but are still within low limits. In addition, the bilevel method still outperforms the full-space one, achieving almost 1 order of reduction in the CPU time compared to the full space method.

Finally, Table 3 shows the results corresponding to the maximum map resolution. As seen, the full space MILP gets intractable when we increase further the number of pixels (i.e., 126 294 pixels), which leads to a prohibitive computational burden. As observed, the full space method must solve an MILP with 631 470 binary variables and 505 192 continuous variables, which turns out to be intractable. In contrast, our bilevel strategy keeps the model size tractable and can thus handle large problems in reasonable CPU times (CPU time around 40−50 s), while still providing near optimal (i.e., optimality gap of 3%) solutions. Hence, our approach allows for

dx.doi.org/10.1021/ie402471w | Ind. Eng. Chem. Res. 2013, 52, 17640−17647

Table 3. Computational Results for 126 294 Pixels with GAP 3% (CPLEX)

	binary variables	continuous variables	equations	time (s)	cost (euro)
		Four Plants			
full space	631 470	505 192	1 389 266	out of memory	
bilevel (UB)	114 280	91 426	251 422	10.97	6 391 374
LB	63 150	50 522	138 936	5.06	6 326 472
		Five Plants			
full space	757 764	631 486	1 641 858	out of memory	
bilevel (UB)	136 728	113 942	296 251	15.16	5 349 945
LB	75 780	63 152	164 197	6.89	5 284 988
		Six Plants			
full space	884 058	757 780	1 894 450	out of memory	
bilevel (UB)	158 879	136 184	340 463	18.27	5 109 052
LB	88 410	75 782	189 458	8.02	5 044 526
		Seven Plants			
full space	1 010 352	884 074	2 147 042	out of memory	
bilevel (UB)	183 064	160 183	389 020	20.36	5 025 745
LB	101 040	88 412	214 719	9.14	4 959 139
		Eight Plants			
full space	1 136 646	1 010 368	2 399 634	out of memory	
bilevel (UB)	206 550	183 602	436 060	32.08	4 970 541
LB	113 670	101 042	239 980	14.28	4 901 357

the solution of MILPs based on maps with higher resolution while keeping the CPU time low.

As seen also in Tables 1−3, the complexity of the model, and therefore the CPU time spent in its solution, increases with the number of plants as well as the number of pixels, being the second factor the most critical one.

Finally, we should note that for this particular problem the objective function does not improve significantly as we increase the map resolution (approximately 1%, which corresponds to 50 000 euros in absolute values). Note, however, that in general it is not possible to predict an exact interval within which the objective function will fall when we increase the number of pixels. Hence, because this difference might be much larger in other problems, it is always recommended to use the highest map resolution available.

7. CONCLUSIONS

This work has proposed a decomposition method for MILPs that are formulated on the basis of GIS maps. Our approach is based on a bilevel decomposition strategy that makes use of a clustering aggregation algorithm. In the first level, we solve a lower bounding problem to identify the aggregated pixels that will receive the sludge from the treatment plants. In the upper bounding problem, this information is disaggregated to obtain a rigorous upper bound on the cost.

We applied our method to a case study based on sewage sludge amendment in Catalonia. Numerical examples showed that our tool provides near optimal solutions in a fraction of the CPU time required by the full space model. Our method thus solves in an efficient manner large-scale MILPs based on GIS maps with a high resolution. The strategy presented herein is general enough to be applied to similar MILPs used in spatial-decision analysis that address problems arising in chemical and process industries.

AUTHOR INFORMATION

Corresponding Author

*G. Guillén-Gosálbez: e-mail, gonzalo.guillen@urv.cat.

Notes

The authors declare no competing financial interest.

ACKNOWLEDGMENTS

The authors acknowledge the financial support of the following institutions: Spanish Ministry of Education and Science (CTQ2009-14420-C02, CTQ2012-37039-C02, DPI2012-37154-C02-02 and ENE2011-28269-CO3-03), Spanish Ministry of External Affairs (projects PHB 2008-0090-PC) and the Catalonian Government (FI programs).

APPENDEX

Indices

i wastewater treatment plants
j agricultural soils
k aggregated soils (i.e., clusters)

JAK^{it} Sets

I i:i is a wastewater treatment plants
J j:j is the agricultural soil contained in a pixel
JK k: set of pixels j contained in the aggregated cluster k
JAK^{it} it: set of pixels j contained in the aggregated clusters k that are active in the solution of the mater MILP (those for which $y^{ML}(k)$ takes a value of one) in iteration it of the algorithm

Parameters

CAPpl(i) capacity of plant i
CAPar(j) capacity of field/pixel j
$\underline{X(i,j)}$ minimum allowable flows of sewage sludge from plant i to field j
$\overline{X(i,j)}$ maximum allowable flows of sewage sludge from plant i to field j
$\underline{Y(j)}$ lower bound on the total amount of SS disposed on field j
$\overline{Y(j)}$ upper bound on the total amount of SS disposed on field j
tc unitary transportation cost from plants to fields
$\lambda(i,j)$ distance between plant i and field j

$ac(j)$ application cost of *SS* in field/pixel j
$ac^{ML}(k)$ application cost defined for the aggregated pixel k (master level)
$\lambda^{ML}(i,k)$ distance between plant i and cluster/aggregated pixel k (master level)
$CAPar^{ML}(k)$ capacity of the aggregated pixel k (master level)
$\underline{X^{ML}(i,k)}$ minimum allowable flows of sewage sludge from plant i to cluster k (master level)
$\overline{X^{ML}(i,k)}$ maximum allowable flows of sewage sludge from plant i to cluster k (master level)
$\underline{Y^{ML}(k)}$ lower bound on the total amount of SS disposed on cluster k (master level)
$\overline{Y^{ML}(k)}$ upper bound on the total amount of SS disposed on cluster k (master level)

Variables

$x(i,j)$ amount of SS sent from plant i to agricultural soil j
$z(i,j)$ binary variable that represents the existence of a transportation link between plant i and field j
$y(j)$ binary variable that represents the use of field j
$x^{ML}(i,k)$ amount of SS sent from plant i to cluster k (master level)
$z^{ML}(i,k)$ binary variable that represents the existence of a transportation link between plant i and cluster k (master level)
$y^{ML}(k)$ binary variable that represents the use of a cluster k (master level)
TRC total transportation cost
AC application cots of SS
TC total cost
TRC^{ML} total transportation cost (master level)
AC^{ML} application cots of SS (master level)
TC^{ML} total cost (master level)

REFERENCES

(1) Nadal, M.; Kumar, V.; Schuhmacher, M.; Domingo, J. L. Definition and GIS-based characterization of an integral risk index applied to a chemical/petrochemical area. *Chemosphere* **2006**, *64*, 1526−1535.
(2) Poggio, L.; Vrščaj, B. A gis-based human health risk assessment for urban green space planningAn example from Grugliasco (Italy). *Science of the total environment* **2009**, *407*, 5961−5970.
(3) Johnson, M. S.; Korcz, M.; von Stackelberg, K.; Hope, B. K. *Decision Support Systems for Risk-Based Management of Contaminated Sites*; Springer, 2009; pp 1−19.
(4) Schriever, C. A.; Liess, M. Mapping ecological risk of agricultural pesticide runoff. *Sci. Total Environ.* **2007**, *384*, 264−279.
(5) Malczewski, J. GIS-based land-use suitability analysis: a critical overview. *Progress in planning* **2004**, *62*, 3−65.
(6) Passuello, A.; Cadiach, O.; Perez, Y.; Schuhmacher, M. A spatial multicriteria decision making tool to define the best agricultural areas for sewage sludge amendment. *Environment international* **2012**, *38*, 1−9.
(7) Grabaum, R.; Meyer, B. C. Multicriteria optimization of landscapes using GIS-based functional assessments. *Landscape and Urban Planning* **1998**, *43*, 21−34.
(8) Wang, X.; Yu, S.; Huang, G. Land allocation based on integrated GIS-optimization modeling at a watershed level. *Landscape and Urban Planning* **2004**, *66*, 61−74.
(9) Mapa, S. M. S.; Lima, R. d. S.; Mendes, J. F. *Combining Geographica Information Systemas (GIS) and mathematical modeling to location-allocation problems in education facilities management*. 2007,
(10) Jung, H.; Lee, K.; Chun, W. Integration of GIS, GPS, and optimization technologies for the effective control of parcel delivery service. *Computers & Industrial Engineering* **2006**, *51*, 154−162.
(11) Marcoulaki, E. C.; Papazoglou, I. A.; Pixopoulou, N. Integrated framework for the design of pipeline systems using stochastic optimization and GIS tools. *Chem. Eng. Res. Des.* **2012**,
(12) Passuello, A.; Schuhmacher, M.; Mari, M.; Cadiach, O.; Nadal, M. A Spatial Multicriteria Decision Analysis to Manage Sewage Sludge Application on Agricultural Soils. *Environmental Modeling for Sustainable Regional Development: System Approaches and Advanced Methods* **2010**, 221.
(13) Vaskan, P.; Passuello, A.; Guillén-Gosálbez, G.; Schuhmacher, M.; Jiménez, L. Combined use of GIS and mixed-integer linear programming for identifying optimal agricultural areas for sewage sludge amendment: A case study of Catalonia. *Environmental Modelling & Software* **2013**,
(14) Hartigan, J. A.; Wong, M. A. Algorithm AS 136: A k-means clustering algorithm. *Journal of the Royal Statistical Society. Series C (Applied Statistics)* **1979**, *28*, 100−108.
(15) Kanungo, T.; Mount, D. M.; Netanyahu, N. S.; Piatko, C. D.; Silverman, R.; Wu, A. Y. An efficient k-means clustering algorithm: Analysis and implementation. *Pattern Analysis and Machine Intelligence, IEEE Transactions on* **2002**, *24*, 881−892.
(16) MatLab, http://www.mathworks.es/. 2013,

7.3 Multi-objective design of heat-exchanger networks considering several life cycle impacts using a rigorous MILP-based dimensionality reduction technique.

Vaskan P., Guillén-Gosálbez G., Jiménez L. Multi-objective design of heat-exchanger networks considering several life cycle impacts using a rigorous MILP-based dimensionality reduction technique. *Applied Energy* 98, 149–161, 2012.

Applied Energy 98 (2012) 149–161

Contents lists available at SciVerse ScienceDirect

Applied Energy

journal homepage: www.elsevier.com/locate/apenergy

Multi-objective design of heat-exchanger networks considering several life cycle impacts using a rigorous MILP-based dimensionality reduction technique

Pavel Vaskan, Gonzalo Guillén-Gosálbez *, Laureano Jiménez

Departament d'Enginyeria Quimica, Universitat Rovira i Virgili, Avinguda Països Catalans 26, 43007 Tarragona, Spain

ARTICLE INFO

Article history:
Received 14 October 2011
Received in revised form 1 February 2012
Accepted 7 March 2012
Available online 17 May 2012

Keywords:
Heat exchangers network
Life cycle assessment
Dimensionality reduction method
Environmental impact

ABSTRACT

This work addresses the optimal design of heat exchanger networks (HENs) considering economic and environmental concerns. The design task is posed in mathematical terms as a multi-objective mixed-integer non-linear programming (MINLP) problem, in which life cycle assessment (LCA) principles are used to quantify the environmental impact. One of the advantages of our approach is that it accounts for the simultaneous minimization of several environmental metrics, as opposed to other models that focus on minimizing a single aggregated indicator. A rigorous dimensionality reduction method based on a mixed-integer linear programming (MILP) formulation is applied to aid the post-optimal analysis of the trade-off solutions. The capabilities of our approach are tested through two examples. We clearly illustrate how the use of a single overall aggregated environmental metric is inadequate in the design of HENs, since it may leave some solutions that are appealing for decision-makers out of the analysis. Our method is aimed at facilitating decision-making at the early stages of the design of HENs.

1. Introduction

The design of heat exchanger networks (HENs) is a theme long considered in the process systems engineering (PSE) literature. This topic started to attract attention during the oil crisis that took place in the 70s. With the recent trend of developing more sustainable processes, there has been a renewed interest on the design of these systems [1,2]. Nowadays, the main methods for designing heat exchanger networks include thermodynamic approaches [3–6] and mathematical programming techniques [7–9]. The latter approach, which is the one followed in this work, relies on postulating a superstructure of design alternatives from which the optimal one is identified using rigorous mathematical programming tools based on mixed-integer non-linear programming (MINLP). The overwhelming majority of methods available for the design of HENs have focused on optimizing the economic performance as unique criterion. Environmental concerns are nowadays becoming a priority, mainly due to tighter governments' regulations. HENs are by themselves "environmentally friendly systems", since their ultimate purpose is to reduce the energy consumption and consequently the environmental damage. However, a trade-off arises in their design, since larger energy savings can be obtained at the expense of compromising the economic performance. Hence, optimizing these systems in terms of a single economic indicator may lead to solutions that do not fully exploit their large potential for reducing the environmental impact in process industries.

The selection of a suitable metric for the environmental assessment of processes still remains as an open issue in the literature [10]. Particularly, LCA has gained wider acceptance in the recent past as an effective tool to support objective environmental assessments. LCA is a methodology for evaluating the environmental loads associated with a product, process or activity over its life cycle. LCA first calculates the emissions and feedstock requirements of a process, and then translates this information into environmental impacts pertaining to several damage categories. These impacts can be employed within a multi-criteria optimization framework to improve the environmental performance of a process. The combined use of multi-objective optimization (MOO) and LCA was first proposed by Livingston and Pistikopoulous [11,12], and then formally defined by Azapagic and Clift [13]. This general approach has been applied to a wide variety of chemical engineering problems, such as the design of cooling absorption cycles [14,15], the design of chemical plants [16], the strategic planning of chemical supply chains [17–21], the strategic planning of industrial networks for the production of biofuels [22], the design of bioprocess [23] and the design of hydrogen infrastructures [24,25].

López-Maldonado et al. [26] were the first to investigate the combined use of LCA and MOO in the design of HENs. The authors focused on optimizing a single aggregated LCA metric that quantified the impact caused in several damage categories. Their model accounted for the impact associated with the operation of the HEN (which is mainly due to the utilities generation) and neglected the emissions of the construction phase.

* Corresponding author. Tel.: +34 977558618.
E-mail addresses: pavel.vaskan@urv.cat (P. Vaskan), gonzalo.guillen@urv.cat (G. Guillén-Gosálbez), laureano.jimenez@urv.cat (L. Jiménez).

0306-2619/$ - see front matter © 2012 Elsevier Ltd. All rights reserved.
http://dx.doi.org/10.1016/j.apenergy.2012.03.018

A critical issue in the combined use of MOO and LCA is the definition of suitable LCA-based metrics to be minimized. No agreement has been reached so far in the literature regarding the use of a universal LCA indicator. Unfortunately, the computational burden of MOO grows rapidly with the number of objectives, which prevents the simultaneous inclusion of many LCA indicators in the optimization model. One way to overcome this limitation consists of omitting some of them thereby reducing the associated complexity. Alternatively, by aggregating a set of environmental objectives into a single indicator, it is possible to alleviate the computation burden of environmental MOO problems. This requires defining weights for every environmental objective, which allows for their translation into a single metric. The resulting bi-criteria problems (i.e., economic vs. environmental performance) are easier to calculate and analyze. Examples of aggregated environmental metrics can be found elsewhere [27,28].

Aggregated LCA-based indicators based on weights defined by a panel of experts have gained wider interest in the recent past. This approach shows two major drawbacks. First, these weights do not necessarily reflect the decision-makers' preferences, since they are fixed beforehand and cannot be modified at will. Second, optimizing aggregated metrics in multi-objective optimization has the effect of leaving some optimal solutions out of the analysis [29]. The question that arises at this point is how to avoid their use while at the same time keeping the problem in a manageable size.

Dimensionality reduction methods widely used in areas like statistics and data mining [30] can be employed for omitting redundant objectives in MOO, thereby reducing the computational burden. Deb and Saxena [31] proposed a method based on PCA to decrease the number of objectives in MOO. Their approach identifies redundant objectives from the analysis of the eigenvectors of the correlation matrix. Brockhoff and Zitzler [32] proposed an alternative approach for reducing the number of objectives based on replacing the original set of objectives by a reduced set that is non-conflicting with the original one. An approximation error was introduced by the authors to quantify to which extent the dominance structure of the problem changes when omitting objectives. They formally defined two different problems: computing the minimum subset of objectives with a given delta value (i.e., error of the approximation) and determining the minimum approximation error for an objective subset of given size. Two algorithms, a greedy and an exact one, were proposed to solve the aforementioned problems. Based on similar ideas, Guillén-Gosálbez [33] developed a MILP-based objective reduction method to tackle these problems.

This work addresses the multi-objective optimization of HENs with economic and environmental concerns. Our approach builds on the MINLP model presented by Yee and Grossmann [8], which is adequately modified to quantify the environmental impact through LCA principles. The contributions of this work are threefold. First, we present a MINLP model for the design of HENs that incorporates the impact caused during their construction. Second, our model accounts for the simultaneous minimization of several LCA impacts that provide a complete picture of the environmental performance of the HEN. Third, we investigate the use of dimensionality reduction techniques in this context, highlighting the existence of redundant environmental objectives.

The remainder of this article is structured as follows: Section 2 provides a formal definition of the problem addressed in this paper, while Section 3 describes the mathematical model. Section 4 presents the methodology proposed to solve the MINLP problem. Two computational examples are then introduced in Section 5 to test the capabilities of our approach, and the conclusions of the work are finally drawn in Section 6.

2. Problem statement

To formally state the problem of interest, we consider a superstructure like the one depicted in Fig. 1. Given are a set of hot process streams (HPSs) and cold process streams (CPSs) to be cooled and heated, respectively, and their associated inlet and outlet temperatures. The flow rates, heat capacities and film transfer coefficients of the process streams are provided, along with a set of available hot (HU) and cold (CU) utilities, their temperature ranges and costs. Environmental data associated with every type of utility and construction material are also given. The goal of the analysis is to determine the optimal design and operating conditions that minimize simultaneously the total cost and a set of environmental impacts quantified via LCA principles. The problem solution is defined by a set of Pareto optimal designs each one achieving a unique combination of cost and environmental impact.

3. Model formulation

The model formulation used in this work is based on the superstructure introduced by Yee and Grossmann [8] and the mixed-integer non-linear programming (MINLP) model proposed by the same authors. An example of a superstructure with two stages is shown in Fig. 1. All possible combinations for heat transfer between cold and hot process streams are allowed in each stage. Cooling and heating utilities are available at the outlets of the superstructure. The intermediate temperatures of the process streams in the limits of each stage are regarded as decision variables. We assume isothermal mixing of streams, which simplifies the calculations. Further details of this model can be found in Biegler et al. [34].

For brevity, the complete mathematical formulation of the model is given in Appendix A. We focus next on describing the equations used for determining the economic and environmental performance of the HEN.

3.1. Cost objective function

The total cost, denoted by the continuous variable TC, accounts for the capital cost of the heat exchangers (CC) and the operation cost (OC) associated with the consumption of hot and cold utilities.

$$TC = CC + OC \tag{1}$$

The operating cost is calculated from the amount of utilities consumed as follows:

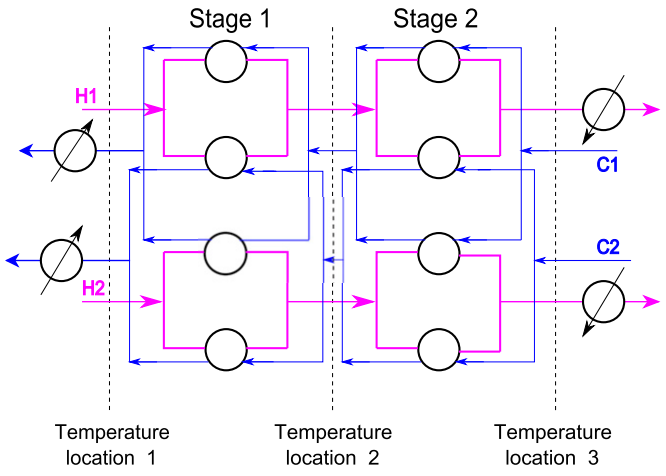

Fig. 1. Superstructure for the HEN synthesis for two cold and hot streams and two stages.

$$OC = \sum_{i\in HP} CCU\ qcu_i\ year + \sum_{j\in CP} CHU\ qhu_j\ year \quad (2)$$

where *CCU* and *CHU* represent the unit cost of cold and hot utilities respectively, qcu_i and qhu_j denote the amount of cold and hot utilities consumed, and *year* is the useful life of the HEN. *HP* and *CP* denote the set of hot and cold streams, respectively. The capital cost is determined from the number and areas of the heat-exchangers as follows:

$$CC = \sum_{i\in HP}\sum_{j\in CP}\sum_{k\in ST} CF_{i,j} z_{i,j,k} + \sum_{i\in HP} CF_i^{CU} zcu_i + \sum_{j\in CP} CF_j^{HU} zhu_j + \sum_{i\in HP}\sum_{j\in CP}\sum_{k\in ST} C_{i,j}(A_{i,j,k})^{\beta_{i,j}} + \sum_{i\in HP} C_i^{CU}\left(A_i^{CU}\right)^{\beta_i^{CU}} + \sum_{j\in CP} C_j^{HU}\left(A_j^{HU}\right)^{\beta_j^{HU}} \quad (3)$$

where $CF_{i,j}$, CF_i^{CU}, CF_j^{HU} represent the fixed cost terms associated with the heat exchanger units; $C_{i,j}$, C_i^{CU}, C_j^{HU} are area cost coefficients; $z_{i,j,k}$, zcu_i, zhu_j denote the existence of the exchangers; $A_{i,j}$, A_i^{CU}, A_j^{HU} represent the areas of the exchangers, and $\beta_{i,j}$, β_i^{CU} and β_j^{HU} are cost parameters.

The remaining process equations of the model are provided in Appendix A. These include mass and energy balances and logic constraints that model the existence of the heat exchangers.

3.2. Environmental impact objective function

LCA is an approach for evaluating the environmental loads associated with a product, process or activity through its entire life cycle. The life cycle assessment methodology [35] comprises four main phases.

1. *Goal and scope definition.* This phase defines the goal of the study, system boundaries, allocation methods and impact categories. We perform a "cradle-to-gate" analysis that embraces all activities associated with the construction and operation of the HEN. Ten impact categories, as defined by the Eco-indicator 99, are considered in our work:
    1. Carcinogenic effects on humans.
    2. Respiratory effects on humans caused by organic and inorganic substances.
    3. Damage to human health caused by climate change.
    4. Human health effects caused by ionizing radiations.
    5. Human health effects caused by ozone layer depletion.
    6. Damage to ecosystem quality caused by ecosystem toxic emissions.
    7. Damage to ecosystem quality caused by the combined effect of acidification and eutrophication.
    8. Damage to ecosystem quality caused by land occupation and land conversion.
    9. Damage to resources caused by extraction of minerals.
    10. Damage to resources caused by extraction of fossil fuels.
2. *Inventory analysis.* The second stage determines the most relevant inputs and outputs of mass and energy associated with the main process. This information will be further translated into environmental impacts. The environmental burdens are given by the production of the amount of stainless steel contained in the heat exchangers and the consumption of cold and hot utilities. The life cycle inventory (LCI) of inputs and outputs is given by the mass of stainless steel (continuous variable mass), and the amount of cold (continuous variable qcu) and hot utilities (continuous variable qhu) consumed as follows:

$$LCI_b = \sum_j qhu_j \omega_b^{HU} + \sum_i qcu_i \omega_b^{CU} + mass\,\omega_b^{M} \quad (4)$$

In this equation, ω_b^{HU}, ω_b^{CU}, ω_b^{M} denote the life cycle inventory entries (i.e., emissions released to the environment or resources taken from the ecosphere) associated with chemical *b* per reference flow of activity (i.e., mass of steam, cooling water and steel generated). These parameters are retrieved from environmental databases (e.g., ecoinvent [36]).

3. *Impact assessment*. This stage quantifies the impact in a set of damage assessment categories. Following the Eco-indicator 99 methodology, the damages in each impact category *c* (denoted by IM_c) are evaluated as follows:

$$IM_c = \sum_b LCI_b \theta_{b,c} \quad (5)$$

where $\theta_{b,c}$ is a damage factor that translates the results of the inventory phase into a set of damages.

4. *Interpretation*. Here, the results of the LCA are analyzed and a set of conclusions and recommendations for the system are formulated. Note that in our approach the decision-makers' preferences are articulated in the post optimal analysis of the Pareto optimal solutions.

4. Solution method

4.1. ϵ-constrain method

The MINLP can be expressed in compact form as follows:

$$\min_{x,y}\ TC(x,y), EI(x,y)$$
$$\text{s.t. constraints } 1\text{—}33$$
$$x \subset \mathbb{R} \quad y \subset \{0,1\}$$

in which *TC* is the total cost, *EI* denotes the LCA impact, *x* and *y* are continuous and binary variables representing design and operating decisions and constraints 1–33 model the HEN performance (see Appendix A for details).

In this work we solve this problem using the ϵ-constrain method [37], which relies on formulating an auxiliary model in which one objective is kept as main objective while the rest are transferred to auxiliary constraints that impose epsilon bounds on their values. These single-objective problems are solved for several epsilon values, generating in each run a different Pareto solution. We follow herein the heuristic-based approach proposed by Kostin et al. [38] that reduces the computational burden of the epsilon constraint method by solving a series of bi-criteria models in which the main objective is optimized against each single secondary objective separately.

4.2. Post-optimal analysis: dimensionality reduction methods

The application of the epsilon constraint method provides a large number of Pareto alternatives. Visualizing and analyzing them considering several objectives simultaneously is a highly difficult task. We describe next how dimensionality reduction methods can be employed in this context to facilitate the post-optimal analysis of the Pareto solutions of the multi-objective model.

The goal of dimensionality reduction methods is to remove redundant objectives from the MOO model in a manner such that its main features are preserved to the extent possible. Our approach builds on the works by Brockhoff and Zitzler [29,32], which are based on the concept of delta error. We provide next a brief outline of this approach.

In what follows, we consider the weakly Pareto dominance relationship, that is, a solution A is said to be weakly efficient if there is no other solution that is strictly better than A in all the objectives. Consider a MOO problem with three solutions (solutions 1, 2 and 3) and three objectives $F = \{f_1, f_2, f_3\}$ that must be simultaneously minimized. Fig. 2 is a parallel coordinates plot that depicts in the bottom axis the objective functions and in the vertical axis the normalized value attained by each solution in every objective.

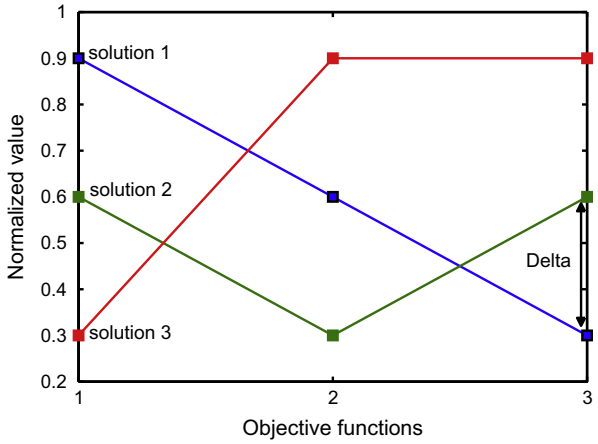

Fig. 2. Dominance structure for the set f_1, f_2, f_3. All solutions are weakly efficient.

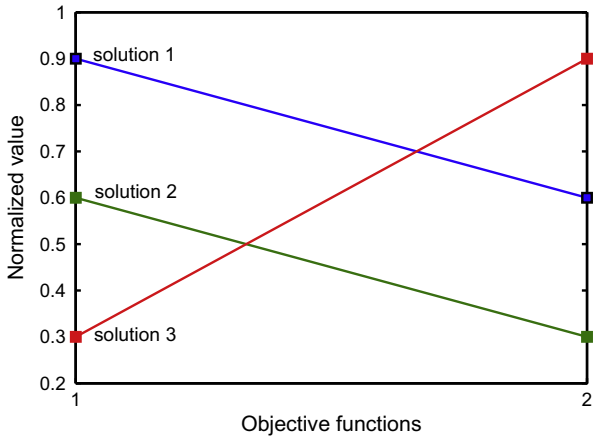

Fig. 3. Dominance structure for the reduced set f_1, f_2. Solution 2 dominate solution 1, since 2 is better than 1 in all objectives. Solution 1 is therefore lost.

As observed, all the solutions are Pareto optimal, since there is no one better than any of the others simultaneously in all the objectives. Particularly, solution 3 is the best in objective 1, solution 2 in objective 2 and solution 1 in objective 3. If we omit the third objective and work in the reduced space $F' = \{f_1, f_2\}$, then the dominance structure changes, as solution 1 is now dominated by 2 (i.e., solution 2 is better than solution 1 in all objectives) (see Fig. 3). That is, solution 1 would be lost, since it would become sub-optimal in the reduced space of objectives. Alternatively, by omitting the second objective from the original set (see Fig. 4), the dominance structure is preserved, since no solution dominates any of the others. In other words, by selecting the objectives to be omitted in a smart way, it is possible to reduce the problem complexity while still preserving its structure. Hence, the second objective is redundant and can thus be discarded from the analysis. The reduced objective set $F'' = \{f_1 f_3\}$ is regarded as non-conflicting with the original set $F = \{f_1, f_2, f_3\}$, since they have the same dominance structure. Thus, non conflicting sets can be replaced by each other in MOO without losing information (i.e., Pareto solutions).

Brockhoff and Zitzler [29,32] proposed to calculate the error of the approximation obtained when removing objectives in MOO. Consider optimizing over the set $F' = \{f_1, f_2\}$, in this case solution 2 would dominate solution 1 (Fig. 3). However, in the original set F, solution 1 is better than 2 in objective 3. In fact solution 2 would dominate 1 in the original 3-dimensional Pareto space $F = \{f_1, f_2, f_3\}$ if it showed the same value in objective function 3 than solution 1.

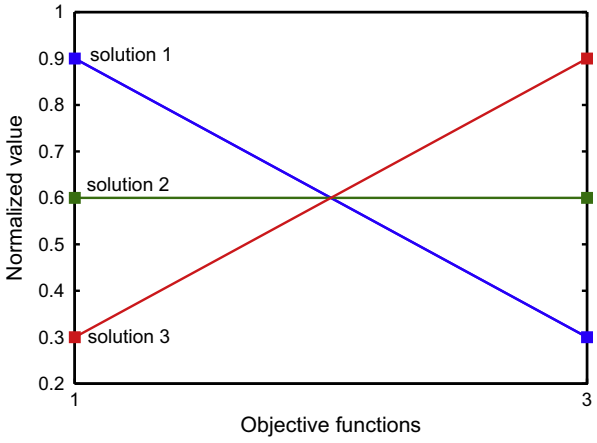

Fig. 4. Dominance structure for reduced set f_1, f_3. No solution dominates any of the others. All solutions are Pareto optimal in the reduced search space, and the dominance structure is preserved.

The difference between the true value of objective 3 in solution 2 and that required to dominate solution 1 in the original space of objectives can be used as a measure to quantify the change in the dominance structure (see Fig. 2). This difference, referred to as delta error [29,32] quantifies the change in the dominance structure after omitting objectives. Hence, the delta value indicates to which extent the initial dominance relationship is modified after removing certain objectives.

The goal of dimensionality reduction methods is to identify a set of objectives of given cardinality such that the delta error of the approximation is minimized. In this work, we apply the MILP method introduced by Guillén-Gosálbez [33] in the post-optimal analysis of the solutions of the HEN problem. This technique identifies redundant objectives that can be omitted, shedding light on the relationships between the environmental indicators. Further details on this method can be found elsewhere [33].

5. Case study

We illustrate next the capabilities of the proposed approach through its application to two case studies, in which we minimize 12 objectives (i.e., total cost and 11 LCA impacts). As environmental objectives, we consider the total Eco-indicator 99, which aggregates the single impacts described in Section 3.2, and all its single impact categories. The motivation for this is to analyze whether the minimization of the aggregated impact is a good practice in the design of HENs (i.e., it preserves the problem structure). The MOO models was implemented in GAMS and solved with DICOPT interfacing with CONOPT and CPLEX on a AMD Athlon 2.99 GHz, 3.49 GB of RAM.

5.1. Example 1

This example considers two hot and one cold process streams. High-pressure steam and cold water are both available. The cost data are presented in Table 1, whereas the environmental data are displayed in Table 2.

We generated 220 Pareto points following the procedure mentioned before. The Pareto solutions were normalized dividing them by the maximum value attained over all solutions. Fig. 5 shows the Pareto points obtained from the bi-criteria problem cost vs. overall Eco-indicator 99 (represented by blue[1] squares in the figure). In the same figure, we have depicted the solutions resulting from the

[1] For interpretation of color in Figs. 1–15, the reader is referred to the web version of this article.

Table 1
Stream data for example 1.

Stream	Tin, °C	Tout, °C	FCp, kW/c	h, kW/m^2 °C	Cost, $/kW
HPS1	105	50	10	0.1	–
HPS2	185	70	15.4	0.1	–
CPS1	25	180	15.5	0.1	–
HU	185	185	–	0.1	300
CU	5	25	–	0.1	30

bi-criteria optimization problems that trade-off cost vs. each single impact. That is, this last set of solutions has been projected onto the 2-D space cost, Eco-indicator 99 (red circles in the plot). As observed, the bi-criteria problem cost vs. Eco-indicator 99 provides only a subset of the solutions of the overall MOO problem. This is because there are many solutions of other bi-criteria problems that are sub-optimal in the 2-D space cost vs. Eco-indicator 99. Hence, it seems clear that using the Eco-indicator 99 as unique indicator is not a good practice, since we might lose solutions that show less impact in other LCA impacts.

Fig. 6 depicts all the results obtained from solving all bi-criteria problems (i.e., cost vs. each single environmental objective separately). As observed, there are metrics that increase as the Eco-indicator 99 decreases and others that behave in the opposite manner, which indicates that some environmental objectives are conflictive. This analysis reveals also that minimizing the Eco-indicator 99 worsens the performance in some LCA impact categories. Note that not all the impacts are decreased to the same extent. For instance, ozone layer cannot be reduced below 10% with respect to its maximum value, whereas the minimum acidification value is around 45% of its maximum.

As seen, LCA metrics can be aggregated into three main groups according to their behavior: (1) those that are monotically increasing and behave in the same manner as the cost function (this group includes climate change, fossil fuel and ozone layer depletion);. (2) those that first decrease and then increase after a minimum value (Eco-indicator 99, ionizing radiation, acidification and eutrophication, carcinogenic, respiratory effects and land occupation); and (3) those that are monotically decreasing and therefore behave in a manner opposite to the cost (mineral extraction and ecotoxicity impacts).

Further analysis of these results reveals that the difference in the metrics' behavior is given by their dependence on the main sources of impact. Particularly, there are two main sources of damage: utilities generation and heat exchangers construction. The consumption of utilities can be reduced by increasing the number and size of heat exchangers, which increases in turn the amount of stainless steel required for their construction. Hence, the first

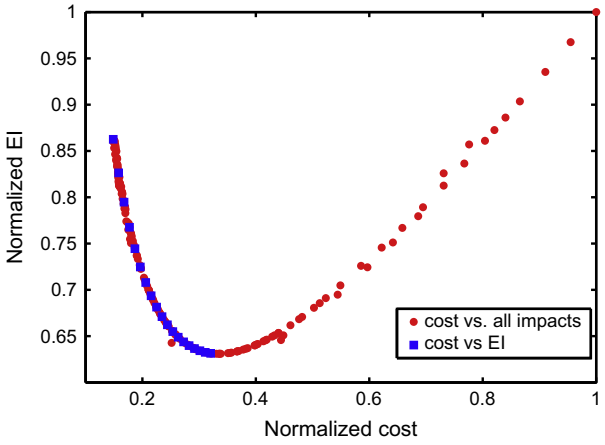

Fig. 5. Results obtained from the bi-criteria problem cost vs. overall Eco-indicator 99 (blue points) and from solving the bi-criteria problems cost vs. single impacts (red points) for example 1.

group of impacts highly depends on the utilities consumption. In contrast, impacts pertaining to the second group are mainly caused by both, utilities generation and stainless steel production. Finally, impacts of the third group are largely attributed to the generation of stainless steel. Note that the optimization of each objective produces a different solution entailing a specific consumption rate of utilities and number and sizes of heat exchangers. Fig. 6 indicates also that the minimization of metrics of type (2) along with the cost as unique criteria is not convenient, since it prevents the identification of Pareto points located after the minimum impact value in the corresponding 2-D curve.

Note that the outcome of the analysis performed here depends on the time horizon considered in the calculations. Fig. 7, which is equivalent to Fig. 6, depicts the results obtained for a time horizon of 15 years. As observed, for a lifetime of 15 years only minerals and ecotoxicity impacts are conflicting with cost. This is because both impacts largely depend on the mass of stainless steel, whereas the remaining impacts along with the cost are highly dependent on the utilities consumption. Hence, the Eco-indicator 99 and cost are mainly attributed to the generation of utilities. Because of this, the simultaneous minimization of both objectives produces one single point in which the environmental and economic indicators attain both their optimal values.

The MILP for dimensionality reduction [33] was next applied iteratively, that is, calculating the best combination of objectives of given size that minimized the delta error, and then executing

Table 2
Eco-indicator 99 from steam, cooling water and stainless steel.

Impacts, ecopoints	Eco-indicator 99 from, steem, ecopoints/kg	Eco-indicator 99 from cooling water, ecopoints/kg	Eco-indicator 99 from stainless steel, ecopoints/kg
Overall eco-indicator 99	0.005672	4.97×10^{-7}	1.132
Carcinogenic	0.00005708	1.71×10^{-8}	0.040332
Climate change	0.00053927	2.99×10^{-10}	0.024494
Ionizing radiation	1.18×10^{-6}	1.95×10^{-11}	0.00050624
Ozone layer depletion	7.86×10^{-7}	1.95×10^{-11}	5.88×10^{-6}
Respiratory effects	0.00065067	1.56×10^{-7}	0.2876
Minerals	4.08×10^{-6}	5.24×10^{-8}	0.32362
Fossil fuel	0.0042286	1.56×10^{-8}	0.09008
Acidification & eutrophication	6.20×10^{-6}	8.30×10^{-8}	0.0063917
Ecotoxicity	0.000086728	5.19×10^{-8}	0.35336
Land occupation	0.000042142	1.23×10^{-8}	0.0056452

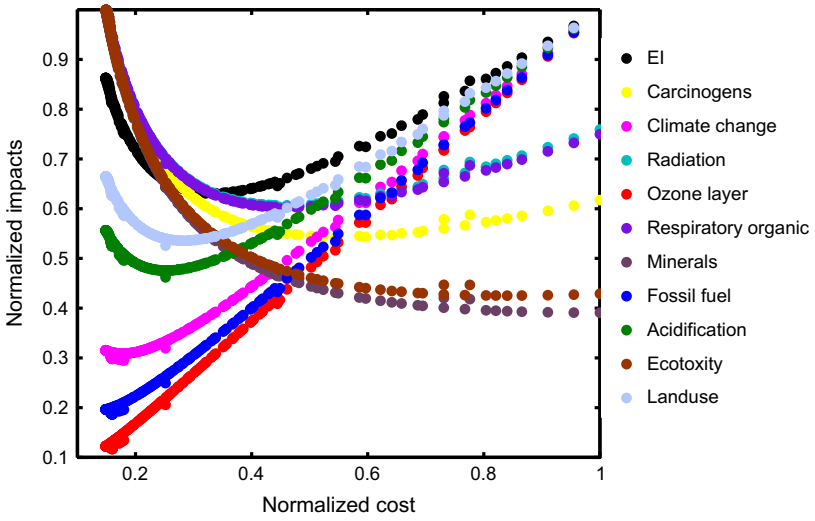

Fig. 6. Results obtained from the bi-criteria problems cost vs. single impacts for a lifetime of 1 year for example 1.

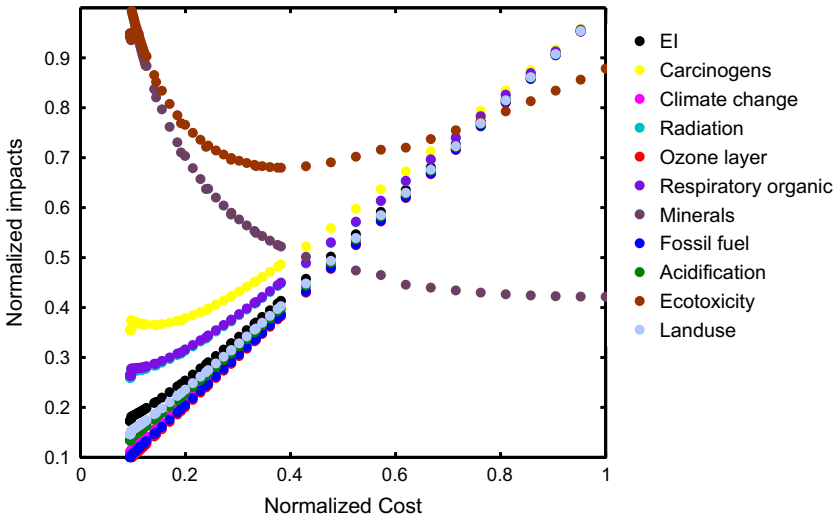

Fig. 7. Results obtained from the bi-criteria problems cost vs. single impacts for a lifetime of 15 years for example 1.

again the MILP with integer cuts added for removing solutions previously identified by the algorithm from subsequent iterations. We repeated the calculations for different useful life times of 1, 5 and 15 years. The results are presented in Tables 3 and 4. Specifically, the tables show the delta value corresponding to every possible combination of cost vs. each single environmental impact for sets of 2 and 3 objectives.

As observed, the delta values change with the life time and so does the dominance structure. The combination of cost and minerals depletion yields a very small delta value. This is because both metrics are conflicting. Hence, optimizing in the space of these two objectives does not alter significantly the problem structure. Furthermore, the triple cost, ozone layer depletion and minerals yields a zero delta error for all life times. In contrast, the couple cost and Eco-indicator 99 leads to large delta values in all the cases. These results indicate that the use of the Eco-indicator 99 as single environmental metric is inadequate in the design of HENs.

Fig. 8 shows the solutions obtained from solving the bi-criteria problem cost vs. minerals for a lifetime of 15 years. As observed, almost all solutions of the bi-criteria problems can be reproduced in the sub space cost vs. minerals depletion.

Table 3
Delta values for example 1 for all combinations of two objectives.

Reduced set		Delta		
		1 Year	5 Years	15 Years
1	2	60.7897	59.9457	52.7001
1	3	17.6811	59.9457	52.7001
1	4	60.7897	59.9457	52.7001
1	5	32.7695	59.9457	52.7001
1	6	60.7897	59.9457	52.7001
1	7	31.4228	59.9457	52.7001
1	8	1.4934	0.0153	0.0000
1	9	60.7897	59.9457	52.7001
1	10	60.7897	59.9457	52.7001
1	11	1.4934	11.5260	41.5601
1	12	60.7897	59.9457	52.7001

Figs. 9 and 10 show the heat exchangers networks with minimum cost and minerals impact, respectively, while Table 5 displays the values of the main variables of both extreme solutions. As observed, to reduce the impact in minerals, the model decides

Table 4
Delta values for example 1 for all combination of three objectives.

Reduced set			Delta			Reduced set			Delta		
			1 Year	5 Years	15 Years				1 Year	5 Years	15 Years
1	2	3	17.6811	59.9457	52.7001	1	5	6	32.7695	59.9457	52.7001
1	2	4	60.7897	59.9457	52.7001	1	5	7	31.4228	59.9457	52.7001
1	2	5	32.7695	59.9457	52.7001	1	5	8	1.4934	0.0153	0.0000
1	2	6	60.7897	59.9457	52.7001	1	5	9	32.7695	59.9457	52.7001
1	2	7	31.4228	59.9457	52.7001	1	5	10	32.7695	59.9457	52.7001
1	2	8	0.7320	0.0153	0.0000	1	5	11	1.4934	11.5260	41.5601
1	2	9	60.7897	59.9457	52.7001	1	5	12	32.7695	59.9457	52.7001
1	2	10	60.7897	59.9457	52.7001	1	6	7	31.4228	59.9457	52.7001
1	2	11	1.0107	11.5260	41.5601	1	6	8	0.0000	0.0000	0.0000
1	2	12	60.7897	59.9457	52.7001	1	6	9	60.7897	59.9457	52.7001
1	3	4	17.6811	59.9457	52.7001	1	6	10	60.7897	59.9457	52.7001
1	3	5	17.6811	59.9457	52.7001	1	6	11	1.0107	11.5260	41.5601
1	3	6	17.6811	59.9457	52.7001	1	6	12	60.7897	59.9457	52.7001
1	3	7	17.6811	59.9457	52.7001	1	7	8	1.4934	0.0153	0.0000
1	3	8	1.4934	0.0153	0.0000	1	7	9	31.4228	59.9457	52.7001
1	3	9	17.6811	59.9457	52.7001	1	7	10	31.4228	59.9457	52.7001
1	3	10	17.6811	59.9457	52.7001	1	7	11	1.4934	11.5260	41.5601
1	3	11	1.4934	11.5260	41.5601	1	7	12	31.4228	59.9457	52.7001
1	3	12	17.6811	59.9457	52.7001	1	8	9	0.0251	0.0000	0.0000
1	4	5	32.7695	59.9457	52.7001	1	8	10	0.7320	0.0153	0.0000
1	4	6	60.7897	59.9457	52.7001	1	8	11	1.4934	0.0153	0.0000
1	4	7	31.4228	59.9457	52.7001	1	8	12	0.7320	0.0153	0.0000
1	4	8	0.1700	0.0151	0.0000	1	9	10	60.7897	59.9457	52.7001
1	4	9	60.7897	59.9457	52.7001	1	9	11	1.0107	11.5260	41.5601
1	4	10	60.7897	59.9457	52.7001	1	9	12	60.7897	59.9457	52.7001
1	4	11	1.0107	11.5260	41.5601	1	10	11	1.0107	11.5260	41.5601
1	4	12	60.78968	59.94572	52.70009	1	10	12	60.7897	59.9457	52.7001
						1	11	12	1.0107	11.5260	41.5601

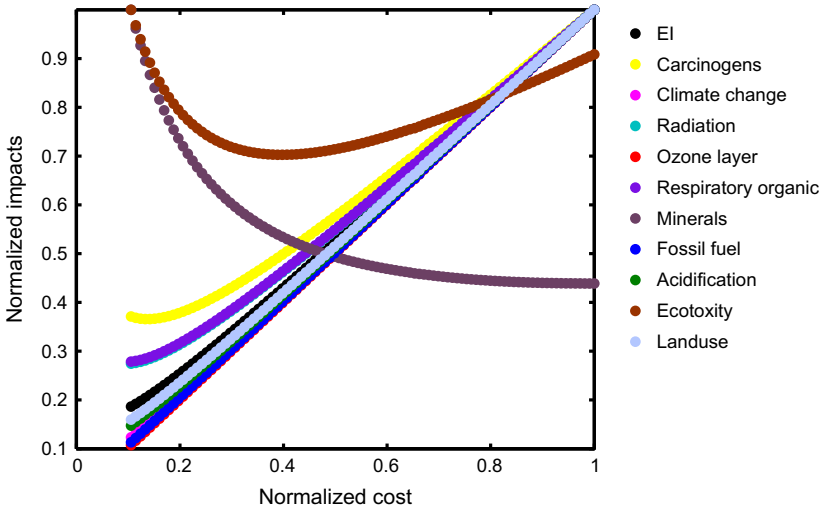

Fig. 8. Results for problem cost vs. minerals for a lifetime of 15 years lifetime for example 1.

to decrease the area of the heat exchangers and therefore the amount of stainless steel required.

5.2. Example 2

This second example was presented by Isafiade and Fraser [39]. Two hot and one cold process streams are considered along with cold and hot utilities. The operating data for this example are shown in Table 6, whereas the environmental data are presented in Table 2.

The results for a lifetime of 1 year are shown in Figs. 11 and 12. Fig. 11 shows the points obtained when optimizing the Eco-indicator 99 vs. cost (blue points), and those resulting from the remaining bi-criteria problems projected onto the same subspace (i.e., cost vs. Eco-indicator 99) (red points). As in the previous example, one branch of solutions would be discarded if cost and Eco-indicator 99 were the only objectives optimized. Note, however, that in this example the contribution of the utilities generation to the total impact is larger. The objectives can be aggregated in three groups: (1) dependent on utilities generation (i.e., Eco-indicator 99, carcinogenic, climate change, respiratory effects, land occupation, ionizing radiation, acidification & eutrophication, fossil fuel and ozone layer depletion); (2) dependent on both emission sources: utilities and steel (cost and ecotoxicity); and (3) dependent on stainless steel (mineral extraction). Note that, as in the previous example, every curve has upper and lower branches.

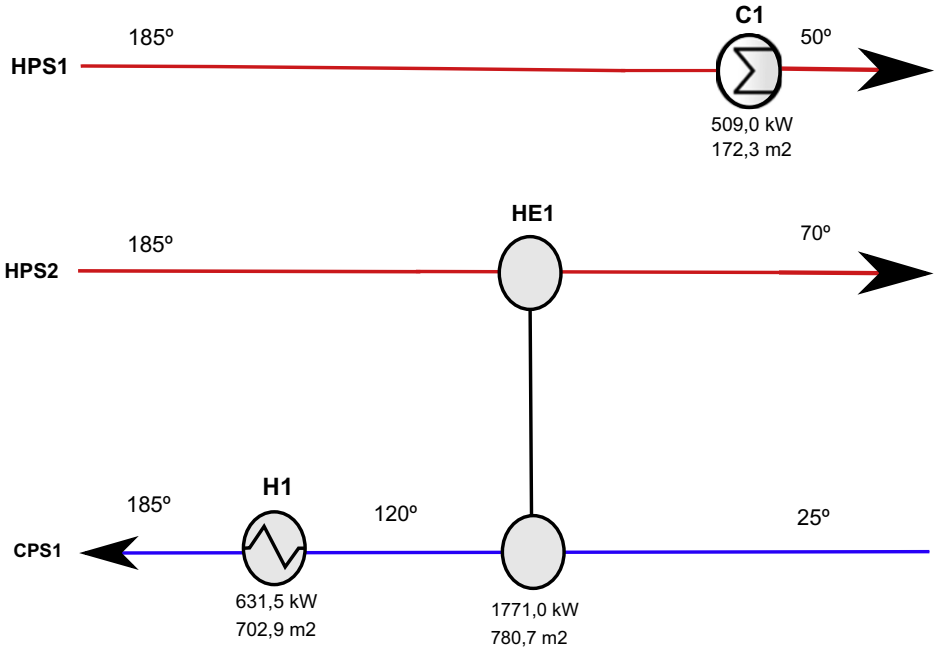

Fig. 9. Network obtained from the bi-criteria problems cost vs. minerals impact for 15 years lifetime with minimum cost for example 1.

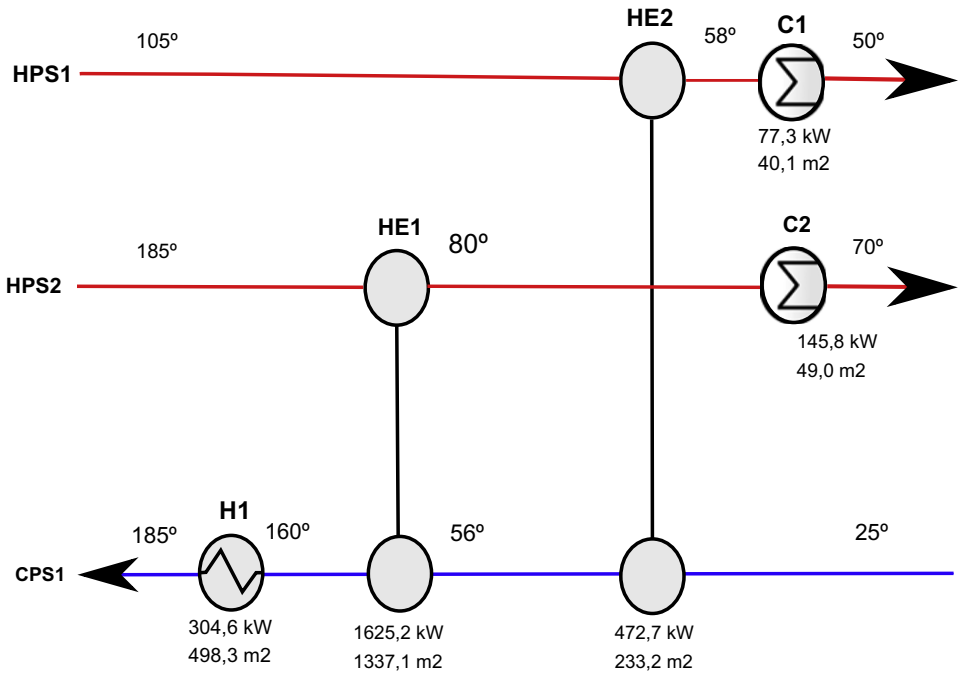

Fig. 10. Network obtained from the bi-criteria problems cost vs. minerals impact for 15 years lifetime with minimum minerals for example 1.

Table 5
Results for example 1 obtained by solving problem cost vs. minerals for 15 years lifetime.

	Total area, m^2	Operation cost, $	Capital cost, $	Total cost, $	Minerals impact, ecopoints
Min minerals	1554.7	4,592,017	40,627.4	4,632,645	25,725.1
Min TC	1664.4	3,089,250	35,215.6	3,124,466	26,791.9

Table 6
Stream data for example 2.

Stream	Tin, °C	Tout, °C	FCp, kW/c	h, kW/m^2 °C	Cost, $/kW
HPS1	105	25	10	0.5	–
HPS2	185	35	5	0.5	–
CPS1	25	185	7.5	0.5	–
HU	210	209	–	5	160
CU	5	6	–	2.6	10

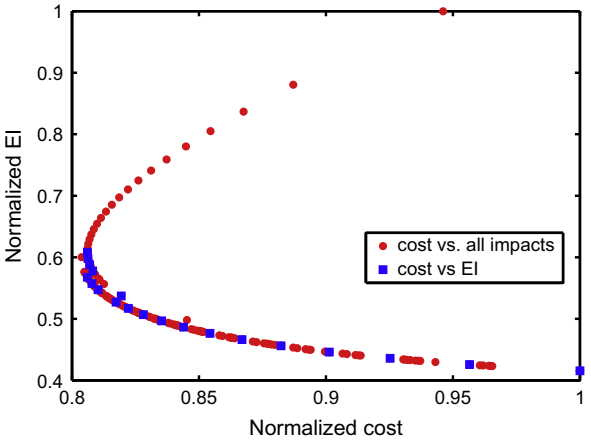

Fig. 11. Points resulting from the bi-criteria optimization cost vs. Eco-indicator 99 and cost vs. every single impact projected onto the subspace cost vs. Eco-indicator 99. Red points above the envelope of the blue ones would be lost if Eco-indicator 99 and cost were optimized as unique objectives (example 2).

The results for lifetimes of 15 years are shown in Fig. 13. The percentage of impact due to utilities generation increases as we move to larger lifetimes. For a useful life of 15 years, minerals depletion is the only impact that is conflicting with cost, since it largely depends on the mass of stainless steel, whereas the others are mainly given by the amount of utilities consumed. Remarkably, there is no trade-off between cost and Eco-indicator 99 for a lifetime of 15 years, since both highly depend on the amount of utilities consumed.

The results obtained with the MILP are shown in Tables 7 and 8. Similarly, as with the previous case, the combination cost vs. depletion of minerals yields a very small error. There are also other combinations of three objectives with small delta values. All these combinations include the environmental impact minerals depletion. As mentioned before, this is because this impact is highly conflicting with the remaining criteria. Fig. 14 shows the solutions obtained from the bi-criteria problem cost vs. minerals for a lifetime of 15 years. As seen, when solving the MINLP problem with these two objectives, all solutions are kept.

Fig. 15 shows the heat exchangers network with minimum cost and minimum minerals impact (i.e, in this case both objective

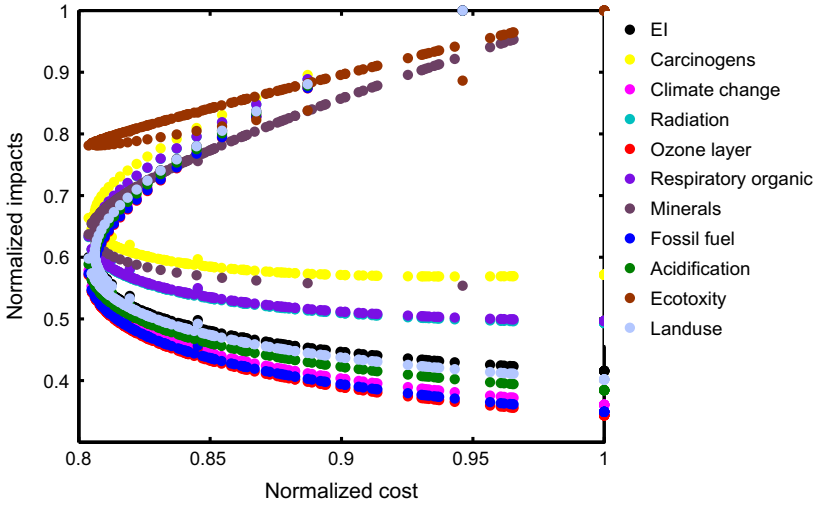

Fig. 12. Results obtained from the bi-criteria problems cost vs. single impacts for a lifetime of 1 year for example 2.

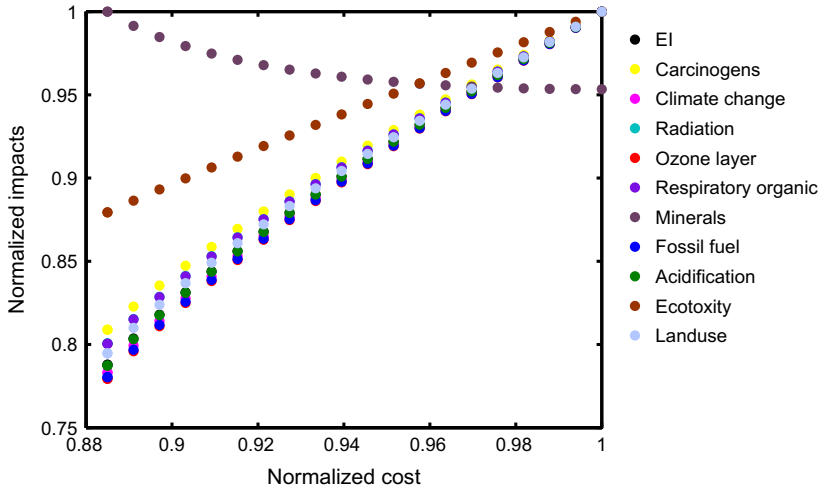

Fig. 13. Results obtained from the bi-criteria problems cost vs. single impacts for a lifetime of 15 year. Depletion of minerals is the only conflicting objective with cost for example 2.

Table 7
Delta values for example 2 for all combinations of two objectives.

Reduced set		Delta		
		1 Year	5 Years	15 Years
1	2	36.7695	20.9273	4.6649
1	3	36.7695	20.9273	4.6649
1	4	36.7695	20.9273	4.6649
1	5	36.7695	20.9273	4.6649
1	6	36.7695	20.9273	4.6649
1	7	36.7695	20.9273	4.6649
1	8	65.6591	4.6835	0.0000
1	9	36.7695	20.273	4.6649
1	10	36.7695	20.9273	4.6649
1	11	65.6591	20.9273	4.6649
1	12	36.7695	20.9273	4.6649

functions lead to the same values of the binary variables and therefore to the same structural design). Further details of these designs are displayed in Table 9. Similarly, as in the previous case, the area is decreased when the minerals impact is minimized.

Note that the results obtained in each case may depend on the LCA data used in the analysis as well as the particular features of the HEN under study. Having said that, we still think that the insight obtained in the examples can be generalized to other HENs problems, since in these systems there is a clear trade-off between the impacts caused during the operation and construction phases. The tool presented herein allows to properly asses such a trade-off and classify the LCA metrics according to their nature. This analysis reduces the problem complexity while still preserving its structure.

Table 8
Delta values for example 2 for all combinations of three objectives.

Reduced set			Delta			Reduced set			Delta		
			1 Year	5 Years	15 Years				1 Year	5 Years	15 Years
1	2	3	17.6811	59.9457	52.7001	1	5	6	32.7695	59.9457	52.7001
1	2	4	60.7897	59.9457	52.7001	1	5	7	31.4228	59.9457	52.7001
1	2	5	32.7695	59.9457	52.7001	1	5	8	1.4934	0.0153	0.0000
1	2	6	60.7897	59.9457	52.7001	1	5	9	32.7695	59.9457	52.7001
1	2	7	31.4228	59.9457	52.7001	1	5	10	32.7695	59.9457	52.7001
1	2	8	0.7320	0.0153	0.0000	1	5	11	1.4934	11.5260	41.5601
1	2	9	60.7897	59.9457	52.7001	1	5	12	32.7695	59.9457	52.7001
1	2	10	60.7897	59.9457	52.7001	1	6	7	31.4228	59.9457	52.7001
1	2	11	1.0107	11.5260	41.5601	1	6	8	0.0000	0.0000	0.0000
1	2	12	60.7897	59.9457	52.7001	1	6	9	60.7897	59.9457	52.7001
1	3	4	17.6811	59.9457	52.7001	1	6	10	60.7897	59.9457	52.7001
1	3	5	17.6811	59.9457	52.7001	1	6	11	1.0107	11.5260	41.5601
1	3	6	17.6811	59.9457	52.7001	1	6	12	60.7897	59.9457	52.7001
1	3	7	17.6811	59.9457	52.7001	1	7	8	1.4934	0.0153	0.0000
1	3	8	1.4934	0.0153	0.0000	1	7	9	31.4228	59.9457	52.7001
1	3	9	17.6811	59.9457	52.7001	1	7	10	31.4228	59.9457	52.7001
1	3	10	17.6811	59.9457	52.7001	1	7	11	1.4934	11.5260	41.5601
1	3	11	1.4934	11.5260	41.5601	1	7	12	31.4228	59.9457	52.7001
1	3	12	17.6811	59.9457	52.7001	1	8	9	0.0251	0.0000	0.0000
1	4	5	32.7695	59.9457	52.7001	1	8	10	0.7320	0.0153	0.0000
1	4	6	60.7897	59.9457	52.7001	1	8	11	1.4934	0.0153	0.0000
1	4	7	31.4228	59.9457	52.7001	1	8	12	0.7320	0.0153	0.0000
1	4	8	0.1700	0.0151	0.0000	1	9	10	60.7897	59.9457	52.7001
1	4	9	60.7897	59.9457	52.7001	1	9	11	1.0107	11.5260	41.5601
1	4	10	60.7897	59.9457	52.7001	1	9	12	60.7897	59.9457	52.7001
1	4	11	1.0107	11.5260	41.5601	1	10	11	1.0107	11.5260	41.5601
1	4	12	60.7897	59.9457	52.7001	1	10	12	60.7897	59.9457	52.7001
						1	11	12	1.0107	11.5260	41.5601

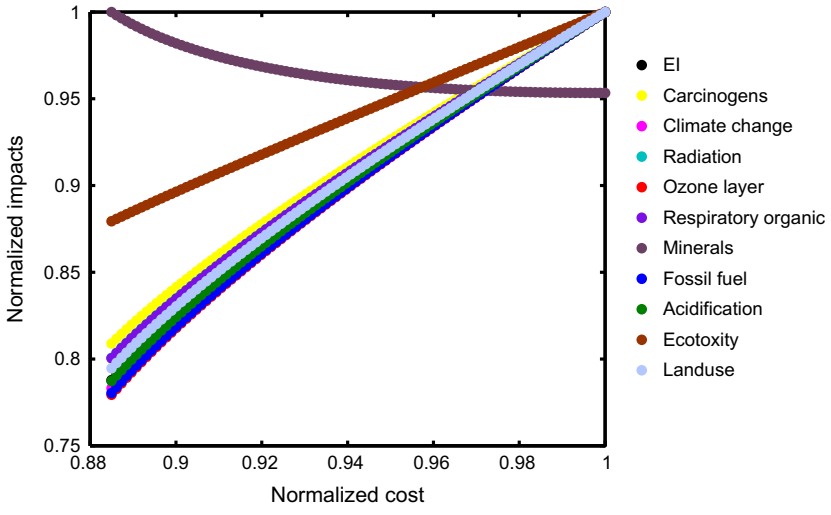

Fig. 14. Results for problem cost vs. minerals for 15 years lifetime. All solution are kept, example 2.

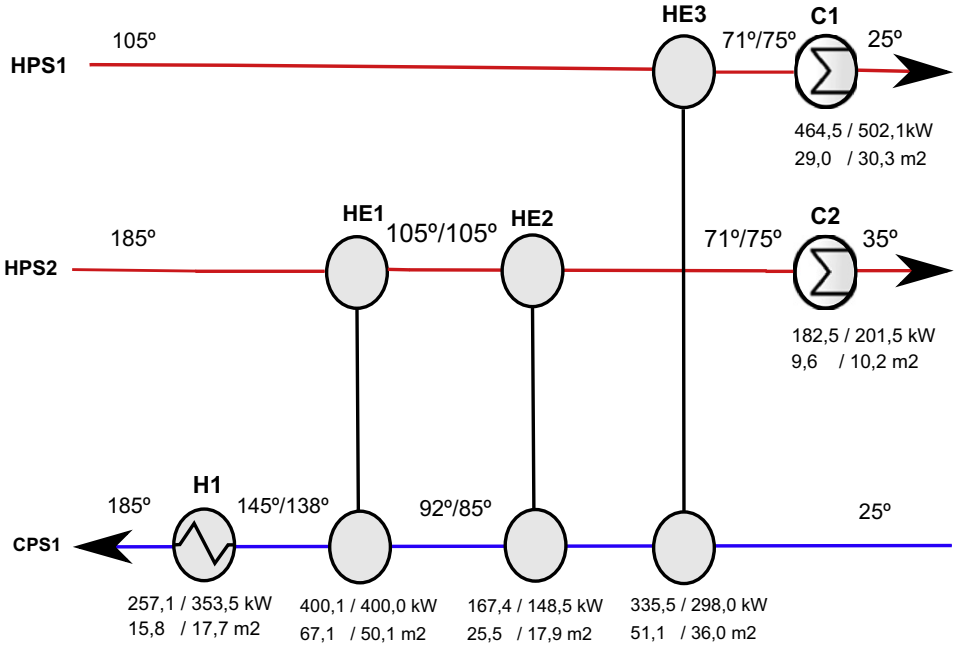

Fig. 15. Network obtained from the bi-criteria problems cost vs. minerals impact for 15 years lifetime with minimum cost/minerals for example 2.

Table 9
Results for example 2 obtained by solving problem cost vs. minerals impact for 15 years lifetime.

	Total area, m^2	Operation cost, $	Capital cost, $	Total cost, $	Minerals impact, ecopoints
Min minerals	162.1	953,960.8	187,507.4	1,141,468.2	6907.1
Min TC	198.1	810,012.3	229,574.7	1,039,587.0	7055.1

6. Conclusion

This work has addressed the optimal design of HENs considering several environmental impacts quantified according to LCA principles. It was clearly shown that the use of an aggregated indicator (i.e., Eco-indicator 99) is inadequate in this context since it leaves solutions that may be appealing for decision makers out of the analysis.

To simplify the visualization and analysis of the Pareto solution, we investigated the use of a rigorous dimensionality reduction method in the post-optimal analysis of the trade-off designs. This technique enables the identification of redundant objectives while still keeping the problem structure to the extent possible. Our approach is aimed at aiding decision-making in the design of HENs with environmental impact considerations.

Acknowledgements

The authors wish to acknowledge support from the Spanish Ministry of Education and Science (Project Nos. CTQ2009-14420-C02, ENE2011-28269-C03-03, and ENE2011-22722) and the Generalitat de Catalunya (FI programs).

Appendix A

The MINLP model of Yee & Grossmann [8] has been used as a test bed to illustrate the usefulness of dimensionality reduction methods in the design of HEN. A detailed description of the equations of the model can be found in Biegler et al. [34]. We provide next an outline of the formulation for the sake of completeness of this work.

A.1. Indices

i	hot process stream
j	cold process stream
k	stage in the superstructure
CU	cooling utility
HU	heating utility

A.2. Sets

HP	(*i*:*i* is a hot stream)
CP	(*j*:*j* is a cold utility)
ST	(*k*:*k* is a stage in the superstructure)

A.3. Parameters

TIN	inlet temperature of stream
F	heat capacity flow rate
CCU	unit cost for cold utility

(*continued on next page*)

CF	fixed charge for exchangers
β	exponent for area cost
Ω	upper bound for heat exchange
$TOUT$	outlet temperature of stream
U	overall heat transfer coefficient
h	film heat transfer coefficient
CHU	unit cost of hot utility
C	area cost coefficient
NOK	total number of stages
Γ	upper bound for temperature difference

A.4. Variables

TC	total cost
OP	operation cost
CC	capital cost
$dt_{i,j,k}$	temperature approach for match i, j at temperature location k
$dtcu_i$	temperature approach for the match of hot stream i and cold utility
$dthu_j$	temperature approach for the match of cold stream j and hot utility
$q_{i,j,k}$	heat exchanged between hot process stream i and cold process stream j in stage k
qcu_i	heat exchanged between hot process stream i and cold utility
qhu_j	heat exchanged between hot utility and cold stream j
$t_{i,k}$	temperature of hot stream i at hot end of stage k
$t_{j,k}$	temperature of cold stream j at hot end of stage k
$z_{i,j,k}$	binary variable to denote existence of match i, j in stage k
zcu_i	binary variable (1 if stream i exchanges heat with the cold utility, 0 otherwise)
zhu_j	binary variable (1 if stream j exchanges heat with the hot utility, 0 otherwise)

Overall heat balance for each stream.

$$(TIN_i - TOUT_i)F_i = \sum_{k\in ST}\sum_{j\in CP} q_{i,j,k} + qcu_i \quad i \in HP \tag{6}$$

$$(TOUT_j - TIN_j)F_j = \sum_{k\in ST}\sum_{i\in HP} q_{i,j,k} + qhu_j \quad j \in HP \tag{7}$$

Heat balance at each stage

$$(t_{i,k} - t_{i,k+1})F_i = \sum_{j\in CP} q_{i,j,k} \quad k \in ST,\ i \in HP \tag{8}$$

$$(t_{j,k} - t_{j,k+1})F_j = \sum_{i\in HP} q_{i,j,k} \quad k \in ST,\ j \in CP \tag{9}$$

Assignment of superstructure inlet temperatures

$$TIN_i = t_{i,1} \tag{10}$$

$$TIN_j = t_{j,NOK+1} \tag{11}$$

Feasibility of temperatures

$$t_{i,k} \geqslant t_{i,k+1} \quad k \in ST,\ i \in HP \tag{12}$$

$$t_{j,k} \geqslant t_{j,k+1} \quad k \in ST,\ j \in CP \tag{13}$$

$$TOUT_i \leqslant t_{i,NOK+1} \quad i \in HP \tag{14}$$

$$TOUT_j \geqslant t_{j,1} \quad j \in CP \tag{15}$$

Hot and cold utility load.

$$(t_{i,NOK+1} - TOUT_i)F_i = qcu_i \quad i \in HP \tag{16}$$

$$(TOUT_j - t_{j,1})F_j = qhu_j \quad j \in CP \tag{17}$$

Logical constraints.

$$q_{i,j,k} - \Omega z_{i,j,k} \leqslant 0 \quad i \in HP, j \in CP, k \in ST \tag{18}$$

$$qcu_i - \Omega zcu_i \leqslant 0 \quad i \in HP \tag{19}$$

$$qhu_j - \Omega zhu_j \leqslant 0 \quad j \in CP \tag{20}$$

$$z_{i,j,k}, zcu_i, zhu_j \quad \in \{0,1\} \tag{21}$$

Calculation of approach temperatures.

$$dt_{i,j,k} \leqslant t_{i,k} - t_{j,k} + \Gamma(1 - z_{i,j,k}) \quad i \in HP,\ j \in CP,\ k \in ST \tag{22}$$

$$dt_{i,j,k+1} \leqslant t_{i,k+1} - t_{j,k+1} + \Gamma(1 - z_{i,j,k}) \quad i \in HP,\ j \in CP,\ k \in ST \tag{23}$$

$$dtcu_i \leqslant t_{i,NOK+1} - TOUT_{CU} + \Gamma(1 - zcu_i) \quad i \in HP \tag{24}$$

$$dthu_j \leqslant TOUT_{HU} - t_{j,1} + \Gamma(1 - zhu_j) \quad j \in CP \tag{25}$$

$$dt_{i,j,k} \geqslant EMAT \tag{26}$$

Objective function.

$$\begin{aligned} Cost = {} & \sum_{i\in HP} CCU\ qcu_i\ year + \sum_{j\in CP} CHU\ qhu_j\ year + \\ & \sum_{i\in HP}\sum_{j\in CP}\sum_{k\in ST} CF_{ij} z_{i,j,k} + \sum_{i\in HP} CF_i^{CU} zcu_i + \sum_{j\in CP} CF_j^{HU} zhu_j + \\ & \sum_{i\in HP}\sum_{j\in CP}\sum_{k\in ST} C_{i,j} (A_{i,j,k})^{\beta_{i,j}} + \sum_{i\in HP} C_i^{CU} \left(A_i^{CU}\right)^{\beta_i^{CU}} + \sum_{j\in CP} C_j^{HU} \left(A_j^{HU}\right)^{\beta_j^{HU}} \end{aligned} \tag{27}$$

$$A_{i,j,k} = \frac{q_{i,j,k}}{U_{ij}\left[(dt_{i,j,k} dt_{i,j,k+1})^{\frac{1}{2}} (dt_{i,j,k} + dt_{i,j,k+1})\right]^{\frac{1}{3}}} \tag{28}$$

$$A_i^{CU} = \frac{qcu_i}{U_i^{CU}\left[(dtcu_i)(TOUT_i - TIN_{CU})^{\frac{1}{2}} (dtcu_i + (TOUT_i - TIN_{CU}))\right]^{\frac{1}{3}}} \tag{29}$$

$$A_j^{HU} = \frac{qhu_j}{U_j^{HU}\left[(dthu_j)(TIN_{HU} - TOUT_j)^{\frac{1}{2}} (dthu_j + (TIN_{HU} - TOUT_j))\right]^{\frac{1}{3}}} \tag{30}$$

$$\frac{1}{U_{ij}} = \frac{1}{h_i} + \frac{1}{h_j} \tag{31}$$

$$\frac{1}{U_i^{CU}} = \frac{1}{h_i} + \frac{1}{h_{cu}} \tag{32}$$

$$\frac{1}{U_j^{HU}} = \frac{1}{h_j} + \frac{1}{h_{HU}} \tag{33}$$

References

[1] Feng X, Pu J, Yang J, Hoong Chu K. Energy recovery in petrochemical complexes through heat integration retrofit analysis. Applied Energy 2011;88:1965–82.
[2] Wang Y, Pan M, Bulatov I, Smith a R, Kim J. Application of intensified heat transfer for the retrofit of heat exchanger network. Applied Energy 2012;89:45–59.
[3] Linnhoff B, Hindmarsh E. The pinch design method for heat exchanger networks. Chemical Engineering Science 1983;38(5):745–63.
[4] Linnhoff B. Pinch analysis: a state-of-the-art overview: techno-economic analysis. Chemical Engineering Research & Design 1993;71(5):503–22.
[5] Tan R, Yee Foo DC, Aviso K, Kok D. The use of graphical pinch analysis for visualizing water footprint constraints in biofuel production. Applied Energy 2009;86:605–9.
[6] Lee SC, Sum Ng DK, Yee Foo DC, Tan RR. Extended pinch targeting techniques for carbon-constrained energy sector planning. Applied Energy 2009;86:60–7.
[7] Papoulias S, Grossmann I. A structural optimization approach in process synthesis – ii:: heat recovery networks. Computers & Chemical Engineering 1983;7(6):707–21.
[8] Yee T, Grossmann I. Simultaneous optimization models for heat integration – ii. Heat exchanger network synthesis. Computers & Chemical Engineering 1990;14(10):1165–84.
[9] Yee T, Grossmann I, Kravanja Z. Simultaneous optimization models for heat integration – i. Area and energy targeting and modeling of multi-stream exchangers. Computers & Chemical Engineering 1990;14(10):1151–64.
[10] Grossmann I, Guillén-Gosálbez G. Scope for the application of mathematical programming techniques in the synthesis and planning of sustainable processes. Computers & Chemical Engineering 2010;34(9):1365–76.

[11] Stefanis S, Buxton A, Livingston A, Pistikopoulos E. A methodology for environmental impact minimization: solvent design and reaction path synthesis issues. Computers & Chemical Engineering 1996;20:1419–24.
[12] Stefanis S, Livingston A, Pistikopoulos E. Minimizing the environmental impact of process plants: a process systems methodology. Computers & Chemical Engineering 1995;19:39–44.
[13] Azapagic A, Clift R. Application of life cycle assessment to process optimization. Computers & Chemical Engineering 1999;23(10):1509–26.
[14] Gebreslassie B, Guillén-Gosálbez G, Jiménez L, Boer D. Design of environmentally conscious absorption cooling systems via multi-objective optimization and life cycle assessment. Applied Energy 2009;86(9):1712–22.
[15] Gebreslassie BH, Guillén-Gosálbez G, Jiménez L, Boer D. A systematic tool for the minimization of the life cycle impact of solar assisted absorption cooling systems. Energy 2010;35(9):3849–62.
[16] Guillén-Gosálbez G, Caballero J, Jiménez L. Application of life cycle assessment to the structural optimization of process flowsheets. Industrial & Engineering Chemistry Research 2008;47(3):777–89.
[17] Hugo A, Pistikopoulos E. Environmentally conscious long-range planning and design of supply chain networks. Journal of Cleaner Production 2005;13(15):1471–91.
[18] Guillén-Gosálbez G, Grossmann I. Optimal design and planning of sustainable chemical supply chains under uncertainty. AIChE Journal 2009;55(1):99–121.
[19] Guillén-Gosálbez G, Grossmann I. A global optimization strategy for the environmentally conscious design of chemical supply chains under uncertainty in the damage assessment model. Computers & Chemical Engineering 2010;34(1):42–58.
[20] Puigjaner L, Guillén-Gosálbez G. Towards an integrated framework for supply chain management in the batch chemical process industry. Computers & Chemical Engineering 2008;32(4-5):650–70.
[21] Pozo C, Ruíz-Femenia R, Caballero J, Guillén-Gosálbez G, Jiménez L. On the use of principal component analysis for reducing the number of environmental objectives in multi-objective optimization: application to the design of chemical supply chains. Chemical Engineering Science 2012;69(1):146–58.
[22] Mele FD, Kostin AM, Guillén-Gosálbez G, Jiménez L. Multiobjective model for more sustainable fuel supply chains. A case study of the sugar cane industry in Argentina. Industrial & Engineering Chemistry Research 2011;50(9):4939–58.
[23] Brunet R, Guillén-Gosálbez G, Jiménez L. Cleaner design of single-product biotechnological facilities through the integration of process simulation, multi-objective optimization, LCA and principal component analysis. Industrial & Engineering Chemistry Research 2012;51(1):410–24.
[24] Guillén-Gosálbez G, Mele F, Grossmann I. A bi-criterion optimization approach for the design and planning of hydrogen supply chains for vehicle use. AIChE Journal 2010;56(3):650–67.
[25] Sabio N, Kostin A, Guillén-Gosálbez G, Jiménez L. Holistic minimization of the life cycle environmental impact of hydrogen infrastructures using multi-objective optimization and principal component analysis. International Journal of Hydrogen Energy 2012;37(6):5385–405.
[26] López-Maldonado L, Ponce-Ortega J, Segovia-Hernandez J. Multiobjective synthesis of heat exchanger networks minimizing the total annual cost and the environmental impact. Applied Thermal Engineering 2011;31(6–7):1099–113.
[27] Cabezas H, Bare J, Mallick S. Pollution prevention with chemical process simulators: the generalized waste reduction (war) algorithm-full version. Computers & Chemical Engineering 1999;23(4–5):623–34.
[28] Mallick S, Cabezas H, Jane C, Sikdar S. A pollution reduction methodology for chemical process simulators. Industrial & Engineering Chemistry Research 1996;35(11):4128–38.
[29] Brockhoff D, Zitzler E. Objective reduction in evolutionary multiobjective optimization: theory and applications. Evolutionary Computation 2009;17(2):135–66.
[30] Liu H, Motoda H. Feature Extraction, Construction and Selection: A Data Mining Perspective. Kluwer Academic Pub; 1998.
[31] K. Deb, D. Saxena, On finding pareto-optimal solutions through dimensionality reduction for certain large-dimensional multi-objective optimization problems, Kangal report.
[32] Brockhoff D, Zitzler E. Are all objectives necessary? on dimensionality reduction in evolutionary multiobjective optimization. Parallel Problem Solving from Nature-PPSN 2006;IX:533–42.
[33] Guillen-Gosalbez G. A novel milp-based objective reduction method for multi-objective optimization: application to environmental problems. Computers & Chemical Engineering 2011;35(8):1469–77.
[34] Biegler L, Grossmann I, Westerberg A. Systematic Methods for Chemical Process Design. Old Tappan, NJ, United States: Prentice Hall; 1997.
[35] Ryding S. Iso 14042 environmental management. The International Journal of Life Cycle Assessment 1999;4(6):307.
[36] Ecoinvent Centre Portal, February, 2012 <http://www.ecoinvent.com/>.
[37] Ehrgott M. Multicriteria optimization, vol. 491. Springer Verlag; 2005.
[38] A. Kostin, G. Guillén-Gosálbez, F. Mele, L. Jiménez. Identifying key life cycle assessment metrics in the multiobjective design of bioethanol supply chains using a rigorous mixed-integer linear programming approach. Industrial & Engineering Chemistry Research 2012.
[39] Isafiade A, Fraser D. Interval-based minlp superstructure synthesis of heat exchange networks. Chemical Engineering Research and Design 2008;86(3):245.

7.4 Multi-objective optimization of utility plants under several environmental indicators using an MILP-based dimensionality reduction approach.

Vaskan P., Guillén-Gosálbez G., Jiménez L. Multi-objective optimization of utility plants under several environmental indicators using an MILP-based dimensionality reduction approach. Pending submission to *Applied Energy*.

Multi-objective optimization of utility plants under several environmental indicators using an MILP-based dimensionality reduction approach

Pavel Vaskan[a], Gonzalo Guillén-Gosálbez [a]*, Laureano Jiménez[a]*

[a] *Departament d'Enginyeria Quimica, Universitat Rovira i Virgili, Avinguda Països Catalans 26, 43007-Tarragona, Spain*

Abstract

We address here the multi-objective optimization of utility plants with economic and environmental concerns. Rather than optimizing a single environmental metric, which was the approach followed in the past, we focus on optimizing these systems considering simultaneously several environmental indicators based on life cycle assessment (LCA) principles. We couple the multi-objective model of the plant with an MILP-based dimensionality reduction method that allows identifying key environmental metrics that exhibit the property that their optimization will very likely improve the system simultaneously in all of the remaining damage categories. This analysis reduces the complexity of the underlying multi-objective optimization problem from the viewpoints of generation and interpretation of its solutions. The capabilities of the proposed method are illustrated through a case study based on a real industrial scenario, in which we show that a few number of environmental indicators suffices to optimize the environmental performance of the plant.

Keywords: dimensionality reduction method, energy systems, life cycle assessment, utility systems.

1. Introduction

The adoption of more sustainable technologies in industry is a central topic in sustainability and green engineering. Particularly, the design and planning of efficient energy systems capable of satisfying a given power and steam demand has recently gained wider interest in this field [1].

Several methods are available in the literature for the synthesis of utility plants. They can be roughly classified into two main groups. The first are based on thermodynamic targets and heuristics [2, 3]. As pointed out by Bruno et al. [4], their main drawback is that even if the design with highest thermal efficiency is obtained, it may not be economically attractive because capital costs may be too high. The second group, to which the present work belongs, relies on rigorous optimization techniques based on mathematical programming (i.e., linear, non-linear, mixed-integer linear, and mixed-integer non-linear programming -LP, NLP, MILP and MINLP, respectively). Optimization approaches based on LP and MILP techniques were originally introduced by Nishio and Johnson [5], Papoulias and Grossmann [6], and Petroulas and Reklaitis [7]. Later on, Hui and Natori [8] developed an MINLP model for the optimization of site utility systems, while Bruno et al.[4] proposed an MINLP formulation for the design of utility systems.

These strategies have traditionally focused on optimizing the utility plant considering the economic performance as unique criterion and disregarding the environmental

*Corresponding author
Email addresses: pavel.vaskan@urv.cat (Pavel Vaskan[a]), gonzalo.guillen@urv.cat (Gonzalo Guillén-Gosálbez [a]), laureano.jimenez@urv.cat (Laureano Jiménez[a])

impact [4, 9, 10]. The design task, however, can be rather formulated as a multi-objective decision-making problem that embeds environmental concerns. This approach allows identifying solutions in which the economic and environmental performance are both simultaneously optimized. A key point in the use of multi-objective optimization as applied to the development of more sustainable processes concerns the assessment of the environmental performance of the system. Among the tools available, Life Cycle Assessment (LCA) has recently gained wider attention in the environmental engineering community. The integration of LCA and multi-objective optimization results in a powerful quantitative tool that facilitates the environmentally conscious design and planning of industrial processes.

Livingston and Pistikopoulous [11, 12] were the first to propose the combined use of multi-objective optimization (MOO) and LCA principles. In the resent past, this approach has been applied to a wide variety of industrial problems, such as the design of chemical plants [15], the strategic planning of supply chains [16–19], the design of heat exchanger networks[20], the design of solar energy plants [21], the design of hydrogen infrastructures [22, 23], and the design and planning of energy systems [1], among others.

Defining a suitable LCA metric to drive the optimization of an energy system is of paramount importance. A plethora of LCA-based indicators are nowadays available for quantifying the impact in several damage categories. The simultaneous optimization of all of them would lead to highly complex models extremely difficult to solve. The prevalent approach to overcome this limitation is to use aggregated metrics that translate several environmental metrics into a single indicator defined by attaching weights to

them. Following this approach, most authors have developed bi-criteria models where the economic performance is traded-off against a single environmental indicator obtained as a weighted sum of individual impacts [24, 25]. This approach simplifies the analysis to a large extent, but has two main drawbacks. The first is that the weights used may not necessarily reflect the decision-makers' preferences. The second is that their optimization might change the structure of the problem, in a manner such that some optimal solutions might be left out of the analysis.

Multi-dimensionality reduction methods aim to overcome these limitations [26]. They allow identifying redundant objectives that can be omitted while still preserving the problem structure to the extent possible. Particularly, Deb and Saxena [29] were the first to investigate dimensionality reduction in MOO. They developed a statistical method based on principal component analysis (PCA) for eliminating non-essential objectives in MOO problems, thereby simplifying the associated calculations. Brockhoff-Zitzler [29] proposed an alternative dimensionality reduction approach based on identifying those objectives whose elimination changes to the minimum extent possible the dominance structure of the multi-objective problem. They formally stated two problems: calculating the smallest objective subset that preserves the dominance structure considering a fixed approximation error; and computing the minimum error for a subset of objectives of given size. The same authors proposed two algorithms to solve these problems, one exhaustive and another one heuristic. More recently, Guillén-Gosálbez [30] proposed an alternative MILP-based method to solve both problems [20] that takes advantage of the latest branch-and-cut methods for MILP.

In this work we optimize utility plants under different environmental metrics and study the relationships between environmental indicators using a rigorous dimensionality reduction strategy. The approach presented relies on the combined use of multi-objective optimization, LCA analysis and dimensionality reduction methods. We first pose the planning task as a multi-objective mixed-integer linear problem (MILP) that simultaneously accounts for the minimization of the cost and environmental impact of the energy system. The environmental performance of the system is quantified using several LCA-based indicators that quantify the damage caused in different categories. We then apply a dimensionality reduction technique to facilitate the post-optimal analysis of the solutions found.

The paper is organized as follows. Section 2 presents a formal definition of the problem under study. In section 3, the mathematical formulation derived to address this problem is presented. Section 4 describes the solution strategy employed to solve the MILP model and the dimensionality reduction strategy. In section 5 the capabilities of the proposed modeling framework and solution strategy are illustrated through two case studies, while in Section 6 we present the conclusions of the work.

2. Problem statement

Given is an electricity and steam demand at various pressure levels to be satisfied Environmental data associated with the production and combustion of fuels as well as with the process of electricity generation are also provided. The objective is to determine the set of planning decisions that simultaneously minimize the total cost and the associated

environmental impact. Decisions to be made include the amounts and types of fuels to be burnt in the boilers and turbines of the system, along with the amount of electricity purchased from an external supplier. The formulation presented in the next section includes empirical models for tanks, boilers and mixers that reproduce the behavior of a standard utility plant.

3. Mathematical formulation

Energy systems utilize fuel, air and other materials to generate electricity and steam demanded by other process units of an industrial system (see Figure 1). The system taken as reference in this work consists of storage tanks to store a set of fuels, boilers that convert fuels into steam at high pressure, and turbines that expand higher pressure steam into lower pressure steam in order to generate electricity.

The flows of materials in the units are denoted by the continuous variables x^{FU}_{jltm} (fuel), x^{HP}_{jlt}, x^{MP}_{jlt}, x^{LP}_{jlt} (steam at high, medium and low pressure, respectively), x^{CO}_{jlt} (condensate) and x^{EL}_{jlt} (electricity). In these variables, the subscript j represents the process unit of the system to which the flow is referred (i.e., tanks, boilers or turbines), l denotes the state of the material (i.e., input or output), and t indicates the time period. Note that there are m different types of fuel available in the system.

The overall problem is formulated as a generalized disjunctive programming (GDP) model that involves Boolean and continuous variables. In this GDP problem, logic decisions correspond to the selection of a specific fuel type from a set of available choices. The complete formulation is described in detail in the next sections.

3.1. Fuel tank models

Fuel tanks can contain different types of fuels that are combusted in the boilers in order to generate HP steam. There are several reasons for considering alternative fuels instead of a single one. One of them is the lack of a certain fuel type due to problems in the supply in a given time period. Another possible reason is the inclusion of economically and/or environmentally attractive fuels in order to improve the economic performance of the system and/or minimize its environmental impact. Specifically, the selection of a specific fuel m in a tank j in period t, can be modeled via the following disjunction:

$$\begin{bmatrix} Y_{jtm} \\ TFC_{jtm} = cost^{FU}_{mt}\theta x^{FU}_{jltm} \qquad l = IN \\ INV_{jtm} = INV_{jt-1m} + \theta x^{FU}_{jltm} - \\ \theta x^{FU}_{jl'tm} \qquad l = IN, l' = OUT \\ \underline{x^{FU}_{jltm}} \leq x^{FU}_{jltm} \leq \overline{x^{FU}_{jltm}} \quad l = IN, OUT \\ \underline{INV_{jtm}} \leq INV_{jtm} \overline{\leq INV_{jtm}} \end{bmatrix} \vee \begin{bmatrix} \neg Y_{jtm} \\ TFC_{jtm} = 0 \\ x^{FU}_{jltm} = 0 \quad l = IN, OUT \\ INV_{jtm} = 0 \end{bmatrix}$$

$$Y_{jtm} \in \{True, False\} \qquad \forall m, t, j \in TANKS \tag{1}$$

If fuel m is stored in tank j in period t, then the Boolean variable Y_{jtm}, will hold True, and the total fuel cost (TFC_{jtm}) and the inventory level in the tank (INV_{jtm}) will take on

positive values that will be calculated using specific equations. If Y_{jtm} is False, all the constraints in the corresponding disjunction will be ignored, and the associated variables set to zero.

The total fuel cost (TFC_{jtm}) is calculated from the fuel consumption and the fuel cost in period t ($cost_{mt}^{FU}$) if the Boolean variable is True, and it is set to zero otherwise. Here, θ represents the duration of each period t. The inventory level in the tank is given by the materials balance, which states that the initial inventory (INV_{jt-1}) plus the amount of fuel introduced in the tank minus the amount transferred from the tank to the boilers must equal the final inventory. The disjunction imposes also lower and upper limits on the mass flows and inventory levels of the fuels ($\underline{x_{jltm}^{FU}}$, $\underline{INV_{jtm}}$, $\overline{x_{jltm}^{FU}}$ and $\overline{INV_{jtm}}$, respectively), if the corresponding fuel is selected, and set them to zero otherwise.

3.2. Boiler models

Boilers generate high pressure steam by burning fuel. The combustion process generates environmentally harmful chemical substances such as SO_x, NO_x, and CO_x. These units require electricity for operating the mechanical equipment and medium pressure steam for heating the feed water. Similarly, as with the tanks, boilers can utilize different fuels with some adjustments in the operating conditions of their equipment. The boilers

are modeled via the following disjunctions:

$$\begin{bmatrix} Y_{jtm} \\ x^{HP}_{jlt} = \frac{hc_m}{\eta_{jm}} x^{FU}_{jl'tm} \quad l = OUT, l' = IN \\ \underline{x^{FU}_{jltm}} \leq x^{FU}_{jltm} \leq \overline{x^{FU}_{jltm}} \quad l = IN \end{bmatrix} \vee \begin{bmatrix} \neg Y_{jtm} \\ x^{HP}_{jlt} = 0 \quad l = OUT \\ x^{FU}_{jltm} = 0 \quad l = IN \end{bmatrix}$$

$$Y_{jtm} \in \{True, False\} \qquad \forall m, t, j \in BOILERS \tag{2}$$

As observed, when Y_{jtm} is True, the amount of HP steam is calculated from the amount of fuel consumed, the heat of combustion of the selected fuel (hc_m), and the boiler efficiency (η_{jm}). Besides, lower and upper bounds are imposed on the total fuel consumption. On the other hand, when Y_{jtm} is False, the fuel consumption in the boiler and the amount of steam generated are both set to zero.

The amount of HP steam generated is also a function of the consumption of MP steam and electricity, as stated in Eqs. 3 and 4.

$$x^{HP}_{jlt} = a^{MP}_j x^{MP}_{jl't} \qquad \forall t, j \in BOILERS, l = OUT, l' = IN \tag{3}$$

$$x^{HP}_{jlt} = a^{EL}_j x^{EL}_{jl't} \qquad \forall t, j \in BOILERS, l = OUT, l' = IN \tag{4}$$

In these equations, a_j^{MP} and a_j^{EL} represent the materials balance coefficients that relate the amount of HP steam generated in boiler j with the consumption of MP steam and electricity.

The total amount of fuel consumed in the boilers must equal the amount sent from the storage tanks:

$$\sum_{j \in BOILERS} x_{jltm}^{FU} = \sum_{j' \in TANKS} x_{j'l'tm}^{FU} \qquad \forall t, m, l = IN, l' = OUT \tag{5}$$

Note that Eqs. 3 to 5 must be satisfied regardless of the fuel selected, and hence can be placed outside the disjunction.

3.3. Turbine models

Turbines expand steam at higher pressure converting the mechanical energy released during the expansion into electricity. A typical multi-stage turbine receives HP steam and produces electricity, MP and LP steams, and condensate, as shown in in Figure1. Electricity generation in a turbine is a function of the amount of HP steam feed, and the amounts of MP and LP steam, and condensate generated, as shown in Eq. 6.

$$\begin{aligned} x_{jlt}^{EL} = b_j^{HP} x_{jl't}^{HP} - g_j^{MP} x_{jlt}^{MP} - g_j^{LP} x_{jlt}^{LP} - g_j^{CO} x_{jlt}^{CO} \\ \forall t, j \in TURBINES, l = OUT, l' = IN \end{aligned} \tag{6}$$

In Eq. 6, the coefficients b_j^{HP}, g_j^{MP}, g_j^{LP} and g_j^{CO} can be obtained by performing a statistical analysis on the existing process data. The upper and lower bounds on the amount of

electricity generated in turbines are defined via Eq. 7.

$$\underline{x_{jlt}^{EL}} \leq x_{jkl} \leq \overline{x_{jlt}^{EL}} \qquad \forall j,t,l = OUT \tag{7}$$

The material balance around turbines is expressed in Eq. 8 8:

$$x_{jlt}^{HP} = x_{jl't}^{MP} + x_{jl't}^{LP} + x_{jl't}^{CO} \qquad \forall t, j \in TURBINES, l = IN, l' = OUT \tag{8}$$

3.4. Demand satisfaction

The demand of electricity, HP, MP and LP steam must be fulfilled in each time period, as stated in constraints 9 to 12:

$$\sum_{j \in TURBINES} \sum_{l \in OUT} \theta x_{jlt}^{EL} + EPU_t - \sum_{j \in BOILERS} \sum_{l \in IN} \theta x_{jlt}^{EL} \geq dem_t^{EL} \tag{9}$$

$$\sum_{j \in BOILERS} \sum_{l \in OUT} \theta x_{jlt}^{HP} - \sum_{j \in TURBINES} \sum_{l \in IN} \theta x_{jlt}^{HP} \geq dem_t^{HP} \tag{10}$$

$$\sum_{j \in TURBINES} \sum_{l \in OUT} \theta x_{jlt}^{MP} - \sum_{j \in BOILERS} \sum_{l \in IN} \theta x_{jlt}^{MP} \geq dem_t^{MP} \tag{11}$$

$$\sum_{j \in TURBINES} \sum_{l \in OUT} \theta x_{jlt}^{LP} \geq dem_t^{LP} \tag{12}$$

Here dem_t^{EL}, dem_t^{HP}, dem_t^{MP} and dem_t^{LP} denote the demands of electricity, HP, MP and LP steam in period t, whereas EPU_t represents the total amount of electricity purchased from the external supplier. Hence, Eq.9 considers that part of the electricity demand can be satisfied by an external supplier (i.e., outsourcing). Note that in Eq. 10, the amount of HP steam available is calculated from the steam generated in the boiler minus the amount consumed in the turbine. Similarly, in Eq. 11, the total amount of MP steam available is obtained by subtracting the consumption of steam in the boiler from the amount of MP steam produced in the turbine.

3.5. Objective function

The model presented must attain two targets: minimum cost and environmental impact. We next describe in detail how to determine both objectives.

3.5.1. Total cost

The total cost of the energy system includes the cost of the fuel purchased, the inventory cost associated with holding fuel in the tanks, and the consumption of external

electricity, as stated in Eq. 13:

$$TC = \sum_{j \in TANKS} \sum_{t} \sum_{m} TFC_{jtm} + \sum_{j \in TANKS} \sum_{t} \sum_{m} cost_{mt}^{INV} \left(\frac{INV_{jt-1m}^{FU} + INV_{jtm}^{FU}}{2} \right) + \sum_{t} cost_{t}^{EL} EPU_{t} \quad (13)$$

Here, $cost_{mt}^{INV}$ represents the unitary inventory cost associated with fuel m and period t, and $cost_{t}^{EL}$ is the electricity cost in period t.

3.5.2. *Environmental impact objective function.*

The environmental performance of the energy system is quantified according to the principles of Life Cycle Assessment (LCA) [31]. Specifically, this work makes use of the Eco-indicator 99 framework, which accounts for 11 impacts aggregated into three damage categories. The computation of this metric follows the four LCA phases: goal and scope definition, inventory analysis, impact assessment and interpretation. Such phases are described in detail in the next sections.

1. Goal and scope definition. In this phase, the system boundaries and the impact categories are identified. Specifically, we perform a "cradle-to-grave" analysis that embraces all the activities of the energy system, starting from the extraction of raw materials (i.e., oil), and ending with the delivery of electricity and steam to the final customers. Eleven impact categories, as defined by the Eco-indicator 99, are considered:

1. Carcinogenic effects on humans.
2. Respiratory effects on humans caused by organic substances.

3. Respiratory effects on humans caused by inorganic substances.
4. Damage to human health caused by climate change.
5. Human health effects caused by ionizing radiations.
6. Human health effects caused by ozone layer depletion.
7. Damage to ecosystem quality caused by ecosystem toxic emissions.
8. Damage to ecosystem quality caused by the combined effect of acidification and eutrophication.
9. Damage to ecosystem quality caused by land occupation and land conversion.
10. Damage to resources caused by extraction of minerals.
11. Damage to resources caused by extraction of fossil fuels.

2. Inventory analysis. The second phase of the LCA provides the inputs and outputs of materials and energy associated with the process (Life Cycle Inventory), which are required to perform the environmental impact calculations. In the context of the energy system, the environmental burdens are given by the production of fuels at the refineries (LCI_b^{FU}), the generation of the external electricity (LCI_b^{EL}), and the direct emissions associated with the combustion of the fuels in the boilers (LCI_b^{DE}). Mathematically, the inventory of emissions can be expressed as a function of some continuous decision vari-

ables of the model, as stated in Eq. 14.

$$LCI_b = LCI_b^{FU} + LCI_b^{EL} + LCI_b^{DE} = \sum_{j \in TANKS} \sum_{l=IN} \sum_t \sum_m \omega_m^{FU} \theta x_{jltm}^{FU} + \sum_t \omega^{EL} EPU_t + \sum_{j \in BOILERS} \sum_{l=IN} \sum_t \sum_m \omega_m^{DE} \theta x_{jltm}^{FU} \quad (14)$$

Here, ω_m^{FU}, ω^{EL} and ω_m^{DE} denote the life cycle inventory entries (i.e., feedstock requirements and emissions released) associated with chemical b per reference flow of activity. In the production of fuels and electricity, the reference flow is one unit of fuel (ton) and electricity(kW), respectively, generated. In the combustion of fuel, the reference flow is one unit of fuel combusted in the boilers.

3. Impact assessment. In this step, we determine the environmental impact of the process using a damage assessment model. These impacts are further aggregated into three main damage categories: human health (expressed in DALYs), ecosystem quality (PDFm2yr), and damages to resources (MJ surplus energy). Mathematically, the damage caused in each impact category c belonging to damage category d (IM_c) is calculated from the life cycle inventory and a set of damage factors (df_{bc}), as stated in Eq. 15.

$$IM_c = \sum_b df_{bc} LCI_b \qquad \forall c \quad (15)$$

The damage factors link the LCI results with the damage in each impact category. There

are three different damage models each of which reflects a different perspective based on Cultural Theory [32]. The impact caused in each damage category can be calculated via Eq. 16:

$$DAM_d = \sum_{c \in ID(d)} IM_c \qquad \forall d \tag{16}$$

Here, $ID(d)$ denotes the set of impact categories c that contribute to damage d. Finally, the damages are normalized and aggregated into a single impact factor (i.e., Eco-indicator 99), as stated in Eq. 17.

$$ECO_{99} = \sum_d n_d w_d \cdot DAM_d \tag{17}$$

This equation makes use of normalization (n_d) and weighting (w_d) factors specified in the Eco-indicator 99 methodology [32].

4. Interpretation. Finally, in the fourth phase, the results are analyzed and a set of conclusions or recommendations are formulated. In our work, the decision-makers' preferences are articulated in the post-optimal analysis of the Pareto optimal solutions.

4. Proposed approach

The methodology followed to solve the multi-objective model describe above comprises several steps. We start by generating a set of solutions of the original multi-objective model using a heuristic-based approach that decomposes it into a set of bi-criteria problems in which we optimize the cost against each single impact. The Pareto solutions generated in this manner are next normalized, and finally used to carry out an MILP-based dimensionality reduction analysis that identifies redundant objectives that can be omitted without disturbing the main features of the problem. We describe in the ensuing sections each of these steps in detail.

5. Solution strategy

5.1. ϵ - constrain method.

The overall bi-criteria GDP can be expressed as follows:

$$\min Z = (TC, EI(ECO99, EI_1, EI_2, ..., EI_{11}))$$

$$\begin{bmatrix} Y_i \\ h_j(x) \leq 0 \\ c_j = \gamma_j \end{bmatrix} \vee \begin{bmatrix} \neg Y_i \\ B_j x = 0 \\ c_j = 0 \end{bmatrix} \qquad i \in D$$

$$\Omega(Y) = TRUE$$

$$x \geq 0 \qquad c_j \geq 0 \qquad Y_i \in \{True, False\}$$

Using the convex hull reformulation technique [33], the GDP is reformulated into a bi-criteria mixed-integer linear programming (MILP) model of the following type:

$$\begin{aligned} \textbf{(MO)} \quad \min_{x,y} \quad & (TC, EI(ECO99, EI_1, EI_2, ..., EI_{11})) \\ \text{s.t.} \quad & g(x,y) \leq 0 \\ & h(x,y) = 0 \\ & x \in \mathbb{R}, y \in \{0,1\} \end{aligned}$$

in which TC is the total cost, EI denotes the LCA impact ($ECO99$ is the overall environmental impacts and $EI_1, EI_2, .., EI_{11}$ represent 11 difference impact categories 3.5.2), while x denotes the continuous variables (mass flows, inventory levels and costs), and y the binary variables that replace the Boolean variables appearing in the GDP model.

As already mentioned, the Pareto points of model MO are computed following an heuristic-based approach based on solving a series of bi-criteria problems in which the cost is traded-off against each single impact category [34]. Each of these bi-criteria problems is calculated via the epsilon-constraint method [35], which solves a set of single objective problems, in each of which one objective is optimized and the other is transferred to an auxiliary constraint that bounds it within some allowable levels. We then normalize the Pareto solutions by dividing each objective value by the maximum value attained by the objective in all of the solutions.

5.2. Post-optimal analysis: dimensionality reduction methods.

After normalizing the solutions, we apply a dimensionality reduction method based on the work by Guillén-Gosálbez [30]. The multi-objective model presented above contains a large number of environmental metrics, which makes it difficult to generate and

analyze the Pareto solutions. Dimensionality reduction methods identify redundant objectives that can be removed, which facilitates the generation and post-optimal analysis of the solutions.

We use a simple illustrative example to clarify how dimensionality reduction works. To derive our approach, we consider the concept of weakly Pareto efficiency. A solution A is called weakly efficient if there are no other solutions that are strictly better than A simultaneously in all of the objectives. Let us now consider 4 weakly efficient solutions of a multi-objective problem (solutions A, B, C and D) that optimize 4 objective functions $F = f_1, f_2, f_3, f_4$ (i.e., we aim to minimize all of them simultaneously). Figure 2 is a parallel coordinates plot which shows in the bottom axis the different objective functions and in the vertical axis the normalized values attained by each solution in every objective. As seen, in this case, the four solutions are weakly Pareto efficient. This is because no solution improves any of the others simultaneously in all of the objectives. This is reflected also in the fact that all of the lines representing the Pareto solutions intersect in at least one point.

Let us now assume that we remove one objective from the search space, let us say objective f_4. Figure 3 depicts the dominance structure of the reduced space $F' = f_1, f_2, f_3$. We can see that now sol. C dominates solution D in the reduced space, since C is better than D in all of the objectives kept. Hence, removing f_4 changes the dominance structure of the problem, as solution D becomes sub-optimal in the reduced space F'.

B and Z proposed a metric to quantify the extent to which the initial dominance structure of a problem changes after removing objectives. This metric, termed delta error, cor-

responds to the difference between the true value of objective f_4 in solution C, and the value required to dominate solution D in the original space of objectives (see Figure 2). In our example, the reduced objective set $F' = f_1, f_2, f_3$, could therefore replace the original set $F = f_1, f_2, f_3, f_4$, assuming a delta error of 0.25.

If we next omit two objectives, say f_4 and f_3, we find that solution C becomes dominated by solution D and B (see Figure 4). In this case, the delta error is 0.5, as it is the maximum value that we have to subtract to the solutions lost so as to be dominated in the original objectives space (and not only in the reduced objectives space) (see Figure 2). Hence, it is clear that higher delta values imply greater changes in the dominance structure of the problem.

Note that the delta value depends on the objectives removed. As an example, discarding the second and third objectives (reduced space $F''' = f_1, f_4$) produces no changes in the dominance structure, since all the solutions are kept (see Figure 5.). In this case, we say that the reduced objective set $F''' = f_1, f_4$ is non-conflicting with the original one $F = f_1, f_2, f_3, f_4$. That implies that F''' can be replaced by F without changing the dominance structure of the problem (delta error = 0). The goal of dimensionality reduction methods is therefore to identify objectives that can be removed with a minimum change in the dominance structure of the problem (i.e., minimum delta error).

In this work we employ an MILP-based dimensionality reduction method introduced by Guillén-Gosálbez [30]. This method identifies redundant objectives that can be omitted from the analysis incurring in minimum delta error. Further details on this method can be found elsewhere [30], [20], [36], [37].

6. Case study

We illustrate the capabilities of our modeling framework and solution strategy using two case studies that address the optimal planning of an energy system with two fuel tanks, two boilers and two turbines (see Figure 6). Both case studies assume the same data concerning fuels types, equipment units and energy demands, but differ in the characteristics of the electricity purchased. We minimize 13 objectives (i.e., total cost and 12 LCA impacts). As environmental objectives, we consider the total Eco-indicator 99, which combines 11 single impacts into a single aggregated metric. To calculate these LCA metrics, we employ data retrieved from environmental databases [38]. The motivation for optimizing the Eco-indicator 99 along with its single impacts is to analyze whether the minimization of an aggregated impact is a good practice when optimizing utility systems (i.e., it preserves the problem structure). As will be shown next, the suitability of the Eco-indicator 99 depends on the problem data.

The initial demand of electricity is 29 MW/hr for both examples. The initial demand of steam (HP, MP and LP) is 2 ton/hr, 92 ton/hr and 98 ton/hr, respectively. A 5% increase in this demand is assumed in every time period. The model covers 7 time periods of 48 hours each. Fuels data are given in Tables 1 and 2. The parameters associated with boilers and turbines are displayed in Tables 3 and 4. The capacity of tanks 1 and 2 are 120 and 50 tons, respectively. The maximum electricity power provided by each turbine is 70 MW. The LCI data associated with the production of the different fuels are presented in Table 5, while the impacts associated with the external electricity are displayed in Table

6. The parameters of the damage model were taken from the Eco-indicator 99 report [32], assuming the average weighting set and the hierarchic perspective.

6.1. *Example 1.*

In this example we consider an external electricity provider (i.e., electricity mix) with a high environmental impact (see Table 6) and low price (2 $/MWh). We calculate 240 Pareto solutions by optimizing each single environmental objective vs the total cost. Figure 7 is a parallel coordinates plot that depicts in the horizontal axis the different objective functions, and in the vertical axis the normalized value attained by each solution in every objective. The normalization is performed by dividing each objective value by the maximum one attained over all the solutions. As observed, the environmental objectives seem to be equivalent, as when one increases so do the others and vice-versa. Hence, the cost on the one hand, and the environmental impacts on the other, behave in an opposite manner, that is, decreasing the first increases the second ones and vice-versa.

Figure 8 depicts the normalized results. The bottom axis shows the normalized total cost and the vertical one the normalized environmental impacts. In the figure, we depict all the solutions in the 2-D space (Eco-indicator 99, cost). The blue squares represent the solutions obtained when optimizing the Eco-indicator 99 against the cost, while the red circles are the solutions resulting from the optimization of the total cost against each single impact category. As observed, the optimization of the Eco-indicator 99 produces solutions that are quite close to those obtained when optimizing each single impact category separately. This observation is therefore consistent with the analysis of the parallel

coordinates plot, where we observed that all the indicators behave similarly.

Note that every solution implies a different combination of fuel and electricity (see Table 7). For example, in solution A (i.e., minimum cost solution in Figure 8), one part of the electricity is purchased from an external supplier, whereas another part is generated from fuel 2. In solution B, the main part of electricity is generated from fuel 2, whereas in solution C the main part is generated from fuel 3. The reason why all of the environmental impacts behave similarly and the cost is conflictive with them is that the cost depends to a large extent on the amount of fuels purchased, while the environmental metrics depend largely on the electricity consumption.

Turning back our attention to Figure 8, we can see how the Pareto curve Eco-indicator 99 vs cost (blue circles in the figure) is rather smooth in the region that goes from B to C, whereas from A to B increases sharply (when the model decides to increase the amount of electricity purchased from outside).

We use next the MILP for dimensionality reduction [20, 30] to uncover the relationships between the different environmental indicators. Figure 9 shows the minimum delta value for different number of objectives kept. As observed, the delta error diminishes with the number of objectives retained. From one to two, this drop is quite significant, while afterwards (as we increase further the number of objectives kept) is close to zero and flat. This is because, as mentioned before, all the impacts behave similarly and one of them is enough to capture the behavior of the remaining ones.

Table 8 shows the delta value corresponding to every possible combination of cost vs. each single environmental impact. All combinations of cost and impact yield a very

small approximation error (delta value). Hence, the original multi-objective problem can be replaced by a bi-criteria one (that optimizes cost against any environmental impact) without significant changes in the problem structure.

6.2. Example 2.

Here we consider an external electricity with high price (243 $/MW*hr) and low environmental impact (see Table 6). This electricity is assumed to be generated by wind energy. We calculate again 240 Pareto solutions by optimizing each single environmental objective vs. the total cost.

Figure 10 presents the normalized values for every objective in a parallel coordinates plot. As observed, some objectives behave in a conflictive manner. Particularly, climate change is conflicting with other objectives, since solutions with low climate change impact show large impacts in other categories and vice-versa. As will be explained later, these conflicts arise when the same decision variable shows opposite contributions in different environmental impacts.

In Figure 11, the bottom axis shows the normalized total cost and the vertical one the normalized Eco-indicator 99. The blue points are the solutions to the bi-criteria problem Eco-indicator 99 vs. total cost, while red points are associated with the remaining bi-criteria problems (total cost vs. each single impact category). As oppose to the previous example, in this case we notice that some solutions would be discarded if cost and Eco-indicator 99 were the only objectives being minimized. This is because solutions that are optimal in the space of individual objectives (when optimizing some individual ob-

jectives vs the total cost) would be lost if we optimized only the Eco-indicator 99 vs the total cost.

Concerning the planning decisions behind each solution (see Table 9), we find that in solution *A* (i.e., minimum cost solution) the electricity is mainly generated from fuel 2, in solution *B* (an intermediate solution), electricity is generated from fuels 2 and 4, while solution *C* (minimum Eco-indicator 99 point) employs fuel 1.

To shed further light on this issue, we next apply the MILP-based dimensionality reduction method. Figure 12 shows the minimum delta value for different sets of objectives kept. As observed, the delta error diminishes with the number of objectives retained. Comparing with example 1 (Figure 9), we see that two objectives are not enough for keeping the problem structure, since no combination of two criteria preserves all the Pareto solutions.

Table 10 displays the delta value corresponding to every possible combination of cost vs each single environmental impact, while Table 11 shows the same information, but this time for sets of 3 objectives. The best combination of two objectives is cost and climate change (1,6). For three objectives, the best combination of criteria is cost, respiratory effects (inorganic) and climate change (1, 5, 6), which yields a delta error close to zero. In contrast, the couple cost and Eco-indicator 99 leads to large delta values (i.e., 4.2). These results indicate that the use of the Eco-indicator 99 as unique environmental metric might be inadequate in the design of utility systems, since it might prevent the identification of Pareto solutions that minimize other impacts and that are therefore potentially appealing for decision-makers.

7. Conclusion

This work proposed an approach to optimize utility plants considering the cost and several environmental indicators simultaneously. The environmental impact associated with the energy system has been assessed through the Eco-indicator 99, which is based on LCA principles. The overall problem was formulated as a multi-objective MILP featuring a large number of objectives.

To overcome the numerical difficulties associated with the calculation and analysis of the Pareto solutions, we investigated the use of a rigorous dimensionality reduction method. Numerical examples show that the number of environmental objectives can be greatly reduced while still preserving the problem structure to a large extent. We observed also that the single optimization of aggregated metrics, such as the widely used Eco-indicator 99, might change the dominance structure of the problem in a manner such that some solutions that are optimal in the original space of LCA impacts, might be lost. Our overall approach is intended to facilitate the identification of more sustainable manufacturing patterns in industry.

8. Acknowledgments

The authors wish to acknowledge support from the Spanish Ministry of Education and Science (Projects (CTQ2012-37039-C02, DPI2012-37154-C02-02 and ENE2011-28269-C03-03) and the Generalitat de Catalunya (FI programs).

[1] A. Eliceche, S. Corvalan, P. Martinez, Environmental life cycle impact as a tool for process optimisation of a utility plant, Computers & chemical engineering 31 (5-6) (2007) 648–656.

[2] C. Chou, Y. Shih, A thermodynamic approach to the design and synthesis of plant utility systems, Industrial & engineering chemistry research 26 (6) (1987) 1100–1108.

[3] M. Nishio, J. Itoh, K. Shiroko, T. Umeda, A thermodynamic approach to steam-power system design, Industrial & Engineering Chemistry Process Design and Development 19 (2) (1980) 306–312.

[4] J. Bruno, F. Fernandez, F. Castells, I. Grossmann, A rigorous minlp model for the optimal synthesis and operation of utility plants, Chemical Engineering Research and Design 76 (3) (1998) 246–258.

[5] M. Nishio, A. Johnson, Strategy for energy system expansion, Chemical Engineering Progress (1977) 73–79.

[6] S. Papoulias, I. Grossmann, A structural optimization approach in process synthesis–i:: Utility systems, Computers & chemical engineering 7 (6) (1983) 695–706.

[7] T. Petroulas, G. Reklaitis, Computer-aided synthesis and design of plant utility systems, AIChE journal 30 (1) (1984) 69–78.

[8] C. Hui, Y. Natori, An industrial application using mixed-integer programming technique: A multi-period utility system model, Computers & chemical engineering 20 (1996) S1577–S1582.

[9] R. Iyer, I. Grossmann, Optimal multiperiod operational planning for utility systems, Computers & chemical engineering 21 (8) (1997) 787–800.

[10] S. Micheletto, M. Carvalho, J. Pinto, Operational optimization of the utility system of an oil refinery, Computers & Chemical Engineering 32 (1-2) (2008) 170–185.

[11] S. Stefanis, A. Buxton, A. Livingston, E. Pistikopoulos, A methodology for environmental impact minimization: Solvent design and reaction path synthesis issues, Computers & chemical engineering 20 (1996) S1419–S1424.

[12] S. Stefanis, A. Livingston, E. Pistikopoulos, Minimizing the environmental impact of process plants: a process systems methodology, Computers & chemical engineering 19 (1995) 39–44.

[13] A. Azapagic, R. Clift, Application of life cycle assessment to process optimization, Computers &

Chemical Engineering 23 (10) (1999) 1509–1526.

[14] B. Gebreslassie, G. Guillén-Gosálbez, L. Jiménez, D. Boer, Design of environmentally conscious absorption cooling systems via multi-objective optimization and life cycle assessment, Applied Energy 86 (9) (2009) 1712–1722.

[15] G. Guillén-Gosálbez, J. Caballero, L. Jiménez, Application of life cycle assessment to the structural optimization of process flowsheets, Industrial & Engineering Chemistry Research 47 (3) (2008) 777–789.

[16] A. Hugo, E. Pistikopoulos, Environmentally conscious long-range planning and design of supply chain networks, Journal of Cleaner Production 13 (15) (2005) 1471–1491.

[17] G. Guillén-Gosálbez, I. Grossmann, Optimal design and planning of sustainable chemical supply chains under uncertainty, AIChE Journal 55 (1) (2009) 99–121.

[18] G. Guillén-Gosálbez, I. Grossmann, A global optimization strategy for the environmentally conscious design of chemical supply chains under uncertainty in the damage assessment model, Computers & Chemical Engineering 34 (1) (2010) 42–58.

[19] L. Puigjaner, G. Guillén-Gosálbez, Towards an integrated framework for supply chain management in the batch chemical process industry, Computers & Chemical Engineering 32 (4-5) (2008) 650–670.

[20] P. Vaskan, G. Guillén-Gosálbez, L. Jiménez, Multi-objective design of heat-exchanger networks considering several life cycle impacts using a rigorous milp-based dimensionality reduction technique, Applied Energy 98 (2012) 149–161.

[21] R. Salcedo, E. Antipova, D. Boer, L. Jimnez, G. Guilln-Goslbez, Multi-objective optimization of solar Rankine cycles coupled with reverse osmosis desalination considering economic and life cycle environmental concerns, Desalination, 286 (2012) 358-371.

[22] G. Guillén-Gosálbez, F. Mele, I. Grossmann, A bi-criterion optimization approach for the design and planning of hydrogen supply chains for vehicle use, AIChE Journal 56 (3) (2010) 650–667.

[23] N. Sabio, A. Kostin, G. Guillén-Gosálbez, L. Jiménez, Holistic minimization of the life cycle environmental impact of hydrogen infrastructures using multi-objective optimization and principal compo-

nent analysis, International Journal of Hydrogen Energy 37 (6) (2012) 5385–5405.

[24] H. Cabezas, J. Bare, S. Mallick, Pollution prevention with chemical process simulators: the generalized waste reduction (war) algorithm–full version, Computers & chemical engineering 23 (4-5) (1999) 623–634.

[25] S. Mallick, H. Cabezas, C. Jane, S. Sikdar, A pollution reduction methodology for chemical process simulators, Industrial & engineering chemistry research 35 (11) (1996) 4128–4138.

[26] D. Brockhoff, E. Zitzler, Objective reduction in evolutionary multiobjective optimization: Theory and applications, Evolutionary Computation 17 (2) (2009) 135–166.

[27] L. Van der Maaten, E. Postma, H. Van Den Herik, Dimensionality reduction: A comparative review, Journal of Machine Learning Research 10 (2009) 1–41.

[28] K. Deb, D. Saxena, On finding pareto-optimal solutions through dimensionality reduction for certain large-dimensional multi-objective optimization problems, Kangal report 2005011.

[29] D. Brockhoff, E. Zitzler, Are all objectives necessary? on dimensionality reduction in evolutionary multiobjective optimization, Parallel Problem Solving from Nature-PPSN IX (2006) 533–542.

[30] G. Guillén-Gosálbez, A novel milp-based objective reduction method for multi-objective optimization: Application to environmental problems, Computers & Chemical Engineering 35 (8) (2011) 1469–1477.

[31] S. Ryding, Iso 14042 environmental management - life cycle assessment, The International Journal of Life Cycle Assessment 4 (6) (1999) 307–307.

[32] PR-Consultants, The eco-indicator 99, a damage oriented method for life cycle impact assessment. Methodology report and manual for designers, Tech. rep., PR Consultants, Amersfoort, The Netherlands (2000).

[33] M. Trkay, I. Grossmann, Logic-based minlp algorithms for the optimal synthesis of process networks, Computers and Chemical Engineering 20(8) (1996) 959–978.

[34] M. Kostina, G. Guilln-Goslbez, D. Mele, L. Jimnez, Objective reduction in multi-criteria optimization of integrated bioethanol-sugar supply chains, 22nd European Symposium on Computer Aided Process Engineering, 17, (2012) 1.

[35] M. Ehrgott, Multicriteria optimization, Vol. 491, Springer Verlag, 2005.

[36] A. Kostin, G. Guilln-Goslbez, L. Jimnez, F. D. Mele, Identifying key life cycle assessment metrics in the multiobjective design of bioethanol supply chains using a rigorous mixed-integer linear programming approach, Industrial & Engineering Chemistry Research, 51(14) (2011) 5282-5291.

[37] E. Antipova, D. Boer, L. F. Cabeza, G. Guilln-Goslbez, L. Jimnez, Uncovering relationships between environmental metrics in the multi-objective optimization of energy systems: A case study of a thermal solar Rankine reverse osmosis desalination plant, Energy, 51 (2013) 50-60.

[38] E. C. portal, http://www.ecoinvent.com/, October, 2012.

Notation

Indices

b	chemical species
c	impact categories
d	damage categories
j	process units
l	material state
m	fuels
t	time periods

Sets

$ID(d)$	set of impacts c contributing to damage category d

Parameters

a_j^{MP}	material balance coefficient
a_j^{EL}	material balance coefficient
b_j^{HP}	material balance coefficient
$cost_{mt}^{FU}$	cost of fuel m in period t
$cost_{mt}^{INV}$	unitary inventory cost associated with fuel m and period t
$cost_t^{EL}$	cost of the electricity in period t
dem_t^{EL}	demand of electricity in period t
dem_t^{HP}	demand of HP steam in period t

dem_t^{MP}	demand of MP steam in period t
dem_t^{LP}	demand of LP steam in period t
df_{bc}	damage factor associated with chemical b and impact c
g_j^{CO}	material balance coefficient
g_j^{LP}	material balance coefficient
g_j^{MP}	material balance coefficient
hc_m	heat of combustion of fuel m
n_d	normalization factor associated with damage category d
w_d	weighting factor associated with damage category d
$\underline{INV_{jtm}}$	lower bound on the inventory of fuel m in unit j in period t
$\overline{INV_{jtm}}$	upper bound on the inventory of fuel m in unit j in period t
$\underline{x_{jltm}^{FU}}$	lower bound on the flow of fuel m in state l in unit j in period t
$\overline{x_{jltm}^{FU}}$	upper bound on the flow of fuel m in state l in unit j in period t
$\underline{x_{jlt}^{EL}}$	lower bound on the flow of electricity in state l in unit j in period t
$\overline{x_{jlt}^{EL}}$	upper bound on the flow of electricity in state l in unit j in period t
ϵ	auxiliary parameter employed in the epsilon constraint method
θ	length of a time period
η_{jm}	efficiency of boiler j combusting fuel m
ω_m^{FU}	life cycle inventory entry associated with chemical b

	per unit of fuel m generated
ω^{EL}	life cycle inventory entry associated with chemical b
	per unit of external electricity generated
ω_m^{DE}	life cycle inventory entry associated with chemical b
	per unit of fuel m combusted

Variables

DAM_d	impact in damage category d
ECO_{99}	Eco-indicator 99 value
EPU_t	purchases of external electricity in period t
IM_c	damage in impact category c t
INV_{jtm}	inventory of fuel m in unit j in period t
LCI_b^{FU}	life cycle inventory associated with chemical b
LCI_b^{FU}	life cycle inventory associated with chemical b due to the generation of fuel
LCI_b^{EL}	life cycle inventory associated with chemical b
	due to the consumption of external electricity
LCI_b^{DE}	life cycle inventory associated with chemical b due to the direct emissions
TFC_{jtm}	total cost of fuel m in unit j in period t
TC	total cost
x_{jltm}^{FU}	flow rate of fuel m in state l in unit j in period t
x_{jlt}^{HP}	flow rate of high pressure steam in state l in unit j in period t

x_{jlt}^{MP} flow rate of medium pressure steam in state l in unit j in period t

x_{jlt}^{LP} flow rate of low pressure steam in state l in unit j in period t

x_{jlt}^{CO} flow rate of condensate in state l in unit j in period t

x_{jlt}^{EL} flow rate of electricity in state l in unit j in period t

y_{jtm} binary variable (1, if fuel m is selected in unit j in period t, 0 otherwise)

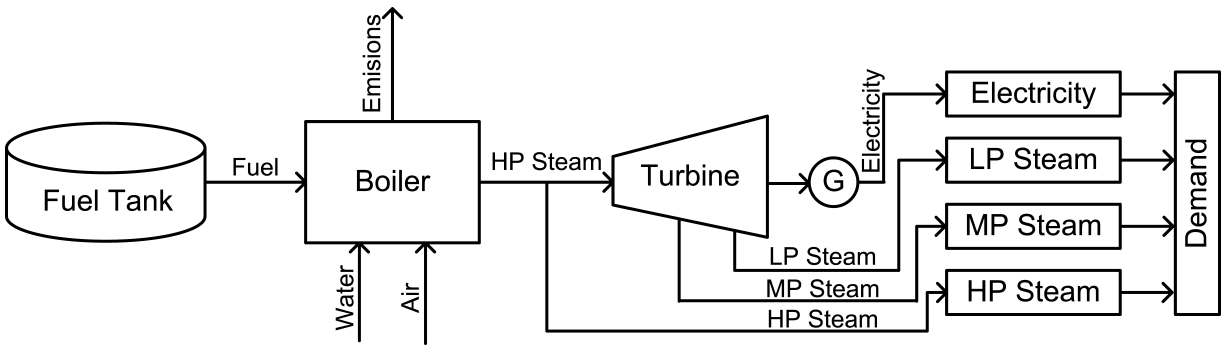

Figure 1. Energy system taken as reference

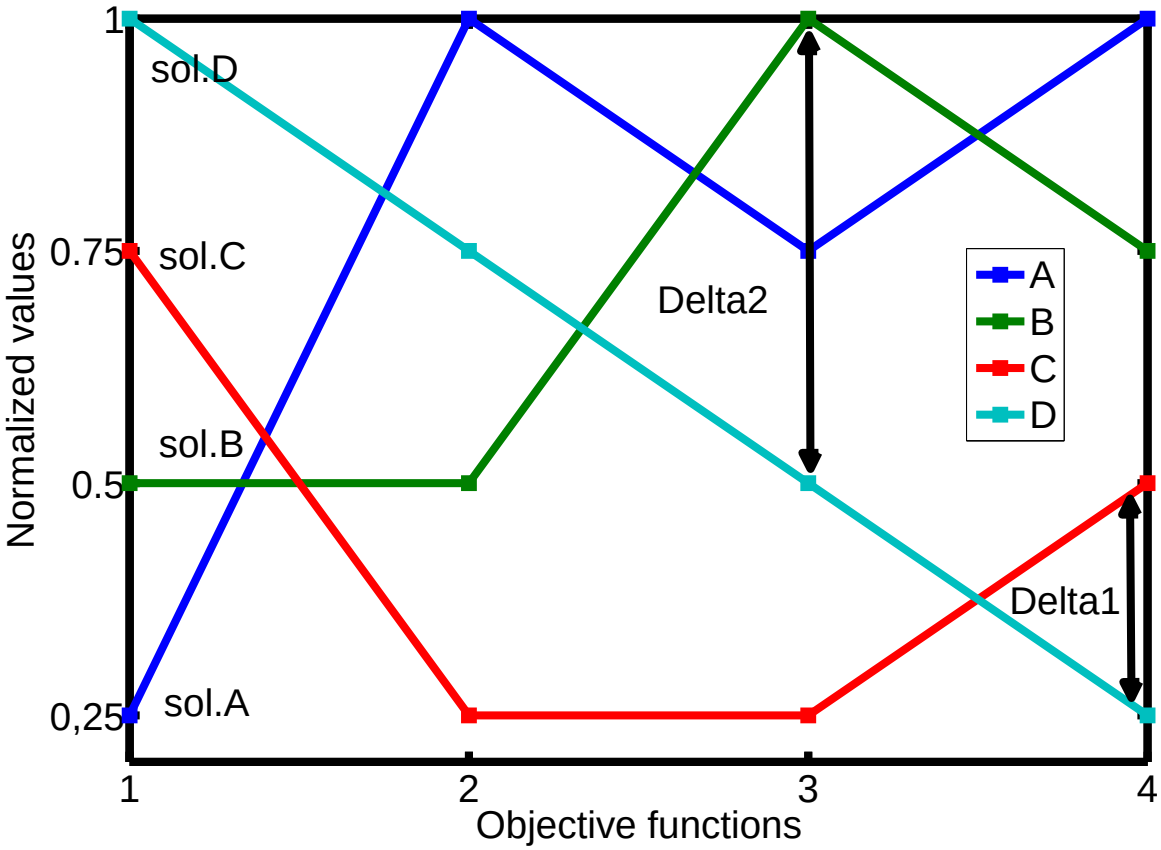

Figure 2. Dominance structure for the set f_1, f_2, f_3, f_4. All solutions are weakly efficient.

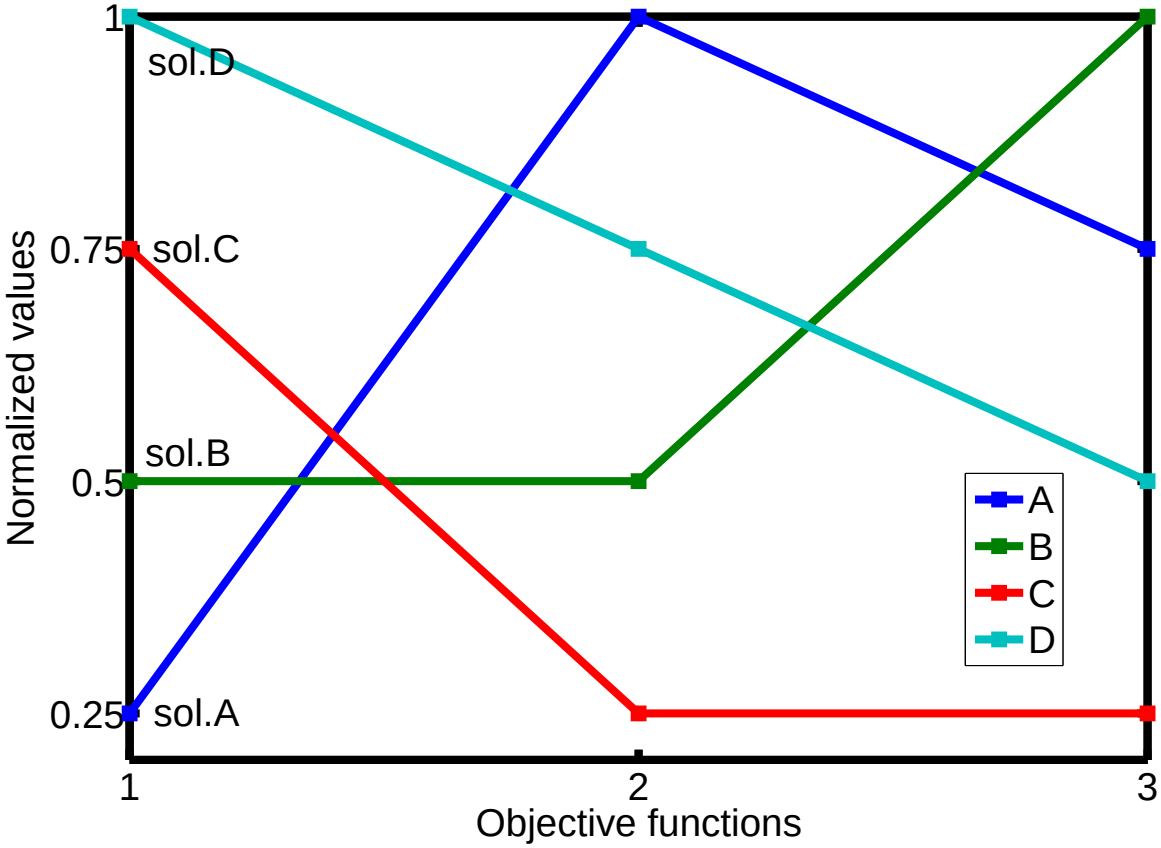

Figure 3. Dominance structure for the reduced set f_1, f_2, f_3. Solution C dominate solution D, since C is better than D in all objectives. Solution D is therefore lost, with the Delta 1 (see Fig. 2).

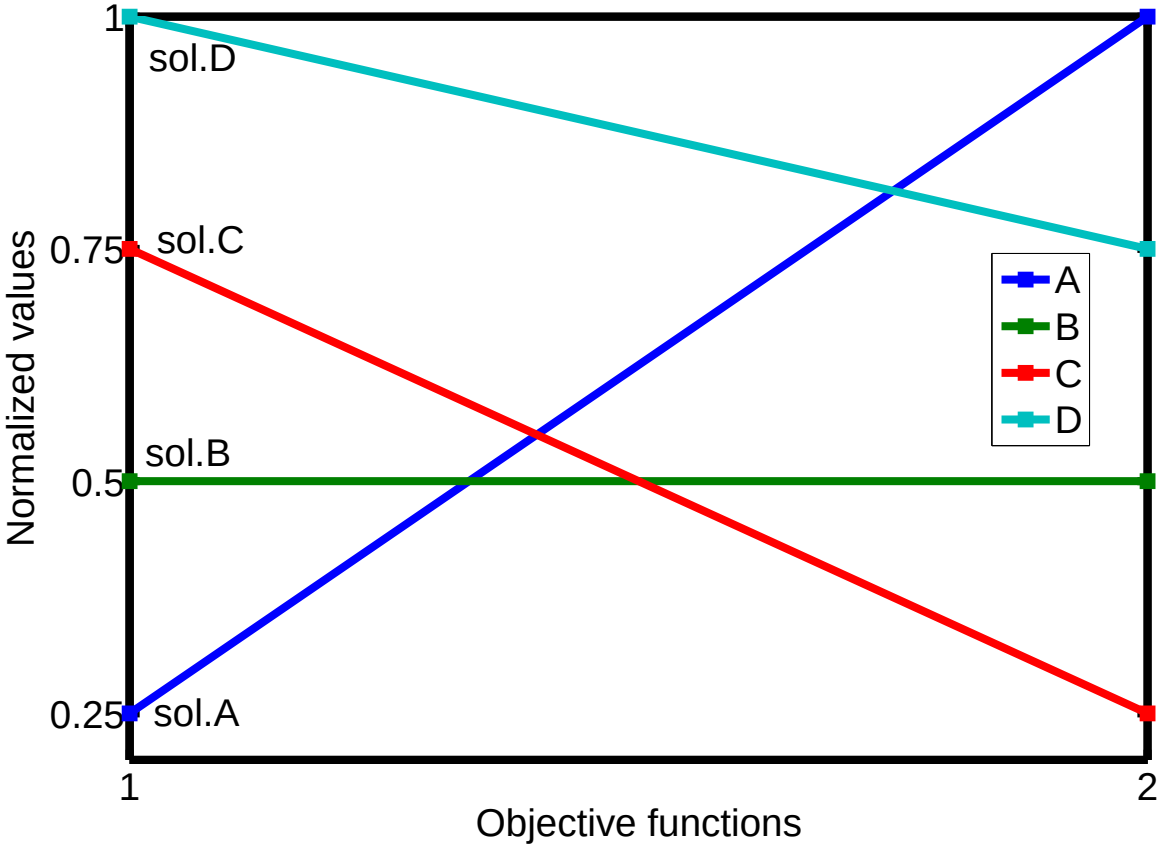

Figure 4. Dominance structure for the reduced set f_1, f_2. Solution C and B dominate solution D, since C and B are better than D in all objectives. Solution D is therefore lost, with the Delta 2 (see Fig. 2).

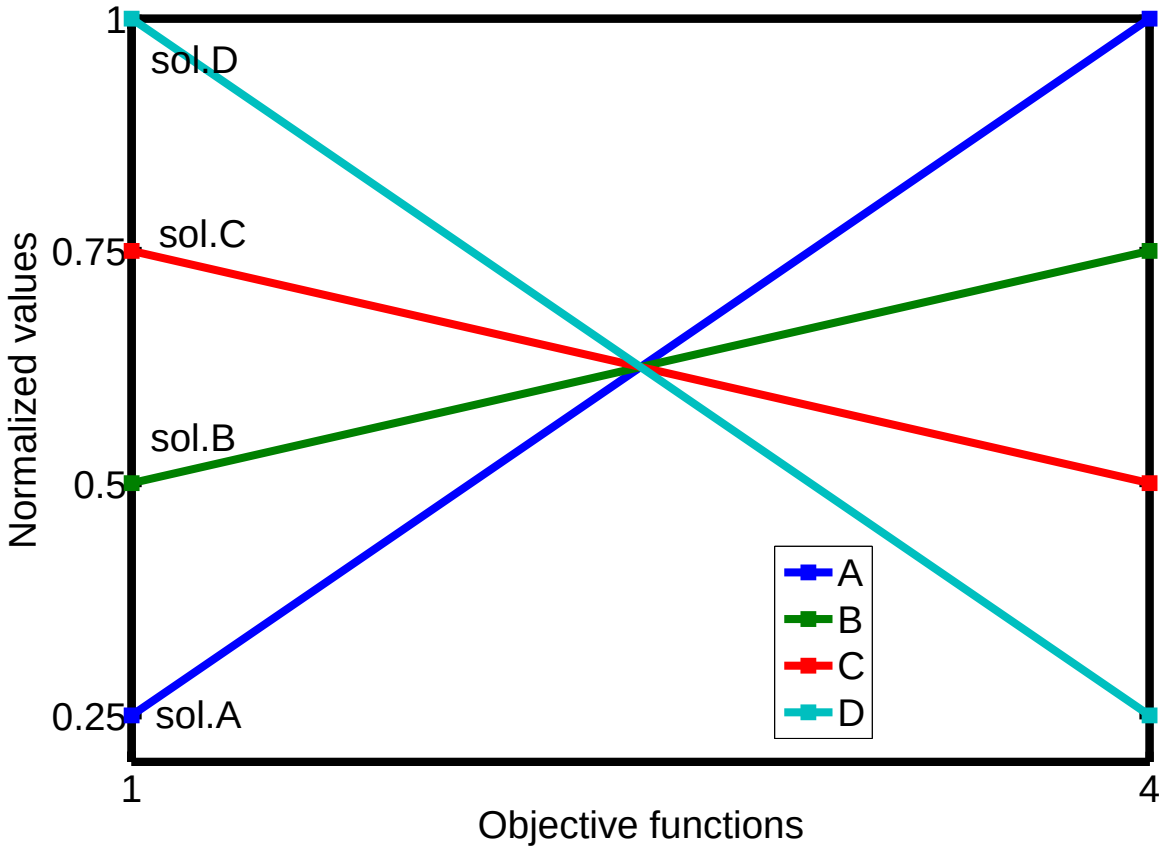

Figure 5. Dominance structure for reduced set f_1, f_4. No solution dominates any of the others. All solutions are Pareto optimal in the reduced search space, and the dominance structure is preserved.

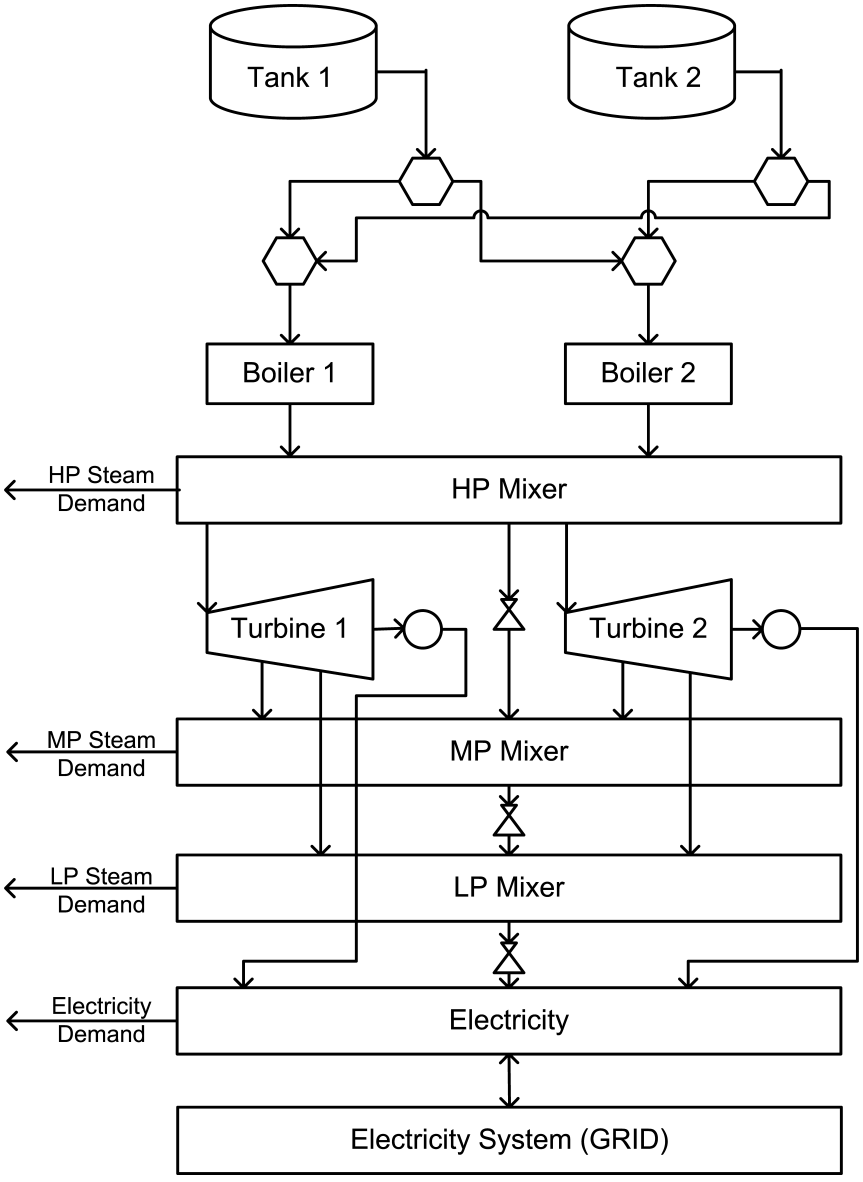

Figure 6. Superstructure of case study.

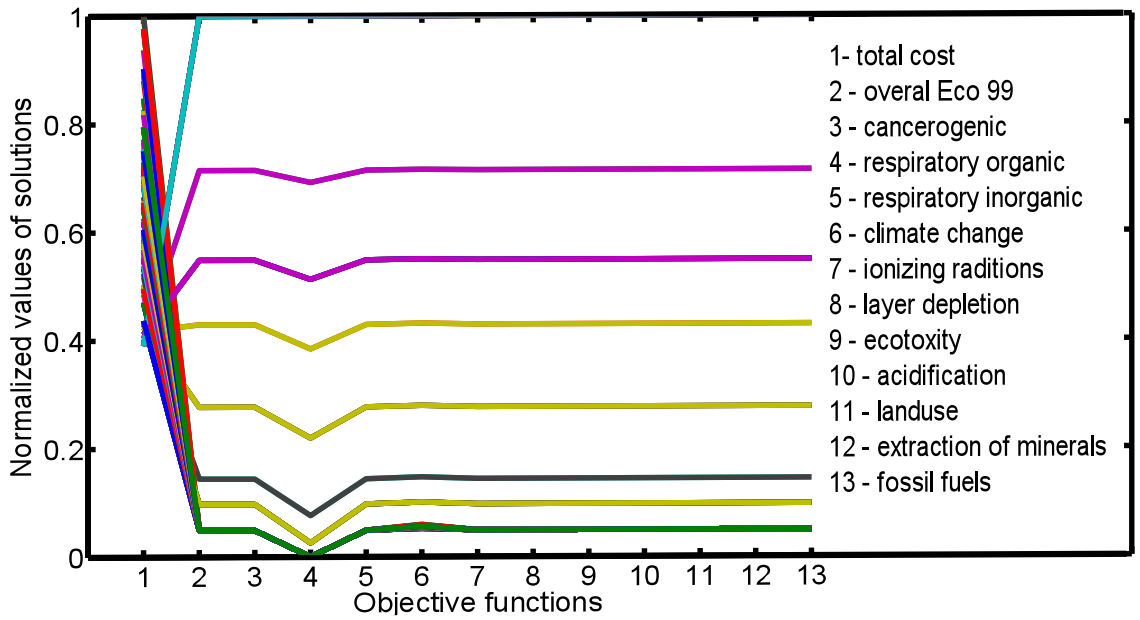

Figure 7. The parallel coordinate plot for Example 1. We show in the horizontal axis the different objectives, and in the vertical one the normalized value of each solution in each objective. Normalization is performed by subtracting the minimum value to each objective function value and dividing by the difference between the maximum and the minimum attained over all the solutions.

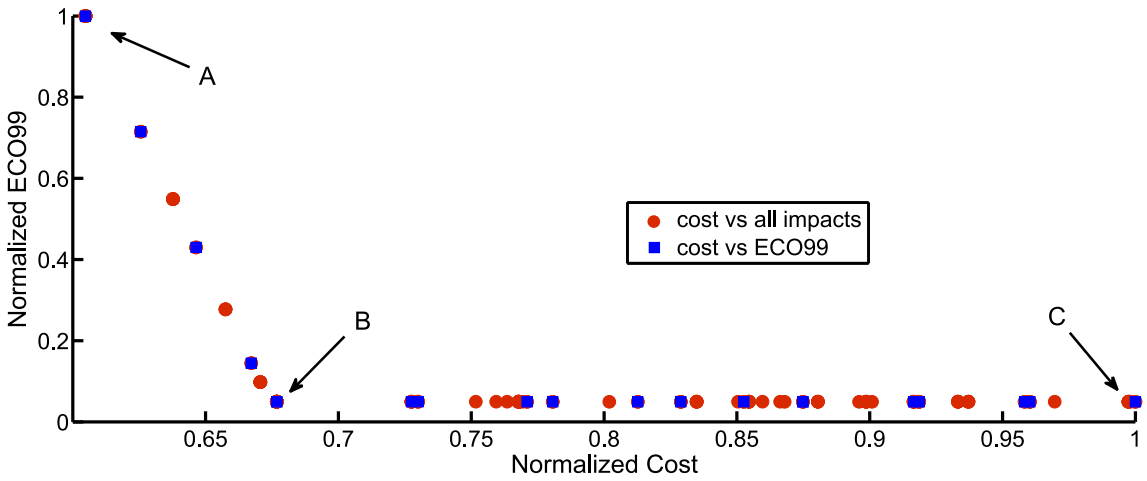

Figure 8. Results obtained from the bi-criteria problem cost vs the overall Eco-indicator 99 (blue points) and from solving the bicriteria problems cost vs. single impacts (red points) for Example 1.

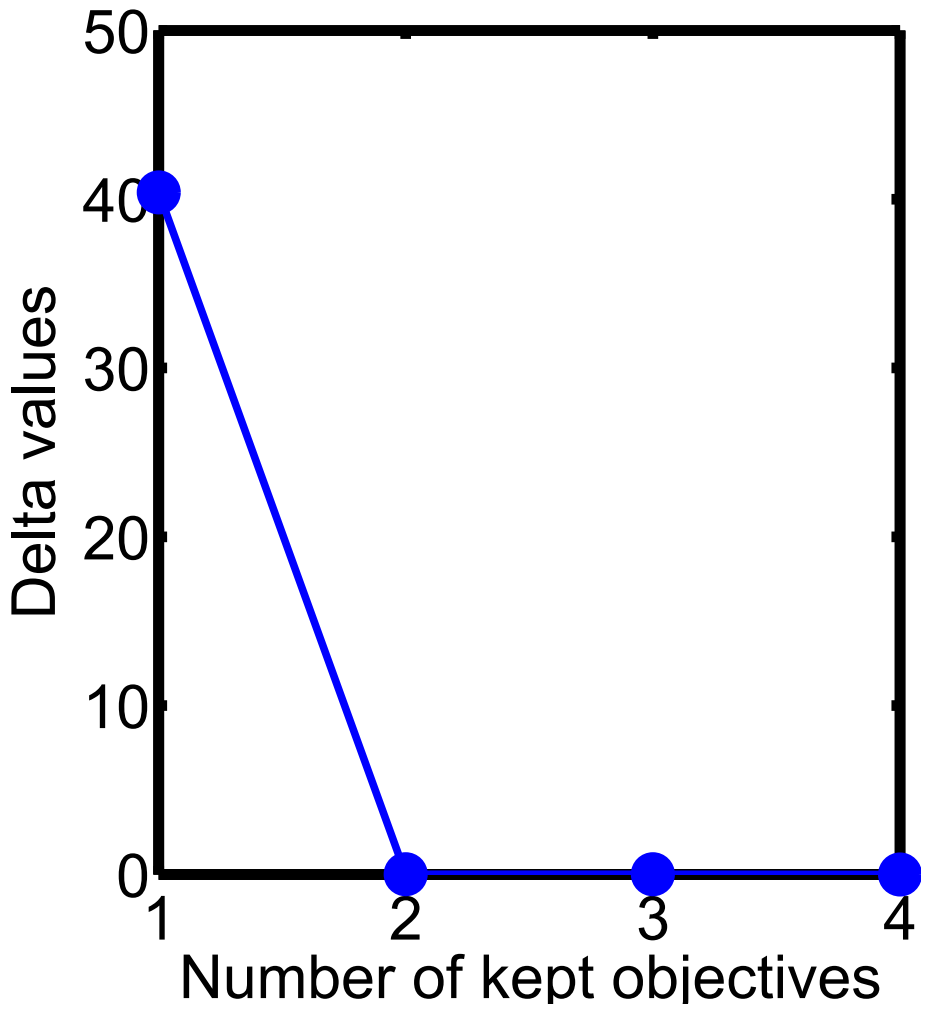

Figure 9. Minimum of delta value for different sets of number of objectives. Example 1.

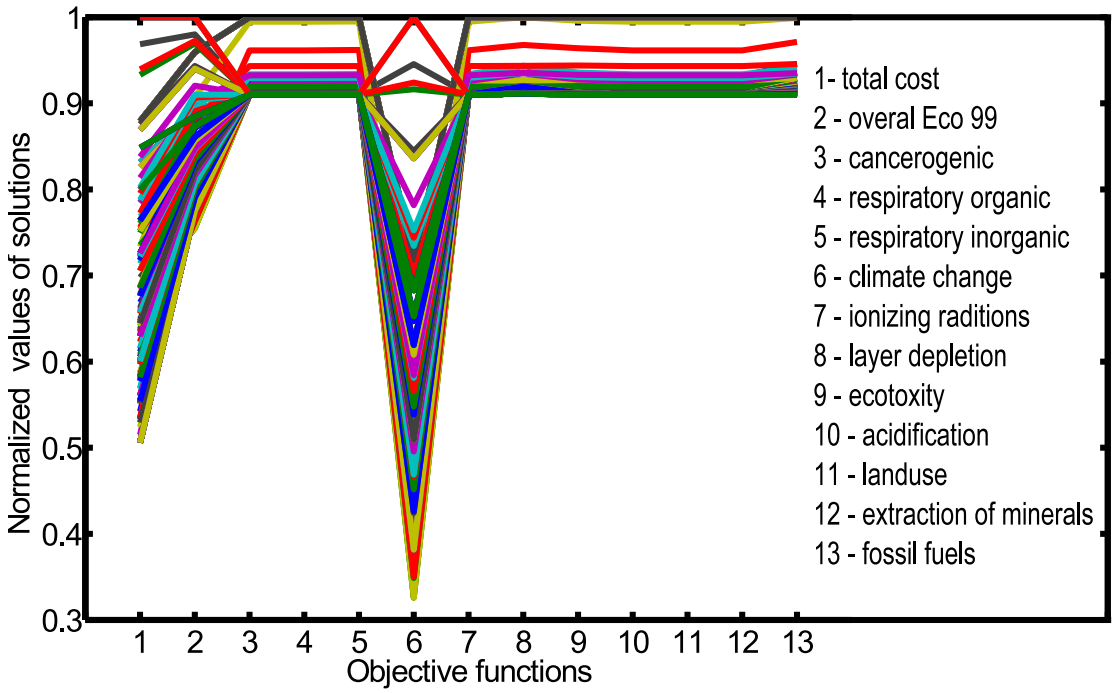

Figure 10. The parallel coordinate plot for Example 2.

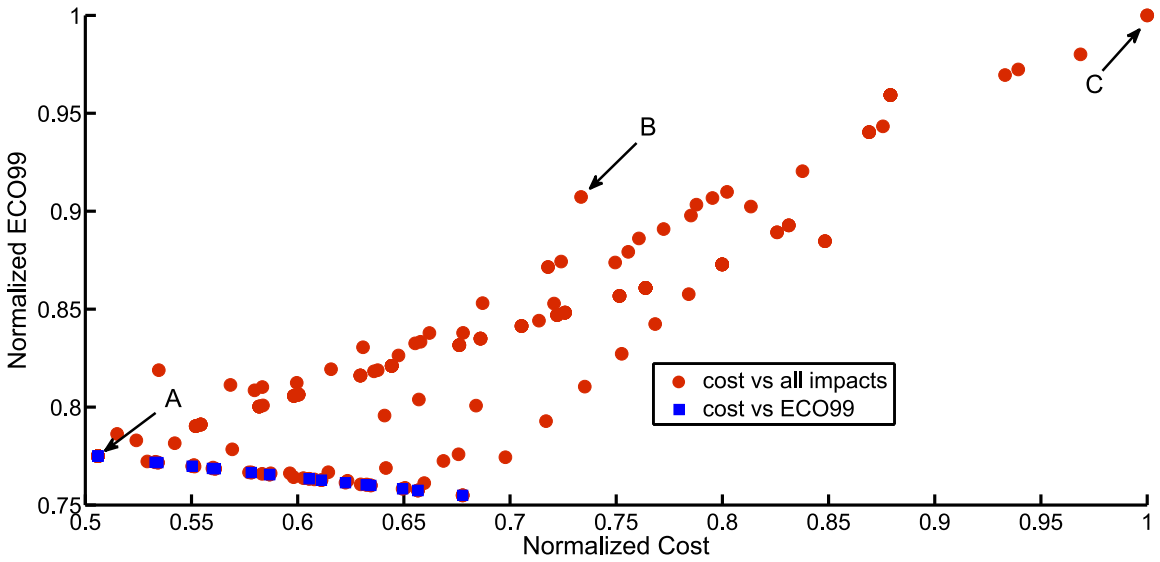

Figure 11. Points resulting from the bi-criteria optimization cost vs. Eco-indicator 99 and cost vs. every single impact projected onto the subspace cost vs Eco-indicator 99. Red points above the envelope of the blue ones would be lost if Eco-indicator 99 and cost were optimized as unique objectives. (Example 2).

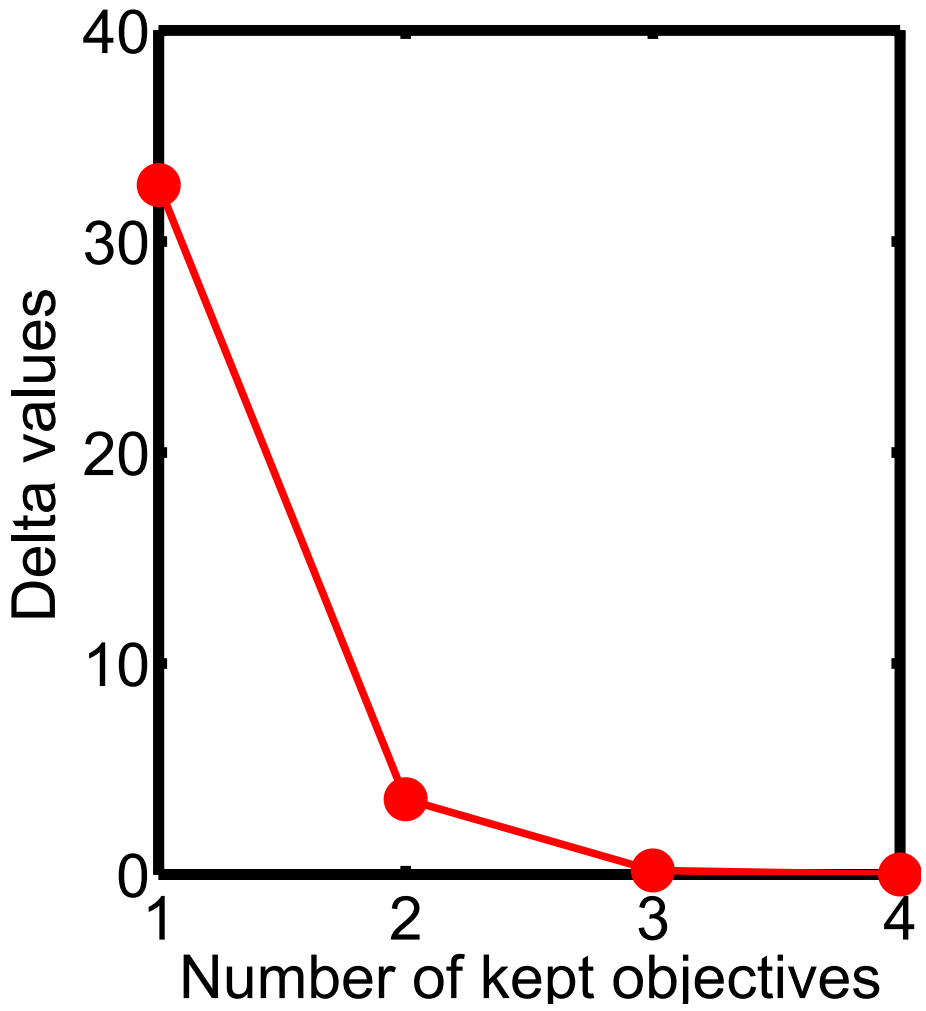

Figure 12. Minimum of delta value for different sets of kept objectives. Example 2.

Table 1. Data for fuels: heat of combustion (hc_m), green house gases content (ghg_m), price ($cost_{mt}^{FU}$), and inventory cost ($cost_{mt}^{INV}$).

	hc_m (kJ/ton)	ghg_m (kg/ton)	$cost_{mt}^{FU}$ (\$/ton)	$cost_{mt}^{INV}$ (\$/ton·hr)
Fuel 1	10.50	17	200	0.50
Fuel 2	9.65	5	76	0.19
Fuel 3	6.65	3	83	0.20
Fuel 4	10.20	10	145	0.35

Table 2. Data for boilers (I): boiler efficiency (η_{jm})

	η_{jm} (kJ/ton)	
Fuel	Boiler 1	Boiler 2
Fuel 1	0.59	0.58
Fuel 2	0.60	0.60
Fuel 3	0.56	0.57
Fuel 4	0.61	0.60

Table 3. Data for boilers (II): materials balance coefficients (a_j^{MP} and a_j^{EL})

	a_j^{MP} (adim)	a_j^{EL} (ton/MW·hr)
Boiler 1	0.11	0.002
Boiler 2	0.12	0.003

Table 4. Data for turbines: materials balance coefficients (g_j^{LP}, g_j^{MP}, b_j^{HP}, and g_j^{CO})

	g_j^{LP} (MW·hr/ton)	g_j^{MP} (MW·hr/ton)	b_j^{HP} (MW·hr/ton)	g_j^{CO} (MW·hr/ton)
Turbine 1	0.01	0.07	0.15	0.00
Turbine 2	0.01	0.08	0.18	0.00

Table 5. Environmental data: production of fuels

	Fuels (impact/kg)			
	1	2	3	4
Carcinogens (DALYs)	1.05×10^{-8}	1.27×10^{-8}	1.29×10^{-8}	2.52×10^{-9}
Respiratory effects (organic) (DALYs)	1.64×10^{-9}	1.69×10^{-9}	1.90×10^{-9}	1.00×10^{-11}
Respiratory effects (inorganic) (DALYs)	3.81×10^{-7}	4.36×10^{-7}	4.54×10^{-7}	8.23×10^{-9}
Climate change (DALYs)	7.18×10^{-8}	8.73×10^{-8}	8.85×10^{-8}	1.92×10^{-9}
Ionizing radiation (DALYs)	7.70×10^{-10}	9.10×10^{-10}	9.40×10^{-10}	2.00×10^{-11}
Ozone layer depletion (DALYs)	4.70×10^{-10}	4.80×10^{-10}	5.40×10^{-10}	0.00×10^{0}
Ecotoxicity (PDF·m^2·year)	4.71×10^{-2}	6.08×10^{-2}	5.88×10^{-3}	8.15×10^{-4}
Acidif./eutroph. (PDF·m^2·year)	1.05×10^{-2}	1.21×10^{-2}	1.25×10^{-2}	2.96×10^{-4}
Land use (PDF·m^2·year)	1.27×10^{-4}	1.44×10^{-4}	1.52×10^{-4}	1.32×10^{-4}
Minerals extraction (MJ)	3.09×10^{-5}	2.50×10^{-5}	2.05×10^{-5}	2.99×10^{-7}
Fossil fuels extraction (MJ)	6.92×10^{0}	7.07×10^{0}	8.02×10^{0}	8.38×10^{-3}

Table 6. Environmental data: generation of electricity

	Electricity	
	Example 1 (impact/MJ)	Example 2 (impact/kWh)
Carcinogens (DALYs)	1.66×10^{-8}	1.06×10^{-8}
Respiratory effects (organic) (DALYs)	7.00×10^{-11}	7.30×10^{-9}
Respiratory effects (inorganic) (DALYs)	1.58×10^{-7}	7.30×10^{-9}
Climate change (DALYs)	3.15×10^{-8}	2.36×10^{-9}
Ionizing radiation (DALYs)	4.72×10^{-9}	4.12×10^{-11}
Ozone layer depletion (DALYs)	5.00×10^{-11}	6.44×10^{-13}
Ecotoxicity (PDF·m^2·year)	2.12×10^{-3}	1.80×10^{-4}
Acidif./eutroph. (PDF·m^2·year)	3.57×10^{-3}	3.68×10^{-3}
Land use (PDF·m^2·year)	6.05×10^{-3}	7.11×10^{-4}
Minerals extraction (MJ)	2.43×10^{-4}	5.93×10^{-3}
Fossil fuels extraction (MJ)	5.20×10^{-2}	5.38×10^{-3}

Table 7. Consumption of fuel and external electricity in different solutions (see Figure 8) for example 1.

Solutions	Purchased electricity, MW	Fuel1, ton	Fuel2, ton	Fuel3, ton	Fuel4, ton
A	2498.88	0	4626.61	0	0
B	673.36	0	5233.41	0	0
C	673.36	0	0	7088.05	0

Table 8. Delta values for Example 1 for all combinations of two objectives. Where 1 is total cost, and other objectives are environmental impacts: 2 is overall Eco 99, 3 is carcinogenic, 4 is respiratory organic, 5 is respiratory inorganic, 6 is climate change, 7 is ionizing radiation, 8 is layer depletion, 9 is ecotoxity, 10 is acidification, 11 is landuse, 12 is extraction of minerals, 13 is fossil fuels.

Reduced set		Delta
1	2	0.0081
1	3	0.2602
1	4	0.2602
1	5	0.2602
1	6	0.0031
1	7	0.2602
1	8	0.2602
1	9	0.1516
1	10	0.2602
1	11	0.2602
1	12	0.2602
1	13	0.2602

Table 9. Consumption of fuel and external electricity in different solutions (see Figure 11) for example 2.

Solutions	Purchased electricity, MW	Fuel1, ton	Fuel2, ton	Fuel3, ton	Fuel4, ton
A	673.36	0	5233.41	0	0
B	736.17	0	2511.72	0	3062.082
C	673.36	4729.59	0	0	0

Table 10. Delta values for Example 2 for all combinations of two objectives. Where 1 is total cost, and other objectives are environmental impacts: 2 is overall Eco 99, 3 is carcinogenic, 4 is respiratory organic, 5 is respiratory inorganic, 6 is climate change, 7 is ionizing radiation, 8 is layer depletion, 9 is ecotoxity, 10 is acidification, 11 is landuse, 12 is extraction of minerals, 13 is fossil fuels.

Reduced set		Delta
1	2	4.2030
1	3	21.2638
1	4	21.2638
1	5	21.2638
1	6	3.5650
1	7	21.2638
1	8	21.2638
1	9	17.7041
1	10	21.2638
1	11	21.2638
1	12	21.2638
1	13	21.2638

Table 11. Delta values for Example 2 for all combinations of three objectives. Where 1 is total cost, and other objectives are environmental impacts: 2 is overall Eco 99, 3 is carcinogenic, 4 is respiratory organic, 5 is respiratory inorganic, 6 is climate change, 7 is ionizing radiation, 8 is layer depletion, 9 is ecotoxity, 10 is acidification, 11 is landuse, 12 is extraction of minerals, 13 is fossil fuels.

Reduced set			Delta	Reduced set			Delta
1	2	3	4.2030	1	5	9	17.7041
1	2	4	4.2030	1	5	10	21.2638
1	2	5	4.2030	1	5	11	21.2638
1	2	6	3.5650	1	5	12	21.2638
1	2	7	4.2030	1	5	13	21.2638
1	2	8	4.2030	1	6	7	0.8065
1	2	9	4.2030	1	6	8	0.6852
1	2	10	4.2030	1	6	9	1.3056
1	2	11	4.2030	1	6	10	0.1869
1	2	12	4.2030	1	6	11	1.4190
1	2	13	4.2030	1	6	12	1.4190
1	3	4	21.2638	1	6	13	0.2524
1	3	5	21.2638	1	7	8	21.2638
1	3	6	0.2167	1	7	9	17.7041
1	3	7	21.2638	1	7	10	21.2638
1	3	8	21.2638	1	7	11	21.2638
1	3	9	17.7041	1	7	12	21.2638
1	3	10	21.2638	1	7	13	21.2638
1	3	11	21.2638	1	8	9	17.7041
1	3	12	21.2638	1	8	10	21.2638
1	3	13	21.2638	1	8	11	21.2638
1	4	5	21.2638	1	8	12	21.2638
1	4	6	0.8065	1	8	13	21.2638
1	4	7	21.2638	1	9	10	17.7041
1	4	8	21.2638	1	9	11	17.7041
1	4	9	17.7041	1	9	12	17.7041
1	4	10	21.2638	1	9	13	17.7041
1	4	11	21.2638	1	10	11	21.2638
1	4	12	21.2638	1	10	12	21.2638
1	4	13	21.2638	1	10	13	21.2638
1	5	6	0.1869	1	11	12	21.2638
1	5	7	21.2638	1	11	13	21.2638
1	5	8	21.2638	1	12	13	21.2638

7.5 Identifying multi-objective design principles in metabolic networks via a rigorous multi-level optimization framework.

Vaskan P., Guillén-Gosálbez G., Alves R., Jiménez L. Identifying multi-objective design principles in metabolic networks via a rigorous multi-level optimization framework. Pending submission to *PLOS Computational Biology*.

Dipòsit Legal: T 952-2014

Identifying multi-objective design principles in metabolic networks via a rigorous multi-level optimization framework

Pavel Vaskan[1], Gonzalo Guillén-Gosálbez[1,*], Rui Alves[2], Laureano Jiménez[1]
1 Departament d'Enginyeria Química (EQ), Escola Tècnica Superior d'Enginyeria Química (ETSEQ), Universitat Rovira i Virgili (URV), Campus Sescelades, Avinguda Països Catalans, 26, 43007 Tarragona, Spain
2 Departament de Ciéncies Médiques Básiques, Universitat de Lleida and IRBLleida, Lleida, Spain
∗ **E-mail: gonzalo.guillen@urv.cat**

Abstract

Flux Balance Analysis (FBA) provides a set of methods to study different aspects of the functioning and evolution of microbial species assuming that biomass growth rate is typically optimized during evolution. Recent work, however, has shown that there might be other meaningful efficiency criteria leading to alternative fitness functions accounting for more than just growth rate. This work addresses this fundamental question: how to identify meaningful biological objective functions that drive the cell's metabolic machinery under different conditions. To this end, we propose an approach that combines bi-level optimization, FBA and mixed-integer nonlinear programming (MINLP) within a single unified framework that enables the identification (in a rigorous and systematic manner) of objective functions that will likely drive the cell's machinery under the studied experimental conditions. We benchmark the method by analyzing which combination of objective functions better explains a set of metabolic fluxes experimentally determined in vivo. We confirm that biomass maximization is a fundamental objective function under the experimental conditions we investigate. In addition, we identify additional sets of functional criteria that, along with growth rate maximization, improve the model fitting to experimental data. Overall, the fitting of FBA models improves with the number of objectives, firstly sharply, and then marginally after a certain number of criteria. We show as well that several biological objectives behave similarly, which suggests the existence of redundant biological criteria.

Author Summary

Evolution of cell metabolism is driven by random mutation processes, generating cells with alternative metabolic phenotypes. These cells then compete for the natural resources of the environment and their differential usage of those resources leads to the survival of the fittest cells with most efficient phenotype. In view of this, a common assumption made in the past is that cells attempt to maximize the biomass growth rate as their optimal function. Based on this assumption, FBA provides a set of methods to study different aspects of the functioning and evolution of microbial species. Recent work, however, has shown that there might be other meaningful efficiency criteria leading to alternative fitness functions accounting for more than just growth rate maximization. Hence, a major challenge in biology concerns the identification of these alternative functions and their relative contribution to fitness under various environmental conditions. In this work we address this challenge by using a systematic framework that combines rigorous mathematical programming techniques (i.e., bi-level optimization) with FBA. By applying this tool, we find that the inclusion of additional biological criteria (apart from biomass growth rate maximization) improves the predictive capabilities of FBA.

Introduction

In industrial settings, humans establish a clear objective function to be met, creating and optimizing designs to attain that objective efficiently under specific constraints and conditions. In contrast, the emergence of new designs in natural systems results from random mutation followed by natural selection. One could argue that this process tends to optimize the structure and behavior of natural systems. Unfortunately, the objective(s) function(s) and constraints (i.e., the optimization-like problem we call natural selection) of this process remain unclear. Determining such a function and set of constraints would allow biologists to identify biological design principles, a central topic in systems biology [1].

The identification of biological design principles can be posed as a *reverse optimization problem* for which the solution (the actual system) is known, and the criteria (if any) that have been optimized to arrive to that solution need to be determined. Several *in silico* frameworks for determining a most-likely objective function have been proposed [2]. For example, **ObjFind**, was built under the assumption that natural systems optimize a linear combination of biological objectives that are related to the fluxes of biological reactions [3]. **ObjFind** seeks to determine the values of the weights (coefficients of importance, CoI) to be attached to a set of reaction fluxes such that when the resulting weighted sum of fluxes is optimized, the difference between the optimal *in silico* flux distribution predicted by the model and the experimentally observed distribution is minimized. In the **ObjFind** framework, a high CoI indicates that a reaction is important for the cellular objective function, while a small weight implies the opposite.

BOSS illustrates another type of optimization framework [4] that assumes that biological systems can add new reactions to their metabolism in order to meet their biological objectives. Effectively, this is implemented by allowing *de novo* reactions to be added to the stoichiometry matrix of the target network. In this approach, the objective reaction is not confined to be one of a subset of existing reactions, but rather is allowed to take on any form (e.g. an existing reaction, a combination of existing reactions, or a previously uncharacteristic reaction). This assumption provides more flexibility to the framework and makes the optimization process closer to what is thought to occur during biological evolution, where changes in regulation (modeled by optimizing the CoIs of existing reactions) can be combined with gene duplication or deletion (modeled by adding new reactions to the network). A third type of framework was proposed by Knorr *et al* [5]. This approach employs a Bayesian-based technique to determine meaningful biological objective functions for a system.

The aforementioned approaches rely on single-objective methods that assume the existence of a unique universal biological objective function. Sauer and co-workers, however, suggested recently the existence of more than one meaningful fitness function driving the metabolic machinery [6, 7]. More precisely, they identified three main biological criteria that microorganisms might attempt to optimize simultaneously: maximum ATP yield, maximum biomass yield, and minimum sum of absolute fluxes.

If we expect to understand the evolution and functional properties of complex metabolic networks, it is of paramount importance to develop a rigorous framework for identifying in a systematic and rigorous manner the criteria underlying design selection in biological systems. Here we report the development of a bi-level linear programming framework inspired on the work by Burgard and Maranas [3]. More precisely, we have developed a method that given a set of experimental observations allows us to infer the form of the multi-objective optimization problem that shapes the adaptation of microorganisms to the environment. We pose this problem in mathematical terms as a bi-level linear program that includes an outer problem and a set of inner models. The outer problem optimizes the least square difference between the experimental observations and the optimal solution predicted *in silico*. The inner problems, which are defined for each experimental condition, optimize a linear combination of objectives subject to the weights imposed by the outer problem. The overall bi-level model identifies those combinations of weights that make fitting of the model to each experimental condition optimal, considering several objectives simultaneously. That is, the model looks for those objectives whose optimization produces solutions that are as close as possible to the experimental observations. A nonzero weight implies that the objective is biologically meaningful, while a zero weight implies the converse. Binary variables are

added for controlling the number of plausible fitness functions. Efficient solution of the bi-level problem is achieved by reformulating it as a standard MINLP.

Our approach represents a significant step forward with respect to the original work by Burgard and Maranas [3] for the following two reasons: (i) it handles several objective functions (as opposed to Burgard's approach that only accounts for a single biological criterion); and (ii) it applies a reformulation method that ensures convergence to the global optimum (i.e., our approach guarantees that the solution of the model used to infer meaningful biological objectives is the best possible, while Burgard's approach can produce sub-optimal solutions that might lead to biological conclusions of less quality).

We test the capabilities of our method through its application to the study of an *in vivo* flux distribution in *Escherichia colis* central metabolism using data derived from 13C isotopomer analysis [8] and an FBA model available in the literature [9] that considers biomass growth rate and a set of reaction fluxes as surrogates for cellular fitness functions. Numerical results produced by our method are consistent with the hypothesis that biomass maximization is a fundamental objective function under the observed experimental conditions. In addition, we find that the combination of biomass growth rate with additional biological criteria improves the predictive capabilities of FBA (it better explains the experimental observations). The fitting of the model to the experimental data improves with the number of objectives considered, first sharply and then marginally after a certain point. Finally, we show that there are several groups of objectives that behave similarly, which suggests a certain degree of redundancy among diverse biological criteria. This may have significant implications in explaining the emergence of alternative and seemingly equally fit solutions in replicate experiments of long term evolution [10].

Method

General overview

We have developed a method inspired on the approach by Burgard and Maranas [3] that can handle several objective functions simultaneously. Particularly, given a set of experimental observations, our framework allows us to infer the form of the multi-objective optimization problem that shapes the adaptation of microorganisms to the environment. Hence, we assume the existence of the following multi-objective model that drives the cells' machinery:

$$
\begin{aligned}
&(\textbf{MOFBA}) \quad \min \{v_{j\in MO}\} \\
&\text{s.t.} \\
&\sum_{j\in M} S_{ij} v_j = 0 \qquad \forall i \in N \\
&\underline{v_j} \leq v_j \leq \overline{v_j} \qquad \forall j \in M
\end{aligned}
$$

This model attempts to optimize a set of velocities (including biomass growth rate), subject to mass balance equations (stoichiometric constraints), and equations imposing lower and upper bounds on the velocities. In this formulation, S_{ij} is the stoichiometric coefficient of metabolite i in reaction j, v_j represents the flux of reaction j, MO refers to the set of velocities that are considered surrogates for cellular fitness functions (in principle, we assume that all velocities can be plausible biological objectives), N is the set of metabolites, and M is the set of reactions. $\underline{v_j}$ and $\overline{v_j}$ are lower and upper bounds, respectively, imposed on the velocities.

The solution to this problem is given by a set of Pareto optimal points representing the trade-off between the criteria considered in the analysis. Figures 2a provides an example of a Pareto front that divide the search space into sub-optimal and unfeasible solutions.

The Pareto front of our problem can be obtained using standard multi-objective optimization techniques, such as the epsilon-constrain or weighted-sum methods [11], which are both valid for the case

of linear programming problems like the ones solved in FBA. The latter is based on solving a set of single-objective models in each of which we optimize a linear combination of objectives as follows:

$$
\begin{aligned}
&(\mathbf{MOS}) \quad \min \sum_{j \in MO} v_j w_j \\
&\text{s.t.} \\
&\sum_{j \in M} S_{ij} v_j = 0 \qquad \forall i \in N \\
&\underline{v_j} \leq v_j \leq \overline{v_j} \qquad \forall j \in M
\end{aligned}
$$

Where w_j is the objective attached to velocity j. Each run of the single-objective model that optimizes a linear combination of the original set of objectives generates a different Pareto point. By solving the model for different weights, we obtain a set of Pareto points each achieving a unique combination of objective function values.

Bearing in mind the concepts and ideas given above, we describe next in detail how our method works. Figure 1 summarizes our systematic approach, which consecutively performs the following steps:

1. For each experimental observation, we define the weights to be attached to the different objectives functions. Our goal is to identify the linear combination of weights whose optimization produces results that are as close to the experimental observations as possible.

2. Solve the minimization problem whose objective function is given by the corresponding weighted sum of objectives.

3. Obtain the optimal velocities for the given linear combination of weights.

4. Calculate the error, quantified by the Euclidean distance, between estimated and experimentally determined rates.

5. Minimize the distance calculated in (4) by iteratively varying the weights proposed in (1).

6. At the end of the optimization, identify the objectives with large weight values and tag them as biologically meaningful, while discarding objectives with low weight values.

Steps (1)-(6) can be automated using a bi-level linear program that includes an outer problem and a set of inner models. The outer problem seeks to optimize the least square difference between the experimental observations and the optimal solution predicted *in silico*. The inner problems, which are defined for each experimental condition, optimize a linear combination of objectives, subject to the weights imposed by the outer problem. Hence, the original bi-level problem has the following form:

$$
\begin{aligned}
&(\mathbf{BIMO}) \quad \min_{w_j, x_j} \sum_{j \in EX} (v_j - v_j^{exp})^2 \\
&\text{s.t.} \\
&\left(\begin{array}{ll}
\min\limits_{v_j} \sum\limits_{j=1}^{jup} (v_j w_j) & \\
s.t. & \\
\sum\limits_{j=1}^{M} S_{ij} v_j = 0 & \forall i \in N \\
\underline{v_j} \leq v_j \leq \overline{v_j} & \forall j \in M
\end{array} \right) \\
&\sum_{j=1}^{jup} w_j = 1 \\
&0 \leq w_j \leq \overline{w_j} x_j \qquad \forall j \in M
\end{aligned}
$$

Where S_{ij} is the stoichiometric coefficient of metabolite i in reaction j, v_j represents the flux of reaction j, v_j^{exp} is the experimental flux, and w_j is a weight associated with objective j, which is given by a reaction flux (note that we can also consider a combination of fluxes by defining aggregated velocities). Set N refers to the set of metabolites, EX contains the set of experimentally determined fluxes, and M is the set of reactions. Hence, the overall bi-level model seeks those combinations of weights w_j that make each experimental condition optimal, considering several objectives simultaneously. A nonzero weight implies that the objective is biologically meaningful, while a zero weight implies the opposite.

To solve the bi-level program efficiently, we reformulate it into a standard MINLP by replacing the inner problems by their corresponding KarushKuhnTucker conditions that are expressed in algebraic form using auxiliary binary variables [12]. The multi-objective optimization problem (MOFBA) is therefore reformulated as a Mixed-Integer Quadratically Constrained Program (MIQCP) with linear constraints and a quadratic objective function. This MIQCP is a special type of MINLP that has a nonlinear quadratic objective function and linear equality and inequality constraints. Binary variables are used for controlling the number of plausible fitness functions. In addition, the KKT-based reformulation requires the definition of one auxiliary binary variable for each inequality of the inner problem. Such binaries take a value of one if the constraint is active in the optimal solution of the inner problem (i.e., it is satisfied as an equality), and zero otherwise. The solution of the MIQCP, which can be obtained by standard branch-and-cut methods, provides the set of meaningful objectives (and corresponding weights) under several experimental conditions.

Our method in the context of Pareto optimality

We next clarify the theoretical connections between our approach and the concept of Pareto optimality. To this end, we will use an illustrative example consisting of a system that is optimized following two different approaches: minimizing objectives 1 and 2; and minimizing objectives 3 and 4. Figures 2a and 2b depict the Pareto front corresponding to the optimization of objectives 1 and 2. Points lying below the curve are sub-optimal, since they can be improved in both criteria simultaneously by those lying on the Pareto front (i.e., there are other solutions that are better simultaneously in both objectives). On the other hand, the region above the curve is infeasible, because no alternative shows better values of obj 1 and obj 2 (simultaneously) than the Pareto solutions. On the other hand, Figures 2c and 2d are obtained by optimizing objectives 3 and 4.

It has been proposed that biological systems effectively evolve by finding the Pareto optimal front of a multi-objective functional optimization [13]. Our method effectively identifies the Pareto front of the biological problem to which it is applied by solving the multi-criteria FBA model *in silico*. Note that selecting weights for the objectives is equivalent to moving along the Pareto set [11]. Hence, when our approach calculates weights, it is indeed searching Pareto points according to some criteria.

We now address the question of how to represent experimental points in these bi-criteria plots and how to quantify the error of the prediction made *in silico* when a given combination of objectives (and associated weights) is considered in the analysis. Ideally, an experimental observation should lead to a single point in the Pareto plot. Unfortunately, experimental observations are not fully defined, since some fluxes are typically missing. Because of this, it is in practice extremely difficult (if not impossible) to represent each of them as a single point in the space of objectives due to the lack of some experimental fluxes values.

One possible manner to overcome this limitation consists of fixing the known velocities (i.e., those measured experimentally) in the FBA model, and then maximize and minimize the values of all of the objectives. These calculations would provide the limits of a "experimental" square (in the space of objectives) within which the experimental observations should fall. We found that this approach is inadequate because it leads to unfeasible problems. That is, when we attempt to solve the FBA model with the known fluxes fixed to their experimental values, we find that it usually renders unfeasible (i.e., there is no solution satisfying the mass balance equations and at the same time showing the same velocity

values as those measured experimentally). This can be attributed to the presence of experimental errors that make experimental fluxes inconsistent with the FBA model

To avoid these difficulties, we propose here to calculate the limits of the "experimental" square assuming a given allowable mismatch between the experimental fluxes and those calculated by the FBA model. To this end, we optimize and minimize each objective subject to the condition that the ED (distance between experimental fluxes and fluxes obtained *in silico*) must be below a given threshold. A zero ED value implies a perfect match with experimental results, a situation that seldom arises in practice.

Note that the size of the "experimental" square grows as we consider larger ED values. Hence, Figure 2b shows the same experimental points as Figure 2a, but considers a larger ED value. As seen, the square in Figure 2b crosses the Pareto curve. This means that obj1 and obj2 are meaningful objectives if we consider a maximum allowable error equal to ED2. Figures 2c and 2d are analogous to Figures 2a and 2b, but they are defined for other objectives. As seen, for these objectives, the "experimental" square does not cross the Pareto curve (even for the largest allowable ED error). Hence, the optimization of these objectives does not explain the observed fluxed (considering a maximum allowable error bellow or equal to ED2). As observed, depending on the objectives selected, and the ED value considered, the "experimental" square may or may not touch the Pareto set calculated *in silico*.

Clarifying further the connection between our approach and the concept of Pareto optimality, we state that if the experimental square touches the Pareto set resulting from the simultaneous optimization of the two objectives in at least one point, then these objectives may be meaningful for explaining the biological system in the experimental conditions considered. If the Pareto front does not intersect the "experimental" square, such objectives are not meaningful under these conditions.

Figure 3 further illustrates this concept. As observed, the error required for a square to touch the Pareto set depends on the combination of objectives being assessed. In addition, for a given combination of objectives, there will always be an error for which the Pareto front will touch the "experimental" square (larger ED values lead to squares of larger size that will ultimately intersect the Pareto set). Our approach systematically identifies those combinations of objectives for which the error is the minimum possible. Note that this analysis is carried out considering several objectives simultaneously, and it is therefore not restricted only to two criteria.

Hence, for the illustrative example containing two objectives, the method we propose would work as follows. It would calculate all the Pareto fronts corresponding to every pair of objectives. It would then determine the minimum square (i.e., the square with minimum Euclidean Distance) that would contain the experimental observations for each such combination of objectives. To this end, our method would search among the points contained in the Pareto front the one whose distance with respect to the "experimental" square is minimum, or equivalently, the point in the Pareto front touching the experimental square with minimum ED. For the illustrative example, and considering a total number of allowable objectives equal to two, the model would chose objectives 1 and 2 as the most meaningful ones. As already mentioned, and further discussed later in the article, our approach performs all these calculations in a systematic and automated manner, without the need to carry out iterations.

Results

To test our approach, we use a previously reconstructed flux balance analysis model of the *E. coli* central carbon metabolism [9], with 102 reactions and 62 metabolites that represents the major carbon flows through the cell (the complete model is provided as supplementary material). We consider as potential biological objectives, all reaction fluxes associated with an energy dissipation (ATP consumed), or redox potential dissipation (NADH consumed), biomass growth and total production of ATP (there are 21 different velocities that generate ATP). For our study, we employ 13C-detected in vivo flux distributions from four growth aerobic conditions.

Numerical experiments were carried out in the modeling systems GAMS. The Mixed-Integer Quadratically Constrained Programming model defined for a single experiment contains 794 continuous variables, 207 binary variables and 1,254 constraints. These MIQCPs were solved with the solver CPLEX on an 2x AMD Athlon 2.99 GHz processor, 3,49 GB of RAM. The CPU time varied according to the instance being solved, but was always below 25-150 CPU seconds. The results generated *in silico* were compared with the 13C detected in vivo flux distributions obtained under four different growth aerobic conditions.

Prediction of meaningful objectives considering one single experiment at once

We first apply our approach to each experimental data set separately. We consider for the analysis the following four experiments: Experiment A: batch growth on glucose under aerobic conditions with fast grow 0.6 h^{-1}; experiment B: chemostat growth 0.02 h^{-1}; experiment C: chemostat growth 0.4 h^{-1}; experiment D: chemostat growth (0.4 h^{-1}) under ammonium limitation. Further details on each experiment can be found in [9].

Each individual velocity of the model is regarded as a potential objective function. Our method automatically finds the optimal weights to be attached to a given maximum number of velocities such that the optimization of this weighted combination of objectives is as close as possible to the experimental results. We first solve the reformulated MIQCP for each data set (obtained under a set of specific conditions) independently, and then consider all the experimental conditions simultaneously.

We start by allowing any number of objectives in the MIQCP, and then constrain the maximum number of criteria to 4, 3, 2 and 1, respectively, imposing an upper bound on the number of binary variables that can take a value of one (recall that these binary variables denote whether one objective is meaningful and therefore optimized in the inner problems of the model). To avoid the calculation of equivalent solutions, we enforce that the summation of all of the weights must equal one. Hence, a weight close to one implies that the associated velocity/flux plays a role in the optimization (i.e., the microorganism attempts to optimize it), while a low weight value implies the opposite.

Figures 4 and 5 (and Table S1 in additional material) summarize the results. Figure 4 shows the Euclidean distance (ED) between the experimental fluxes and those predicted by the model for each experiment. This distance quantifies the extent to which predicted fluxes match their experimental values (lower distances imply more accurate predictions). As observed, the ED decreases as we increase the maximum number of allowable objectives (Figure 4). Note, however, that in almost all of the cases the addition of more objectives leads to marginal reductions in ED, which suggests the existence of a small number of meaningful biological objectives.

To further investigate the importance of biomass maximization as a meaningful biological objective, we repeated the calculations but this time fixing a zero weight for biomass growth rate. Figure 4 and Table S2 (in additional materials) show the results obtained following the above commented procedure. The comparison between the initial calculations and those performed fixing the weight for biomass growth to zero shows that the ED between the best model solution and the experimental data increases drastically for all of the experiments when biomass growth rate maximization is omitted. Hence, our results confirm the importance of biomass growth rate maximization as a meaningful biological objective.

Figure 5 displays the weights calculated by our method for each objective function for the individual experiments. The figure shows only those velocities with weights above 0.01 (the number of bars does not always match with the number of objectives considered, because objectives with small weights are not shown; the complete set of values are nevertheless given in supplementary Table S1). As observed, in all of the experiments the MIQCP calculates a large weight for biomass growth (velocity 102). This is in agreement with previous findings [3], in which biomass maximization was found to be a fundamental biological objective driving the evolution of the cells machinery.

We next studied the robustness of the weights identified by the MIQCP for the case of biomass. For this, we solved again the MIQCP by fixing the minimum ED obtained in every run of the model and maximizing and minimizing the value of the weight attached to biomass growth rate. These calculations

provide the minimum and maximum weight that should be attached to biomass growth rate so as to produce estimated fluxes whose ED (i.e., error) with respect to experimental observations is bellow the ED threshold defined beforehand. This is a necessary calculation because the bi-level model may have alternative solutions (i.e., solutions showing different weight values), that produce the same ED value. Hence, by performing this step, we establish the feasible limits of the weight attached to biomass growth rate for a given ED value.

The results of this analysis are summarized in Figure 6 (see also supplementary Table S3). The minimum and maximum weights for growth rate optimization are close to one in all of the cases, confirming that this criterion is dominant under the tested experimental conditions. Although some variation is observed in different experiments, the range of this variation is below 20 %, implying a substantial robustness in the weights in all of the experimental conditions considered.

We finally investigate the existence of equivalent biological objective functions. To this end, we solve our model iteratively, that is, we first identify a solution (i.e., combination of objectives) leading to minimum error, and then remove it from the search space using integer cuts. An integer cut is a tailored inequality that eliminates a given binary solution (see [14]). Hence, a combination of objectives cannot be calculated twice during the calculations. The results obtained for experiment A, and 2, 3 and 4 objectives are shown in Table 1 and Table S4 (we show only the first 6 solutions identified in the calculations). As observed, there are several combinations of 2, 3 and 4 objectives leading to similar ED values, suggesting that equivalent sets of biological objective functions may exist.

Prediction of meaningful objectives considering all of the experiments simultaneously

We next repeat the calculations considering all the experimental conditions simultaneously, that is, forcing the model to select the same objectives for all of the experiments under study. The results obtained, which are similar to the ones produced for each single experiment separately, are displayed in Figures 7 and 8, and Table S5 (see additional materials).

Figure 7 shows the Euclidean distance (ED) between experimental and *in silico* fluxes considering all of the experiments simultaneously. Recall that lower ED values imply more accurate predictions. As seen, the ED decreases as we increase the maximum number of allowable objectives. The ED values are larger than those reported in Figure 4, in which we adjusted each individual experiment separately. This was expected, since we are attempting to adjust more experimental points in each single run.

Figure 8 shows the weights calculated for each velocity for different numbers of allowed objectives. Note that in this case the model must choose the same set of objectives for all of the experiments, as opposed to what happens in Figure 5, in which the model can choose different objectives for each experimental condition (although in practice some of these objectives appear several times under different experimental conditions). Again, biomass growth (102) shows the largest weight.

Theoretical connections with the concept of Pareto optimality

Optimality goals are tailored for specific conditions and different, eventually competing, objectives cannot be optimized simultaneously without compromising each other. As a result, cells face a trade-off that is described by a Pareto front in which each Pareto optimal point achieves a unique combination of objectives [13].

To investigate the relationship between our method and the concept of Pareto front we built the Pareto plot for experiment A, considering velocities 102 (biomass growth) and 13 (Phosphoenolpyruvatesynthase), which yield the minimum ED (i.e., better fit with experimental data) for the case of 2 objectives.

Figure 9 shows the Pareto set v102 vs. v13 calculated *in silico*. In the same figure, we have depicted also three squares associated with different ED values. These squares contain the set of feasible solutions

of the FBA model (projected onto the space of the aforementioned two objectives) whose ED value (distance with respect the experimental data) is bellow a given threshold. To obtain these squares, we fix the ED in the model and then maximize and minimize each single objective separately. As seen, the Pareto front intersects the squares corresponding to ED = 300,000 and ED = 150,000, but not the one associated with ED= 100,000 (see Table S6, additional materials). This means that we cannot generate *in silico* solutions (by solving the model for these two objectives) with an ED value (error with respect to experimental data) bellow 100,000. Note that this is consistent with what we observed in Figure 2 , in which the error for the best combination of two objectives is above 100,000. Hence, these two objectives are more successful in explaining the experimental observations than any other combination of two criteria. Note, however, that the extent to which they may be regarded as "biologically meaningful" will depend on the maximum error (i.e., Euclidean distance) we are willing to assume in the calculations.

We now construct the Pareto set for velocities 69 and 3, and the feasible squares corresponding to ED values equal to 150,000 and 400,000 (Figure 10 and Table S6 in additional materials). As opposed to the previous case, the Pareto set does not intersect the feasible square with a ED=150,000, but it does intersect the one defined for an ED equal to 400,000. Hence, it is clear that depending on the velocities considered as objectives and the maximum allowable ED values, the "experimental" square may or may not intersect the Pareto set. If the square intersects the Pareto set, then the predictions made *in silico* fit the experimental observations within the error considered in the calculations. Hence, for this particular example, it turns out that the optimization of objectives v102 and v13 produces feasible solutions that are closer to experimental data than those obtained by optimizing velocities v69 and v3. In practice, the model automatically selects those velocities for which the ED is minimum, without the need of neither calculating nor plotting the corresponding Pareto sets explicitly.

Conclusions

We have presented a novel framework that integrates network stoichiometry and experimental flux data to determine the most likely set of objective functions for a given biological system. We illustrate the utility of our method on a model of *E. coli* central metabolism, for which we identify the coefficients of importance (i.e., extent to which each objective can explain the experimental observations) under a variety of experimental conditions. The problem of identifying meaningful biological objectives is mathematically posed as a bi-level optimization problem. We solve this model by reformulating it into a single-level mixed-integer quadratically constrained program using the KarushKuhnTucker conditions. This reformulated problem can then be solved by standard optimization algorithms.

We found that biomass growth rate maximization is the objective that better explains the experimental observations (i.e., the one with the largest coefficient of importance). In addition, the error of the approximation decrease as we include more biological objectives in the analysis. Thus, the maximization of cellular biomass appears to be an important descriptor, although not the unique one, in explaining the observed fluxes. Numerical results show also that experimental observations can be well explained by a reduced number of objectives (i.e., around 3), and that there are different combinations of objectives leading to similar errors.

Hence, we hypothesize that microorganism evolution optimizes simultaneously a subset of biological criteria so as to stay as close as possible to the so called Pareto optimal frontier of a "universal" multi-objective model [15]. This implies that there is no single universal objective function for microorganisms; rather, there is a set of fitness functions that cells seek to optimize simultaneously. The relative importance of each of these functions depends on the external conditions. Under different conditions, different criteria may emerge as predominantly controlling the optimization at the expense of worsening the remaining objectives. In addition, the cell might seek regions where at least one objective can be improved without necessarily worsening any of the others. That is, if one objective can be improved with no additional performance drop in any other criterion, then the microorganism will move towards this win-win situation. In this context, our method can be used to test the validity of different hypotheses leading to a better

characterization of the underlying driving forces of cellular metabolism.

Materials and Methods

Our approach is built under the assumption that metabolic networks are designed to optimize simultaneously several objectives that are unknown. Hence, the goal of the method is to find these objectives considering a set of experimental fluxes against which we compare the solutions produced *in silico* using a multi-objective algorithm (i.e., weighted-sum approach). Flux Balance Analysis are steady-stage stoichiometric models of metabolic networks that are based on linear programming (LP). The stoichiometric information used to construct FBA models defines a feasible search space from which we need to identify the solution that optimizes a given objective function, typically biomass growth rate maximization. In a recent work, Sauer and co-workers [9] suggested that there might be more than one meaningful biological objective driving the metabolic machinery. This hypothesis can be mathematically translated into the following multi-objective FBA model (**MOFBA**):

$$\begin{aligned} &(\mathbf{MOFBA}) \quad \min U\{v_j, .., v_{jup}\} \\ &\text{s.t.} \\ &\sum_{j=1}^{M} S_{ij} v_j = 0 \qquad \forall i \in N \\ &\underline{v_j} \leq v_j \leq \overline{v_j} \qquad \forall j \in M \end{aligned}$$

Where U is the multi-dimensional objective function being optimized, jup is the number of objective functions (which in our calculations was assumed to be equal to the number of reactions), N is the set of metabolites and M is the set of reactions. Note that $|MO| = jup$. The solution to this problem is given by a set of Pareto optimal points with the property that it is impossible to improve them in one objective without necessarily worsening at least one of the others. We use here the weighted sum method to obtain the Pareto-optimal solutions. This method relies on optimizing a linear combination of jup objectives by solving a set of single-objective problems of the following form (for different values of the weights wj):

$$\begin{aligned} &(\mathbf{MOS}) \quad \min \sum_{j=1}^{jup} v_j w_j \\ &\text{s.t.} \\ &\sum_{j=1}^{M} S_{ij} v_j = 0 \qquad \forall i \in N \\ &\underline{v_j} \leq v_j \leq \overline{v_j} \qquad \forall j \in M \end{aligned}$$

Figure 1 illustrates the main idea underlying our approach. First, we define a set of weights w_j to be attached to the different objectives. We then minimize (or maximize) the linear combination of such objectives to obtain the global optimum of the problem according to this objective. This solution is guaranteed to be Pareto optimal, that is, there is no other point improving it simultaneously in both criteria. This global optimum satisfies all the constraints of the model (i.e., steady state operation and bounds on velocities) while minimizing at the same time the linear combination of objectives. We next calculate the ED between this global optimum and the experimental observations by measuring the distance between the fluxes calculated in silico and those obtained experimentally. Finally, we repeat the calculations until the ED cannot be improved any further. The final goal is to identify the set of weights to be attached to the different objectives such that when this linear combination is optimized, the ED takes its minimum value. Every putative biological objective that is given a nonzero weight, plays a role, while those that are assigned a zero weight are not biologically meaningful. As will be shown, this whole procedure can be performed in one single step by reformulating the bi-level model.

Our approach is inspired on the **ObjFind** method proposed by Burgard and Maranas [3], which is based on a bi-level optimization model composed of an outer problem and inner problem. The outer problem finds the best values of the weights to be attached to a set of velocities regarded as plausible biological objectives. The objective of this outer problem is to minimize the sum-squared error between experimentally-measured (*in vivo*) fluxes and framework-computed (*in silico*) fluxes. That is, the outer problem must find the best weight values, understanding by best values those that show the following property: when we optimize a weighted sum of velocities using these weight values, the distance between the fluxes calculated *in silico* and the experimental ones is minimal.

The inner problems, which are defined for every experimental condition, minimize the linear combination of objectives proposed by the outer problem subject to steady state and stoichiometric constraints and considering also lower and upper bounds on the velocities. Hence, the inner problems are single-objective problems whose solutions are Pareto optimal in the space of the underlying multi-objective FBA model. The original bi-level problem has the following form:

$$
\begin{aligned}
(\mathbf{BIMO}) \quad & \min_{w_j, x_j} \sum_{j \in EX} (v_j - v_j^{exp})^2 \\
& \text{s.t.} \\
& \left(\begin{array}{ll} \min\limits_{v_j} \sum\limits_{j=1}^{jup} (v_j w_j) & \\ s.t. & \\ \sum\limits_{j=1}^{M} S_{ij} v_j = 0 & \forall i \in N \\ \underline{v_j} \leq v_j \leq \overline{v_j} & \forall j \in M \end{array} \right) \\
& \sum_{j=1}^{jup} w_j = 1 \\
& 0 \leq w_j \leq \overline{w_j} x_j \qquad \forall j \in M
\end{aligned}
$$

Where S_{ij} is the stoichiometric coefficient of metabolite i in reaction j, represents the flux v_j of reaction j, v_j^{exp} is the experimental flux, and w_j is a weight associated with objective j, which can be a reaction flux or a combination of fluxes v_j . Set N refers to the set of metabolites, EX contains the set of experimentally determined fluxes, and M is the set of reactions. Thus, the goal of the bi-level model is to determine the linear combination of reaction fluxes weighted by that explain in a better manner the experimental fluxes.

In order to make this bi-level optimization problem computationally tractable, we reformulate it as a single-level optimization problem via the KarushKuhnTucker (KKT) conditions (see [12]). The idea is to substitute the inner problems by their KKT conditions and solve the outer problem subject to the KKT conditions of the inner models. The bi-level optimization problem (MOO) is therefore reformulated as a MIQCP. Note that by replacing the inner problems by the KKT conditions, we obtain a convex MINLP model that can be solved to global optimality using standard MINLP solvers. This is a major advantage with respect to the approach used by Burgard and Maranas [3] to reformulate the bi-level problem, which led to a nonconvex model with multiple potential local minima. The main drawback of the latter method is that standard optimization algorithms may get trapped in a local optimum during the search, thereby leading to less meaningful conclusions. Another advantage of our method is that it can handle several objectives simultaneously, as oppose to the approach by Burgard and Maranas [3] that considers only one single objective function. Our tool can in turn consider at the same time several experimental data sets obtained under various conditions.

In order to control the number of objectives in the outer problem, we add a binary variable that takes the value of one if the objective is selected and zero otherwise. The reformulated problem takes finally the following form:

$$
\begin{aligned}
&(\textbf{BIMO}) \quad \min_{w_j, x_j} \sum_{j \in EX} (v_j - v_j^{exp})^2 \\
&\text{s.t.} \\
&\left(\begin{array}{ll}
w_j + \sum_{i=1} S_{ij}\mu_i + \lambda_j^{lo} - \lambda_j^{up} = 0 & \forall j \in M \\
\sum_{j=1}^{M} S_{ij} v_j = 0 & \forall i \in N \\
\underline{v_j} - v_j + slack_j^{lo} = 0 & \forall j \in M \\
v_j - \overline{v_j} + slack_j^{up} = 0 & \forall j \in M \\
slack_j^{lo} \leq (\overline{v_j} - \underline{v_j})(1 - y_j) & \forall j \in M \\
slack_j^{up} \leq (\overline{v_j} - \underline{v_j})(1 - y_j) & \forall j \in M \\
\lambda_j^{lo} \leq y_j \overline{\lambda_j^{lo}} & \forall j \in M \\
\lambda_j^{up} \leq y_j \overline{\lambda_j^{up}} & \forall j \in M \\
\mu_i, \lambda_j^{lo}, \lambda_j^{up}, slack_j^{lo}, slack_j^{up} \leq 0 & \forall j \in M
\end{array} \right) \\
&\qquad \sum_{j=1}^{jup} w_j = 1 \\
&\qquad 0 \leq w_j \leq \overline{w_j} x_j \qquad \forall j \in M
\end{aligned}
$$

Where μ_i and λ_j are the Lagrangean multipliers associated with the equality and inequality constraints, respectively. $slack_j$ is a slack variable that is zero if the inequality constraint is active and positive otherwise. Y is a binary variable that is one if the inequality is active and it is zero otherwise. Hence, the first equation inside the parenthesis (obtained after reformulating the inner problems) models the stationary KKT conditions of the inner problems, the second enforces the steady-state of the network, while the remaining ones are used in order to determine the values of the Lagrangian multipliers of the inequality constraints. Note that we need to define one binary variable for each inequality constraint in order to model the complementary slackness condition (i.e., if the inequality is inactive, its multiplier is zero). Finally, the two last equations constrain the number of objectives through the addition of the binary variable x_j, which is one if the objective is included and zero otherwise.

Acknowledgments

The authors wish to acknowledge support from the Spanish Ministry of Education and Science (Projects (CTQ2012-37039-C02, DPI2012-37154-C02-02 and ENE2011-28269-C03-03) and the Generalitat de Catalunya (FI programs).

References

1. Savageau MA, Rosen R (1976) Biochemical systems analysis: a study of function and design in molecular biology, volume 725. Addison-Wesley Reading, MA.

2. Feist AM, Palsson BO (2010) The biomass objective function. Current opinion in microbiology 13: 344–349.

3. Burgard AP, Maranas CD (2003) Optimization-based framework for inferring and testing hypothesized metabolic objective functions. Biotechnology and bioengineering 82: 670–677.

4. Gianchandani EP, Oberhardt MA, Burgard AP, Maranas CD, Papin JA (2008) Predicting biological system objectives de novo from internal state measurements. BMC bioinformatics 9: 43.

5. Knorr AL, Jain R, Srivastava R (2007) Bayesian-based selection of metabolic objective functions. Bioinformatics 23: 351–357.

6. Bachmann H, Fischlechner M, Rabbers I, Barfa N, dos Santos FB, et al. (2013) Availability of public goods shapes the evolution of competing metabolic strategies. Proceedings of the National Academy of Sciences 110: 14302–14307.

7. Schuetz R, Zamboni N, Zampieri M, Heinemann M, Sauer U (2012) Multidimensional optimality of microbial metabolism. Science 336: 601–604.

8. Fischer E, Zamboni N, Sauer U (2004) High-throughput metabolic flux analysis based on gas chromatography–mass spectrometry derived 13c constraints. Analytical biochemistry 325: 308–316.

9. Schuetz R, Kuepfer L, Sauer U (2007) Systematic evaluation of objective functions for predicting intracellular fluxes in escherichia coli. Molecular systems biology 3.

10. Teotónio H, Rose MR (2000) Variation in the reversibility of evolution. Nature 408: 463–466.

11. Ehrgott M (2005) Multicriteria optimization, volume 2. Springer.

12. Ben-Ayed O (1993) Bilevel linear programming. Computers & operations research 20: 485–501.

13. Shoval O, Sheftel H, Shinar G, Hart Y, Ramote O, et al. (2012) Evolutionary trade-offs, pareto optimality, and the geometry of phenotype space. Science 336: 1157–1160.

14. Balas E, Jeroslow R (1972) Canonical cuts on the unit hypercube. SIAM Journal on Applied Mathematics 23: 61–69.

15. Milo R, Itzkovitz S, Kashtan N, Levitt R, Shen-Orr S, et al. (2004) Superfamilies of evolved and designed networks. Science 303: 1538–1542.

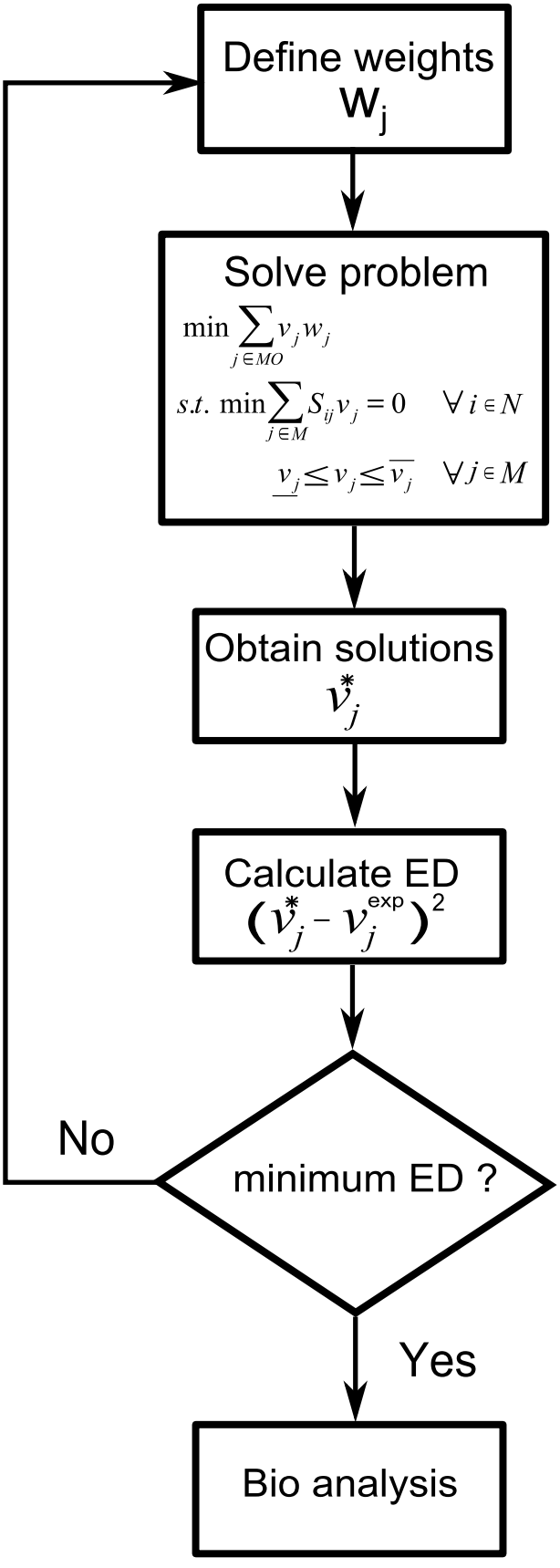

Figure 1. Scheme of the optimization steps carried out by our method. Our approach performs these steps in a simultaneous fashion by reformulating the bi-level problem into a single algebraic optimization model.

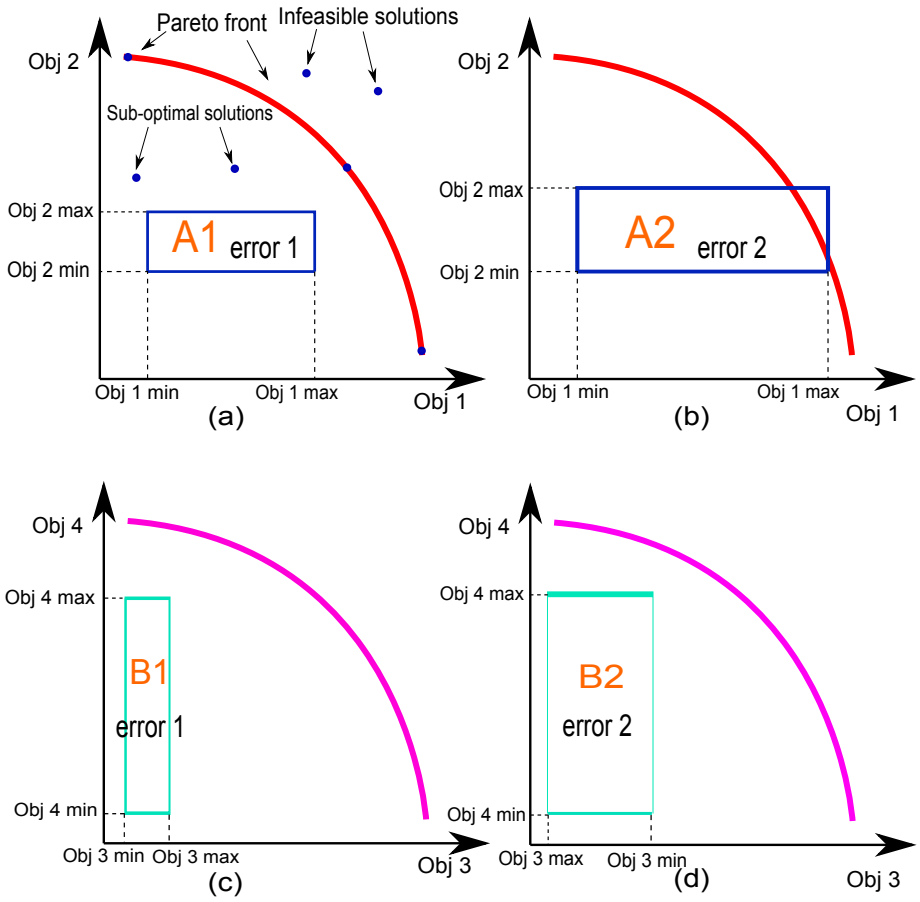

Figure 2. Concept of Pareto optimality. Figures 2a and 2b show the Pareto curve Obj1 vs Obj2, for different ED values, which leads to squares of different sizes. Note that the squares define the space of points projected onto the space of objectives whose distance with respect to the experimental data is bellow a given error. Figures 2c and 2d are analogous to 2a and 2b, but consider other objectives. As observed, depending on the objectives considered, the experimental points may fall within or outside the corresponding square for a given ED value.

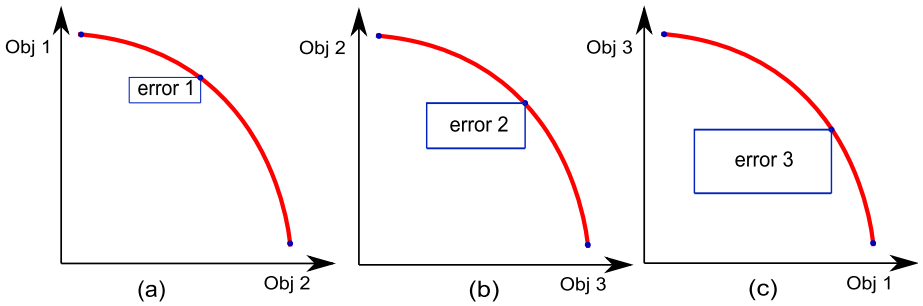

Figure 3. Pareto sets for different combinations of objectives and associated error

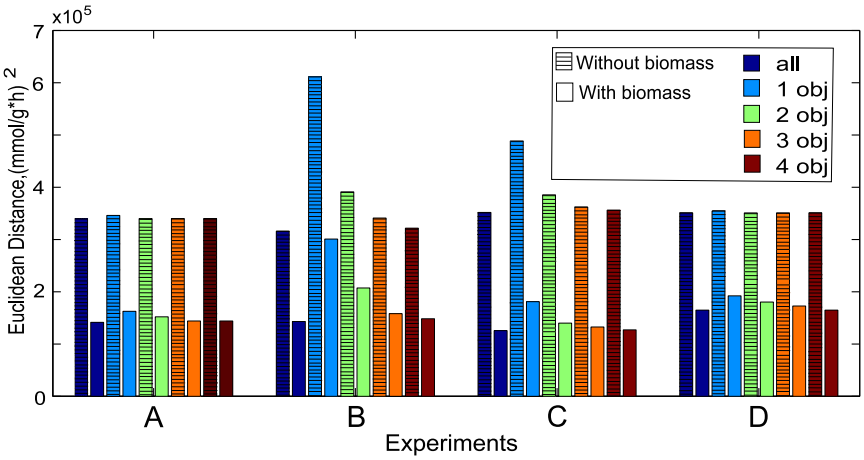

Figure 4. Results for four experiments with and without biomass growth. The ED decreases as we increase the number of objectives. The inclusion of biomass growth as a potential objective function leads to better ED values.

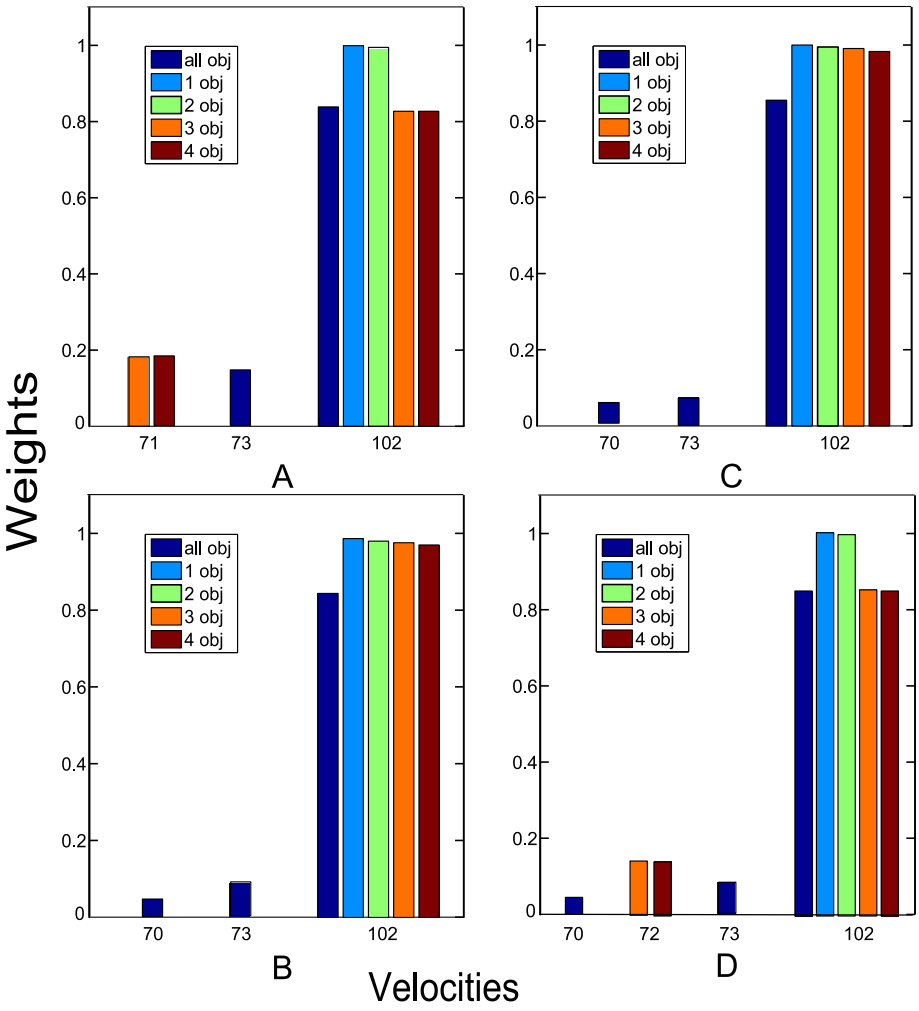

Figure 5. Weights calculated for all of the velocities with the MINLP for different limits on the total number of objectives considered in the analysis. In all of the cases the weight attached to biomass growth rate is above 0.8, which confirms its importance as a meaningful biological objective driving the cell's machinery. Velocity 70 is Acetaldehyde dehydrogenaseII R1, 71 is Acetaldehyde dehydrogenase R2, 72 is Ethanol dehydrogenase, 73 is Alcohol dehydrogenase classIII, 102 is biomass production (see additional materials).

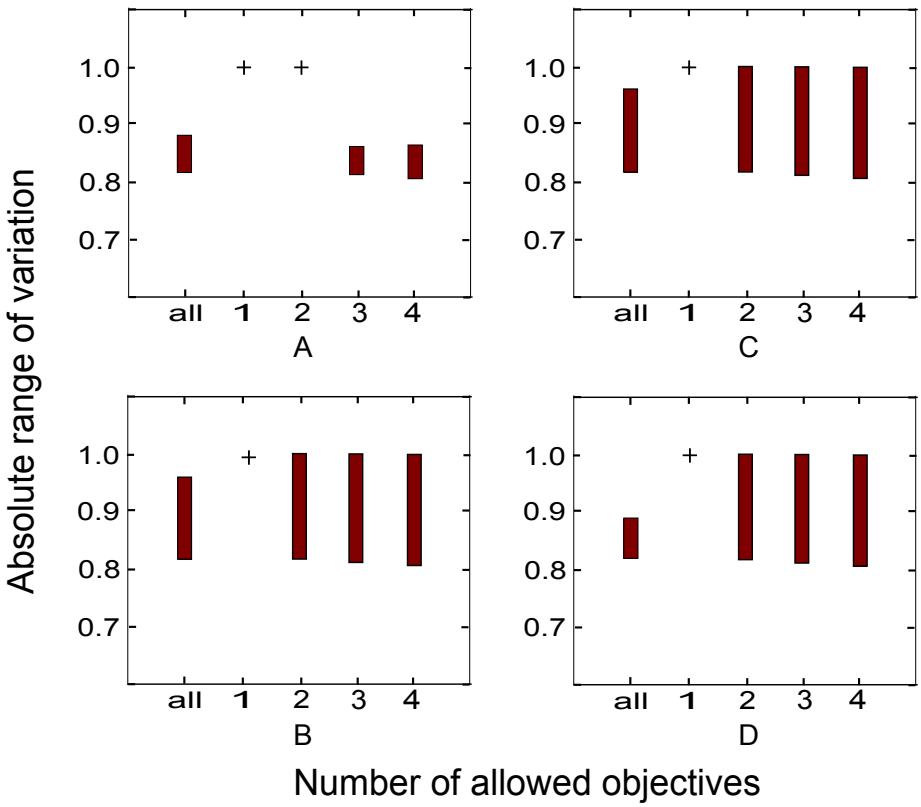

Figure 6. Results for the case of maximizing and minimizing the value of the weight attached to biomass growth rate for different limits on the number of objectives. The interval gets wider as we increase the number of objectives. The values of the biomass growth rate weight are quite large, confirming its importance as a meaningful objective function.

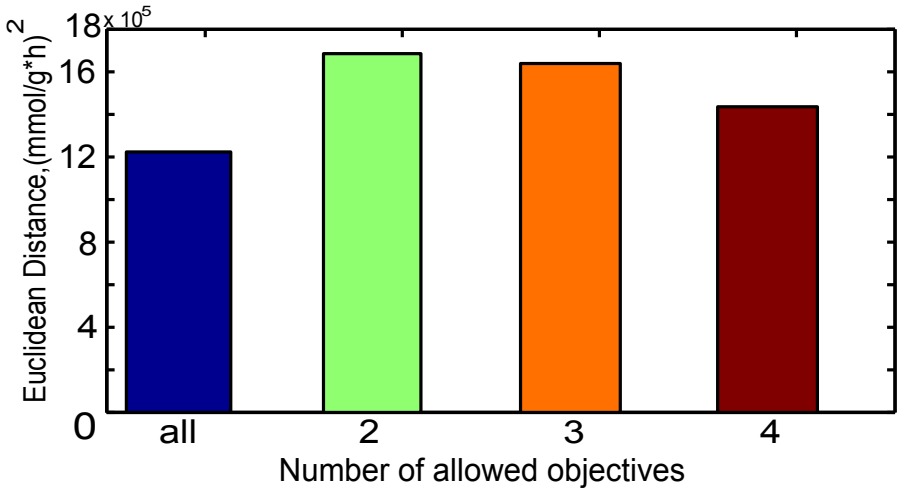

Figure 7. ED values for all the experiments simultaneously.

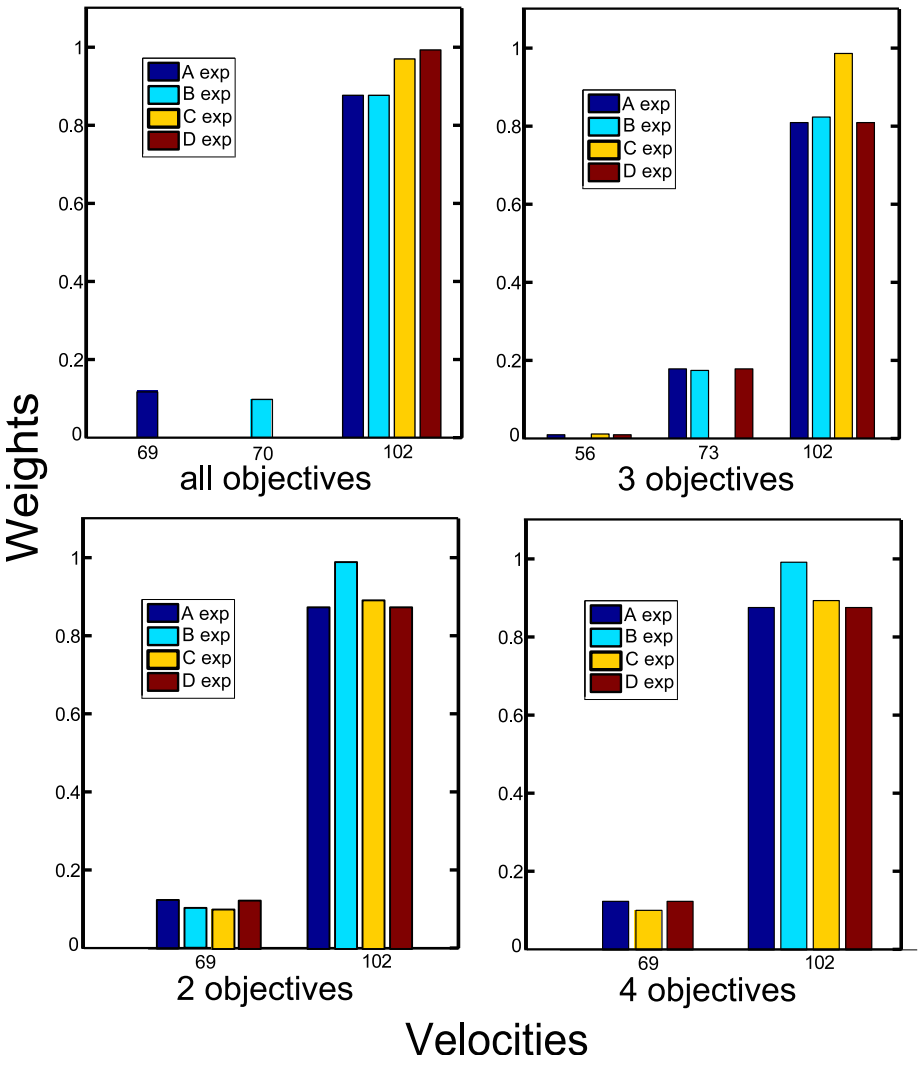

Figure 8. Results for all the experiments simultaneously. In all of the cases the weight attached to biomass growth rate is above 0.8, which confirms its importance as a meaningful biological objective driving the cell's machinery. Velocity 56 is NADH dehydrogenaseI, 69 is Acetaldehyde dehydrogenaseI R1, 70 is Acetaldehyde dehydrogenaseII R1, 73 is Alcohol dehydrogenase classIII , 102 is biomass production. For simplicity, velocities with weights lower than 0.01 are not shown.

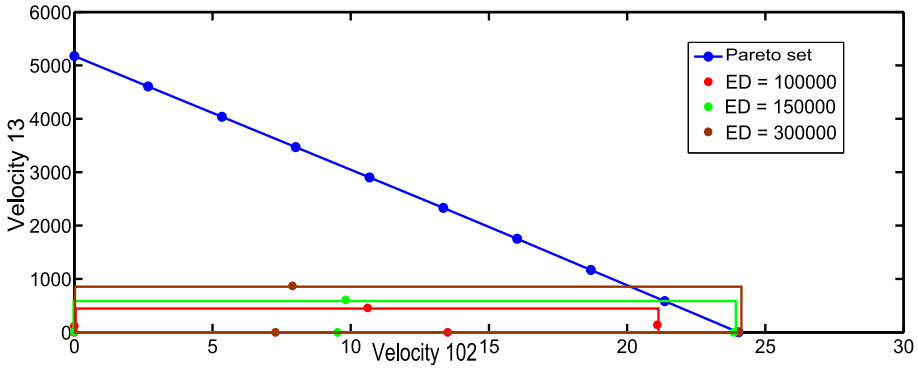

Figure 9. Results obtained from the bi-criteria problems biomass growth vs. velocity 13 and feasible squares for a given ED

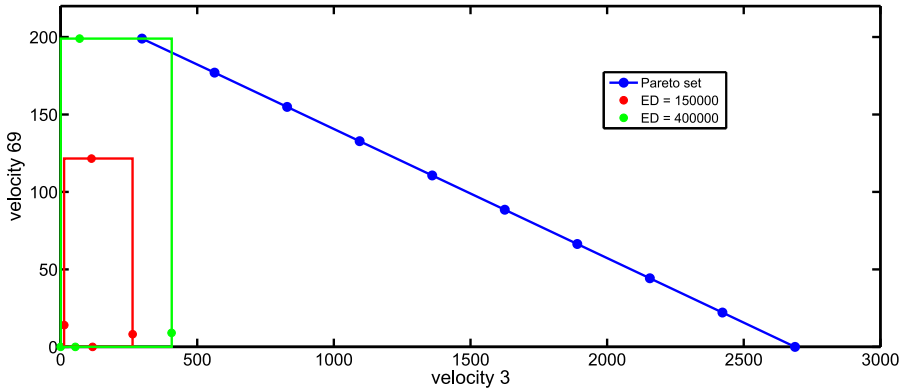

Figure 10. Results obtained from the bi-criteria problems velocity 3 vs. velocity 69 and areas bordered by extreme solutions

Tables

Table 1. Results for integer cuts method for first experiments

2 obj		3 obj		4 obj	
ED	Velocities	ED	Velocities	ED	Velocities
152045.2	102, 13	144073.8	102, 56, 73	141425.4	102, 73, 13, 4
157980.2	102, 69	144073.8	102, 56, 70	142558.6	102, 3, 13, 73
157980.2	102, 73	144073.8	102, 56, 69	142558.6	102, 3, 13, 72
157980.2	102, 72	144073.8	102, 56, 71	144073.8	102, 101, 73, 56
157980.2	102, 70	144073.8	102, 56, 72	144073.8	102, 71, 56
157980.2	102, 71	148354	102, 13, 73	144073.8	102, 71, 56, 57

Appendices

Three articles were published; two article are currently under review.

A List of publications

1. **Vaskan P.**, Passuello A., Guillén-Gosálbez G., Schuhmacher M., Jiménez L. **Combined use of GIS and mixed-integer linear programming for identifying optimal agricultural areas for sewage sludge amendment: A case study of Catalonia.** *Environmental Modelling & Software* 48, 163–169, 2013.

2. **Vaskan P.**, Guillén-Gosálbez G., Kostin A., Jiménez L. **Decomposition Algorithm for Geographic Information System Based Mixed-Integer Linear Programming Models: Application to Sewage Sludge Amendment**. *Industrial & Engineering Chemistry Research*, 52(49), 17640–17647, 2013.

3. **Vaskan P.**, Guillén-Gosálbez G., Jiménez L. **Multi-objective design of heat-exchanger networks considering several life cycle impacts using a rigorous MILP-based dimensionality reduction technique**. *Applied Energy* 98, 149–161, 2012.

4. **Vaskan P.**, Guillén-Gosálbez G., Jiménez L. **Multi-objective optimization of utility plants under several environmental indicators using an MILP-based dimensionality reduction approach**. Pending submission to *Applied Energy*.

5. **Vaskan P.**, Guillén-Gosálbez G., Alves R., Jiménez L. **Identifying multi-objective design principles in metabolic networks via a rigorous multi-level optimization framework**. Pending submission to *PLOS Computational Biology*.

B Contributions to congresses

1. **Vaskan P.**, Guillén-Gosálbez G., Sorribas A., Alves R., Jiménez L.**Multi-level optimization framework for the identification of multi-objective design principles in metabolic networks** . *AIChE 2013 Annual Meeting*, San Francisco, USA, 2013.

2. **Vaskan P.**, Guillén-Gosálbez G., Jiménez L. **Indentifying redundant environmental objectives in the design of heat-exchanger networks using rigorous dimensionality reduction techniques**. *ESCAPE-22 European Symposium on Computer Aided Chemical Engineering*, London, UK, 2012.

3. **Vaskan P.**, Passuello A., Guillén-Gosálbez G., Schuhmacher M., Jiménez L. **Integrated use of geographic informational system and mixed integer linear programming for indentifying optimal agricultural areas for sewage sludge amendment: A case study of Catalonia**. *AIChE 2012 Annual Meeting*, Pittsburgh, USA, 2012.

4. **Vaskan P.**, Passuello A., Guillén-Gosálbez G., Schuhmacher M., Jiménez L. **Coupled use of geographic informational system and mixed-integer linear programming for indentifying optimal agricultural areas for sewage sludge amendment: A case study of Catalonia**, *ANQUE's International Congress of Chemical Engineering*, Sevilla, Spain, 2012.

5. **Vaskan P.**, Guillén-Gosálbez G., Jiménez L. **Indentifying redundant environmental objectives in the design of heat-exchanger networks using rigorous dimensionality reduction techniques**, *12th Mediterranean Congress of Chemical Engineering*, Barcelona, Spain, 2011.

C Book chapters

1. **Vaskan P.**, Guillén-Gosálbez G., Jiménez L. **Indentifying redundant environmental objectives in the design of heat-exchanger networks using rigorous dimensionality reduction techniques.**. *Computer-Aided Chemical Engineering*, 30 , pp. 202-206, ISBN: 978-0-444-59431-0, Pergamon-Elsevier Science Ltd, 2012.